# GEOLOGY AND MINERAL DEPOSITS OF THE GALLINAS MOUNTAINS, LINCOLN AND TORRANCE COUNTIES, NEW MEXICO; PRELIMINARY REPORT

Virginia T. McLemore

New Mexico Bureau of Geology and Mineral Resources
New Mexico Institute of Mining and Technology
Socorro, NM 87801
ginger@gis.nmt.edu

Open-file Report OF-532

**September 2010**

*This information is preliminary and has not been reviewed according to New Mexico Bureau of Geology and Mineral Resources standards. The content of this report should not be considered final and is subject to revision based upon new information. Any resource or reserve data are historical data and are provided for information purposes only and does not reflect Canadian National Instrument NI 43-101 requirements, unless specified as such.*

*Cougar Mountain, looking east from the top of Gallinas Peak.*

## ABSTRACT

Rare earth elements (REE) are used in the electronics, automotive and metallurgical industries. Deposits containing REE are found throughout New Mexico. With the projected increase in demand of REE, domestically and globally, areas such as the Gallinas Mountains in New Mexico are being re-examined for additional REE potential. Minimal past production of REE in the 1950s, as bastnaesite, came from the Gallinas Mountains, Lincoln and Torrance Counties. Since then, several companies and the U.S. Bureau of Mines (USBM) have conducted various exploration programs to identify and delineate REE resource potential. The igneous rocks in the Gallinas Mountains are metaluminous to peraluminous, alkaline volcanic rocks, and have chemical compositions similar to A-type granitoids. Trachyte/syenite and latite are possibly related, but the rhyolite could be a separate magmatic event. The geochemical data suggest a crustal source for the igneous rocks. Four types of deposits are found in the Gallinas Mountains: epithermal REE-F veins, Cu-REE-F veins, REE-F breccia pipes and iron skarn deposits; all are associated with Tertiary alkaline to alkalic-calcic igneous rocks. District zonation is defined by Cu-REE-F (±Pb, Zn, Ag) veins that form center of the district, surrounded by REE-F veins. The magmatic-hydrothermal breccia pipe deposits form a belt partially surrounding the veins. Iron skarns formed at the top and edge of the trachyte/syenite body and are likely the earliest stage of mineralization. The iron skarns are probably related to the REE-F veins and breccias because they typically contain bastnaesite and fluorite and are similar in trace element geochemistry. The paragenesis is defined by four stages of brecciation and faulting with three stages of fluorite deposition. REE minerals were deposited during the $1^{st}$ and $2^{nd}$ stage of fluorite deposition. A genetic model is summarized by intrusion/extrusion of crustal-derived igneous source rock in an extensional terrain possibly related to an alkaline-carbonatite complex with mineralization related to mixing of magmatic-hydrothermal and formation fluids. In 1991-1992, USBM calculated an inferred resource of 537,000 short tons with a grade of 2.95% total REE (not NI-43-101 compliant).

## TABLE OF CONTENTS

## FIGURES

## TABLES

## INTRODUCTION

Rare earth elements (REE) are increasingly becoming more important in our technological society and are used in many of our electronic devices. REE include the 15 lanthanide elements (atomic number 57-71), yttrium (Y, atomic number 39), and scandium (Sc; Table 1) and are commonly divided into two chemical groups, the light REE (La through Eu) and the heavy REE (Gd through Lu, Sc, and Y). REE are lithophile elements (or elements enriched in the crust) that have similar physical and chemical properties (Table 1), and, therefore, occur together in nature. However, REE are not always concentrated in easily mined economic deposits and only a few deposits in the world account for current production (Committee on Critical Mineral Impacts of the U.S. Economy, 2008; Hedrick, 2009). Thorium (Th), uranium (U), niobium (Nb) and other elements typically are found with REE. Most deposits are radioactive because of their Th and U content.

TABLE 1. Description of rare earth elements (REE) (from Taylor and McClennan, 1985; Samson and Wood, 2005; Rudnick and Gao, 2005; Castor and Hedrick, 2006; and Hedrick, 2009). * Promethium does not occur naturally.

| Rare Earth Element | Symbol | Oxide | Conversion factor (% element x conversion factor - % oxide) | Atomic Number | Abundance in the upper crust (ppm) |
|---|---|---|---|---|---|
| Scandium | Sc | $Sc_2O_3$ | | 21 | 14 |
| Yttrium | Y | $Y_2O_3$ | 1.269 | 39 | 21 |
| Lanthanum | La | $La_2O_3$ | 1.173 | 57 | 31 |
| Cerium | Ce | $Ce_2O_3$ | 1.171 | 58 | 63 |
| Praseodymium | Pr | $Pr_2O_3$ | 1.17 | 59 | 7.1 |
| Neodymium | Nd | $Nd_2O_3$ | 1.166 | 60 | 27 |
| Promethium | Pm | * | * | 61 | * |
| Samarium | Sm | $Sm_2O_3$ | 1.16 | 62 | 4.7 |
| Europium | Eu | $Eu_2O_3$ | 1.158 | 63 | 1.0 |
| Gadolinium | Gd | $Gd_2O_3$ | 1.153 | 64 | 4.0 |
| Terbium | Tb | $Tb_2O_3$ | 1.151 | 65 | 0.7 |
| Dysprosium | Dy | $Dy_2O_3$ | 1.148 | 66 | 3.9 |
| Holmium | Ho | $Ho_2O_3$ | 1.146 | 67 | 0.83 |
| Erbium | Er | $Er_2O_3$ | 1.143 | 68 | 2.3 |
| Thulium | Tm | $Tm_2O_3$ | 1.142 | 69 | 0.30 |
| Ytterbium | Yb | $Yb_2O_3$ | 1.139 | 70 | 2.2 |
| Lutetium | Lu | $Lu_2O_3$ | 1.137 | 71 | 0.31 |
| Thorium | Th | $ThO_2$ | 1.138 | 90 | 10.5 |
| Zirconium | Zr | $ZrO_2$ | 1.351 | 40 | 193 |
| Niobium | Nb | $Nb_2O_5$ | 1.431 | 41 | 12 |

REE have many highly specialized applications in our industry and for many applications there is no other known substitute (Naumov, 2008; Hedrick, 2009). Europium is the red phosphor used in color cathode-ray tubes and liquid-crystal displays in computer monitors and televisions, with no known substitute (Committee on Critical Mineral Impacts of the U.S. Economy, 2008). Erbium is used in fiber-optic telecommunication cables that transmit signals over long distance and provide greater bandwidth than the traditional copper wires. Erbium also is used in fiber-optics telecommunication cables, ceramics, dyes for glass, optical filters and lasers. Permanent magnets utilize Nd, Sm, Gd, Dy and Pr, which are used in appliances, audio and video equipment, computers, automobiles, communication systems, and wind turbines. Rechargeable lanthanum-nickel-hydrogen (La-Ni-H) batteries are replacing nickel-cadmium (Ni-Cd) batteries in computers, communication systems, and automobiles. Dysprosium is used in hybrid car motors. As electric automobiles become more viable, La-Ni-H and other REE batteries will be in more demand. Cerium magnetic switches are an important component of modern cell phones. Scandium is used in high-strength aluminum-scandium (Al-Sc) alloys and electron beam tubes. Catalytic converters require La and Ce and there are no known substitutes (Committee on Critical Mineral Impacts of the U.S. Economy, 2008). Cerium, as $CeO_2$, is used to polish mirrors and lenses because of its unique physical and chemical attributes in aqueous medium (Committee on Critical Mineral Impacts of the U.S. Economy, 2008). Yttrium is used in fluorescent lamps, capacitors, cathode-ray tube (CRT) phosphors, microwave filters, glasses oxygen sensors, radars, lasers, structural ceramics, and superconductors. A small amount of Y in steel produces a fine-grained structure and improves the mechanical, electrical, and magnetic properties (Naumov, 2008). Scandium is alloyed with aluminum and used in baseball and softball bats and in metallurgical research, semiconductors, and specialty lighting (Hedrick, 2009). Approximately 35% of the REE produced are used as catalysts in the refining of crude oil to improve cracking and in automobiles to improve oxidation of pollutants, although use of REE as catalysts is declining (Committee on Critical Mineral Impacts of the U.S. Economy, 2008).

The U.S. once produced enough REE for U.S. consumption, but since 1999 more than 90% of the REE required by U.S. industry have been imported from China (Haxel et al., 2002). However, the projected increase in demand for REE in China, India, U.S., and other countries has resulted in increased exploration and ultimate production from future deposits in the U.S. and elsewhere. Furthermore, specific REE are becoming more economically important. Recently, the Chinese government announced that it is examining the economic feasibility of continuing to export REE from their deposits. REE deposits have been reported from New Mexico (McLemore et al., 1988a, b; McLemore, 2010a), but were not considered important exploration targets because the demand in past years has been met by other deposits in the world. However, with the projected increase in demand and potential lack of available production from the Chinese deposits, these areas in New Mexico are being re-examined for their REE potential. One of these areas in New Mexico is the Gallinas Mountains.

The Gallinas Mountains are in northern Lincoln County and southern Torrance County where a series of alkaline igneous bodies, including porphyritic latite, trachyte/syenite, andesite, and rhyolite laccoliths, flows, dikes, and plugs, have intruded Permian sedimentary rocks belonging to the Abo, Yeso, and Glorieta Formations (Perhac, 1961, 1970). A small amount of bastnaesite, a REE mineral, was recovered during processing for fluorite. Alteration includes brecciation, silicification, chloritization, and fenitization (Griswold, 1959; Woodward and Fulp, 1991; Schreiner, 1993). Carbonatites are inferred at depth by the presence of fenitization, carbonatization of the breccias, presence of REE and similarity of the intrusive rocks and mineralization to areas with known carbonatites.

A number of previous reports have examined the geology and mineral resources of the Gallinas Mountains, but few examined the resource potential for REE and re-examination of the Gallinas Mountains is warranted in light of today’s potential economic importance of REE. Therefore, the purposes of this report are 1) to compile and interpret available published and unpublished data from the Gallinas Mountains, 2) to summarize the geology, geochemistry, resource potential, and origin of the mineral deposits in the Gallinas Mountains, and 3) relate the mineral deposits to other REE deposits in New Mexico and elsewhere.

## METHODS OF STUDY

Published and unpublished data were inventoried and compiled on existing mines and prospects within the Gallinas Mountains. Mineral databases were examined, including the Mineral Resource Data System (MRDS) of the U.S. Geological Survey (Mason and Arndt, 1996), the Minerals Industry Location System (MILS) of the U.S. Bureau of Mines (U.S. Bureau of Mines, 1995), U.S. Forest Service Abandoned and Inactive Mines database, AMLIS (U.S. Bureau of Land Management), and unpublished files at the New Mexico Bureau of Geology and Mineral Resources (NMBGMR). Using these data, mineral occurrences, deposits, mines, prospects, and mills were identified, plotted on base maps, and compiled in the New Mexico Mines Database (McLemore et al., 2005a, b). Mineralized areas were examined and sampled in 1980 and 2009-2010 by the author and in 1991-1992 by the U.S. Bureau of Mines (Schreiner, 1993). Mineral production by commodity and year since the late 1880s is in Tables 1 and 2. Mining and production records are generally poor, particularly for the earliest times, and many early records are conflicting. These production figures are the best data available and were obtained from published and unpublished sources (NMBGMR, file data). However, production figures are subject to change as new data are obtained.

A geologic map was compiled in ARCMAP@ using U.S. Geological Survey topographic maps as the map base and by modifying Kelley et al. (1946), Perhac (1961, 1970), Fulp and Woodward (1991), Schreiner (1993), and field reconnaissance by the author (1980, 2009-2010). Samples were collected and analyzed and compared with published data (Appendix 1). Igneous rock lithologies were identified on the basis of mineralogy and chemistry as defined by LeMaitre (1989).

This report has not been reviewed according to NMBGMR standards. The contents of the report should not be considered final and complete until reviewed and published by the NMBGMR. The views and conclusions contained in this document are those of the author and should not be interpreted as necessarily representing the official policies, either expressed or implied, of the State of New Mexico. Any resource or reserve data presented here are historical data and are provided for information purposes only and do not conform to Canadian National Instrument NI 43-101 requirements.

## MINING AND EXPLORATION HISTORY AND PREVIOUS INVESTIGATIONS

The Gallinas Mountains mining district is in the central Gallinas Mountains, mostly in Lincoln County and is also known as the Corona, Iron Mountain, Red Cloud, and Gallinas districts (File and Northrop, 1966). The Gallinas Mountains were first examined about 1881 when the Red Cloud, Buckhorn, Deadwood, and Summit mining claims were established; production started around 1885 for copper, silver, and lead (File and Northrop, 1966). Small quantities of ore were sent to Socorro for smelting (Jones, 1904), but there are no early production records remaining. The first recorded production for base metals was in 1909, which continued until 1955 (Table 2). By 1920, the ore was shipped to El Paso for refining at the smelter. Iron ore was found by 1904 (Jones, 1904) and in 1942-1943, iron ore was produced from the American Iron and Red Cliff mines (Kelley, 1949). Kelley et al. (1946) and Kelley (1949) mapped the geology and described the iron resources.

Fluorite was discovered in the Gallinas Mountains before the 1930s (Johnson, 1928; Perhac, 1970). In 1951-1954, fluorite was produced from the Red Cloud and Conqueror mines. Bastnaesite was discovered in the area about 1943 (Glass and Smalley, 1943; Dean, 1944; Soulé, 1943, 1946) and approximately 142,000 lbs of bastnaesite was produced from the Red Cloud mine in the 1950s (Zandra et al., 1952). Between 1954 and 1956, the New Mexico Copper Corp. set up a small mill facility near Carrizozo, NM and produced 55,000 pounds of bastnaesite. Phelps Dodge drilled a 532-ft deep hole at the Rio Tinto mine in 1980 and Molycorp, Inc. conducted a more extensive exploration program in 1980-1981, including a geochemical survey, geophysical survey, and two drill holes on a magnetic high anomaly (Schreiner, 1993). Other companies examined the area in 1989-1992, including Canyon Resources (1989), Hecla Mining Co. (1991-1992), American Copper and Nickel, Inc. and Romana Resources (1992). Woodward and Fulp (1991) reported gold assays as high as 183 ppb in brecciated trachyte/syenite sills that intruded Yeso sandstone. The U.S. Bureau of Mines conducted extensive mapping and sampling of the REE deposits in 1991-1992 (Schreiner, 1993). Williams-Jones et al. (2000) and associates (Gagnon et al., 2003; Salvi et al, 2005; Samson and Wood, 2005) examined the geochemistry of selected deposits in the Gallinas Mountains. Strategic Resources, Inc. staked claims in 2009 and began exploration activities (http://www.strategicresourcesinc.ca/index.php, accessed 5/14/2010).

TABLE 2. Yearly metals production data compiled from U.S. Geological Survey (1902-1927) and U.S. Bureau of Mines Mineral Yearbooks (1927-1990) and (McLemore, 1991a, b).

| Year | Ore (tons) | Copper (lbs) | Gold (oz) | Silver (oz) | Lead (lbs) | Zinc (lbs) | Value $ |
|---|---|---|---|---|---|---|---|
| 1900-1908 | | | | | | | 0 |
| 1909 | 14 | 361 | | 42 | 7,907 | | 409 |
| 1910 | | | | | | | 0 |
| 1911 | 8 | 555 | | 70 | 6,620 | | 404 |
| 1912 | 131 | 8,337 | | 879 | 103,911 | | 6,593 |
| 1913 | 157 | 7,068 | 0.18 | 895 | 94,010 | | 5,777 |
| 1914 | 82 | 15,068 | 3.44 | 649 | 10,641 | | 2,849 |
| 1915 | 46 | 5,091 | 0.11 | 243 | 13,277 | | 1,640 |
| 1916-1919 | | | | | | | 0 |
| 1920 | 363 | 11,386 | | 1345 | 171,925 | | 17,315 |
| 1921 | 378 | 49,240 | | 2,552 | 155,222 | | 15,889 |
| 1922 | 1,893 | 213,072 | | 11,015 | 700,072 | | 78,284 |
| 1923 | 578 | 38,966 | | 3,065 | 232,657 | | 24,527 |
| 1924 | 121 | 8,596 | | 409 | 26,912 | | 3,553 |
| 1925-1926 | | | | | | | 0 |
| 1927 | 60 | 3,382 | | 381 | 21,683 | | 2,025 |
| 1928 | 18 | 667 | | 77 | 7,000 | | 547 |
| 1929 | | | | | | | 0 |
| 1930 | 23 | 700 | 0.19 | 151 | 12,000 | | 753 |
| 1931 | | | | | | | 0 |
| 1932 | 24 | 1,000 | 0.58 | 103 | 11,500 | | 449 |
| 1933 | 42 | 1,000 | 0.39 | 123 | 14,000 | | 633 |
| 1934 | 30 | 4,400 | 0.29 | 221 | 13,850 | | 1,017 |
| 1935 | 61 | 2,000 | 0.4 | 185 | 17,300 | | 1,005 |
| 1936-1947 | | | | | | | 0 |
| 1948 | 1,015 | 10,000 | | 854 | 74,000 | 16,000 | 18,317 |
| 1949-1950 | | | | | | | 0 |
| 1951 | 11 | | | 31 | 4,000 | | 720 |
| 1952 | | | | | | | 0 |
| 1953 | 39 | 4529 | | 183 | 14,351 | 1344 | 3,466 |
| 1954 | 23 | | | 45 | 6,000 | | 863 |
| 1955 | 250 | | 1 | 205 | 79,000 | | 1,398 |
| Total | 5,367 | 385,418 | 6.58 | 23,723 | 1,797,838 | 17,344 | 188,433 |

TABLE 3. Minerals production from the Gallinas Mountains, New Mexico.

| Mineral Produced | Mine name | Years of production | Amount (short tons) | Grade % | Reference |
|---|---|---|---|---|---|
| Copper | various | 1909-1953 | 192.7 | | McLemore (1991a, b) |
| Gold | various | 1913-1955 | 6.58 ounces | | McLemore (1991a, b) |
| Silver | various | 1909-1955 | 23,723 ounces | | McLemore (1991a, b) |
| Lead | various | 1909-1055 | 863.4 | | McLemore (1991a, b) |
| Zinc | various | 1948-1953 | 8.7 | | McLemore (1991a, b) |
| Iron ore | American | 1942-1943 | 3,944 | 55.7 | Kelley (1949) |
| | Gallinas | 1942 | 6,410 | 48.7 | Kelley (1949) |
| | Other mines | | 3,326 | | Kelley (1949) |
| Total iron ore | | 1942-1943 | 11, 540 | | Kelley (1949) |
| Fluorite | All American | 1951-1954 | 129 | | Griswold (1959), McAnulty (1978) |
| | Conqueror (Rio Tinto) | 1951-1954 | 300 | | Griswold (1959), McAnulty (1978) |
| | Red Cloud | 1951-1954 | 1,000 | | Griswold (1959), McAnulty (1978) |
| Total fluorite | | 1951-1954 | 1,608 | | |
| Bastnaesite | Conqueror No. 9 | 1954-1955 | 60 | | Griswold (1959) |
| | Conqueror No. 10 | 1956 | 11 | | Griswold (1959) |
| Total bastnaesite | | 1954-1956 | 71 | | |

## REGIONAL GEOLOGIC AND TECTONIC SETTING

Lindgren (1915, 1933) was one of the first geologists who noted that a belt of alkaline-igneous rocks extends from Alaska and British Columbia southward into eastern New Mexico, Trans-Pecos Texas, and eastern Mexico (Fig. 1) and that these rocks contain relatively large quantities of fluorine (F), zirconium (Zr), REE, and other elements. Since then, the North American Cordilleran alkaline-igneous belt has been explored and exploited for numerous types of mineral deposits, especially gold and silver (Mutschler et al., 1985, 1991; Clark, 1989), fluorite (Van Alstine, 1976), and REE (Woolley, 1987). Economic mineral deposits found within this belt have produced nearly 13% of the total lode gold production in the U.S. and Canada (Mutschler et al., 1991). Consequently, numerous companies have examined the belt for additional deposits, including REE deposits.

In New Mexico, the North American Cordilleran alkaline-igneous belt extends from the Sangre de Cristo Mountains near Raton, southward to the Cornudas Mountains, east of El Paso, Texas (Fig. 2; North and McLemore, 1986, 1988; McLemore, 1996, 2001). Significant mineral production, especially gold and silver, has come from deposits spatially associated with Tertiary alkaline-igneous rocks in the New Mexico alkaline-igneous belt (McLemore, 1996, 2001). These mineral deposits in New Mexico have been referred to as Great Plains Margin (GPM) deposits by North and McLemore (1986, 1988) and McLemore (1996, 2001). Alternative classifications by other workers include alkalic-gold or alkaline-igneous related gold deposits (Fulp and Woodward, 1991; Thompson, 1991a, b; Bonham, 1988; Mutschler et al., 1985, 1991; Richards, 1995), porphyry gold deposits, and Rocky Mountain gold province.

The Lincoln County porphyry belt (LCPB) in central New Mexico is part of the North American Cordilleran alkaline-igneous belt and is at the intersection of the north-trending Pedernal arch and the east-west-trending Capitan lineament in Lincoln County, which appears to have localized magmatic and volcanic activity in the LCPB (Fig. 3; Table 4; Kelley and Thompson, 1964; Kelley, 1971; Allen and Foord, 1991; McLemore and Zimmerer, 2009). Alkaline to subalkaline igneous rocks are found in all districts in the LCPB, but mineralization is locally associated with silica-saturated (monzonite) or oversaturated (quartz monzonite) rocks (Table 5; Seagerstrom and Ryberg, 1974; McLemore and Phillips, 1991; Thompson, 1991a, b). K-Ar and sparse $^{40}Ar/^{39}Ar$ dating (Fig. 4, Table 4) suggests the LCPB likely represents two stages of magmatism, an early alkaline belt emplaced along a N-S trend (Pedernal uplift) between 38 and 30 Ma and a younger bimodal suite emplaced along an E-W trend between 30 and 25 Ma (Fig. 2; Allen and Foord, 1991). The GPM deposits consist of seven associated deposit types: (1) polymetallic, epithermal to mesothermal veins, (2) breccia pipes and quartz veins, (3) porphyry Cu-Mo-Au, (4) Cu, Pb/Zn, and/or Au skarns or carbonate-hosted replacement deposits, (5) Fe skarns and replacement bodies, (6) placer Au, and (7) Th-REE-fluorite epithermal veins, breccias, and carbonatites. The GPM veins have high Au/base metal ratios and typically low Ag/Au ratios (North and McLemore, 1988; McLemore, 1996, 2001) in contrast with other high Ag/Au deposits in western New Mexico (McLemore, 2001).

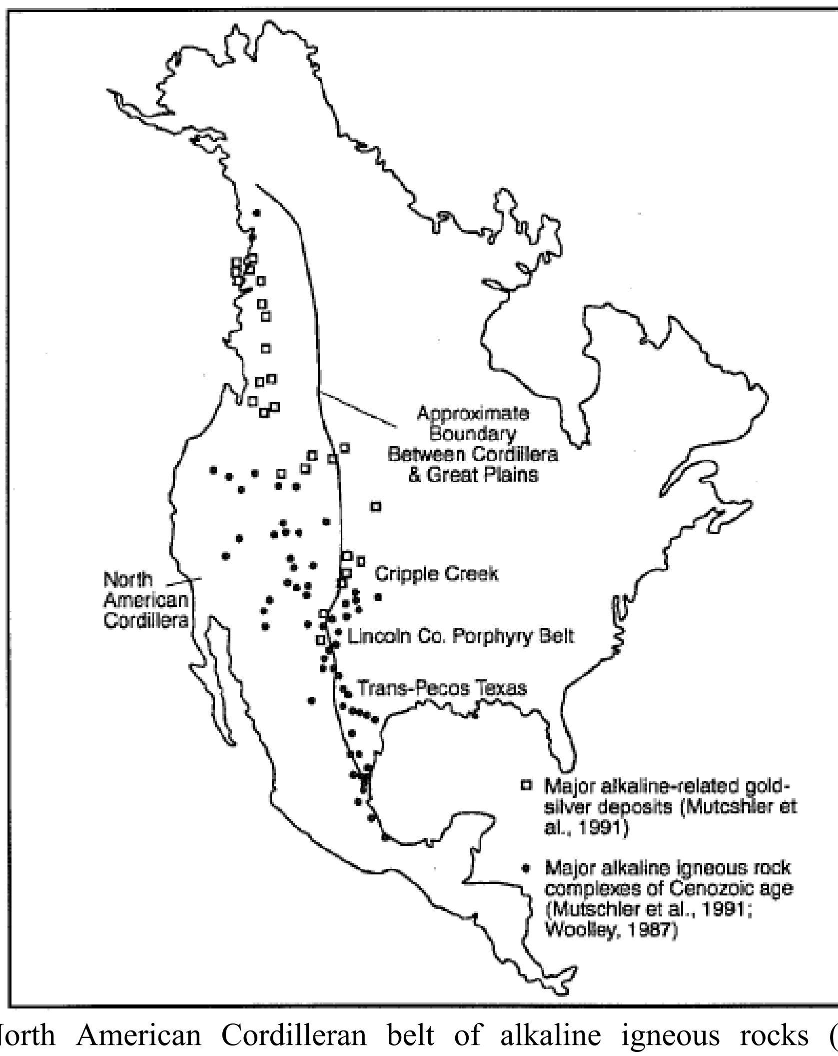


FIGURE 1. North American Cordilleran belt of alkaline igneous rocks (Woolley, 1987; Mutschler et al., 1991; McLemore, 1996).

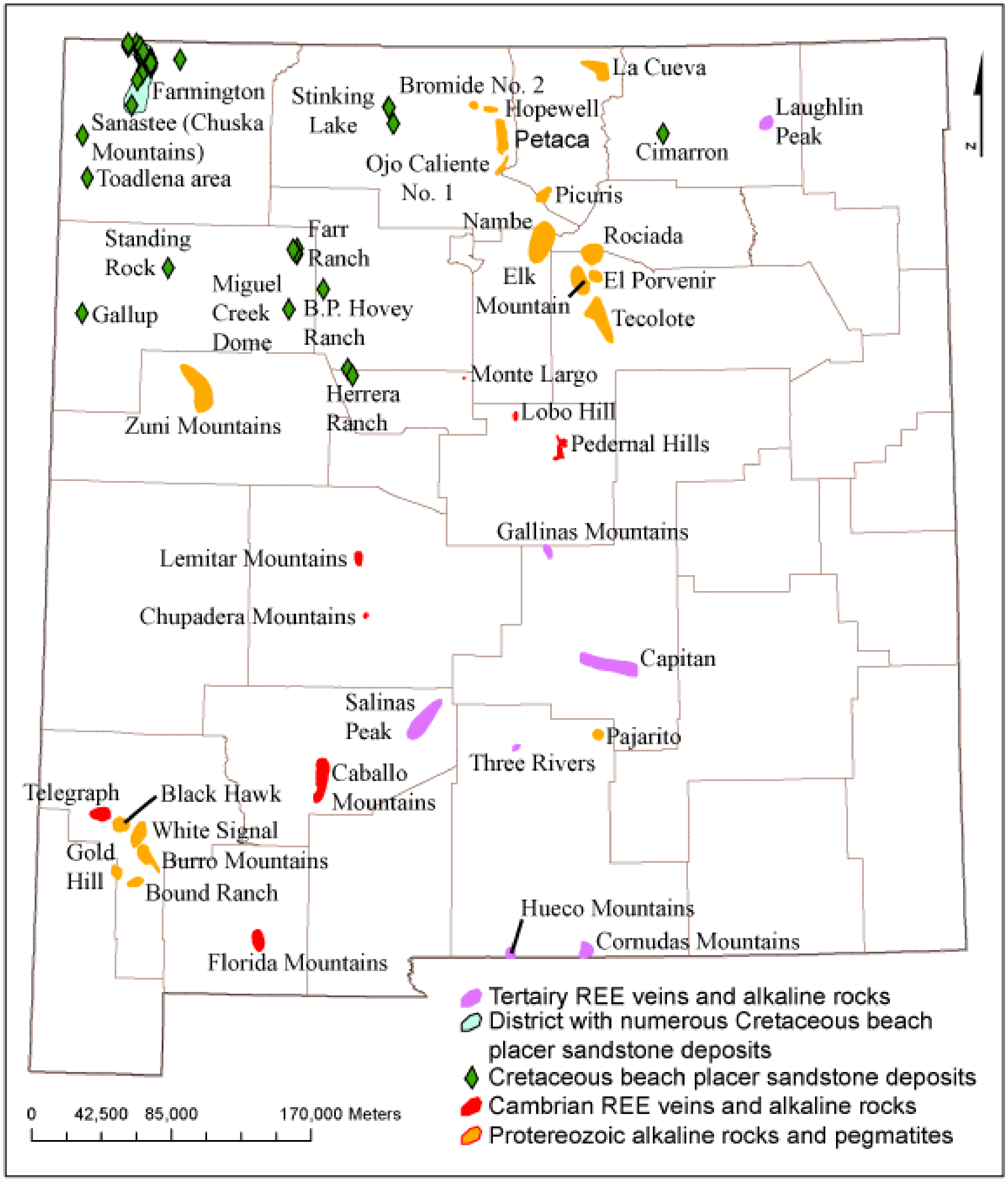


FIGURE 2. Mining districts and areas in New Mexico that contain REE deposits (modified from Adams, 1965; Northrop, 1996; McLemore et al., 1988a, b; 2005a).

The North American Cordilleran alkaline-igneous belt in New Mexico coincides with a belt of alkaline igneous rocks and eastward lithospheric thickening, which follows the tectonic boundary from Texas to Colorado between the tectonically stable Great Plains and tectonically active Rocky Mountains and Basin and Range Provinces. The lithosphere of the Basin and Range and Southern

Rocky Mountains is thinner, has a higher heat flow, and is more permeable and fractured than the lithosphere of the Great Plains (Eaton, 1980; Prodehl and Lipman, 1989; McLemore, 1996). This belt of alkaline-igneous rocks occurs along this boundary and continues northward into Canada and southward into Mexico (Clark et al., 1982; Clark, 1989; Mutschler et al., 1991). The diversity of igneous rocks and associated mineral deposits within this belt (Mutschler et al., 1985, 1991; McLemore, 1996) suggests that the boundary between the Great Plains and Rocky Mountains and Basin and Range provinces is a region of highly fractionated and differentiated magmas (Thompson, 1991a, b; Allen and Foord, 1991). Low initial $^{87}Sr/^{86}Sr$ ratios suggest intrusive rocks associated with GPM deposits are derived from upper mantle to lower crustal sources (Allen and Foord, 1991; McLemore, 1996).

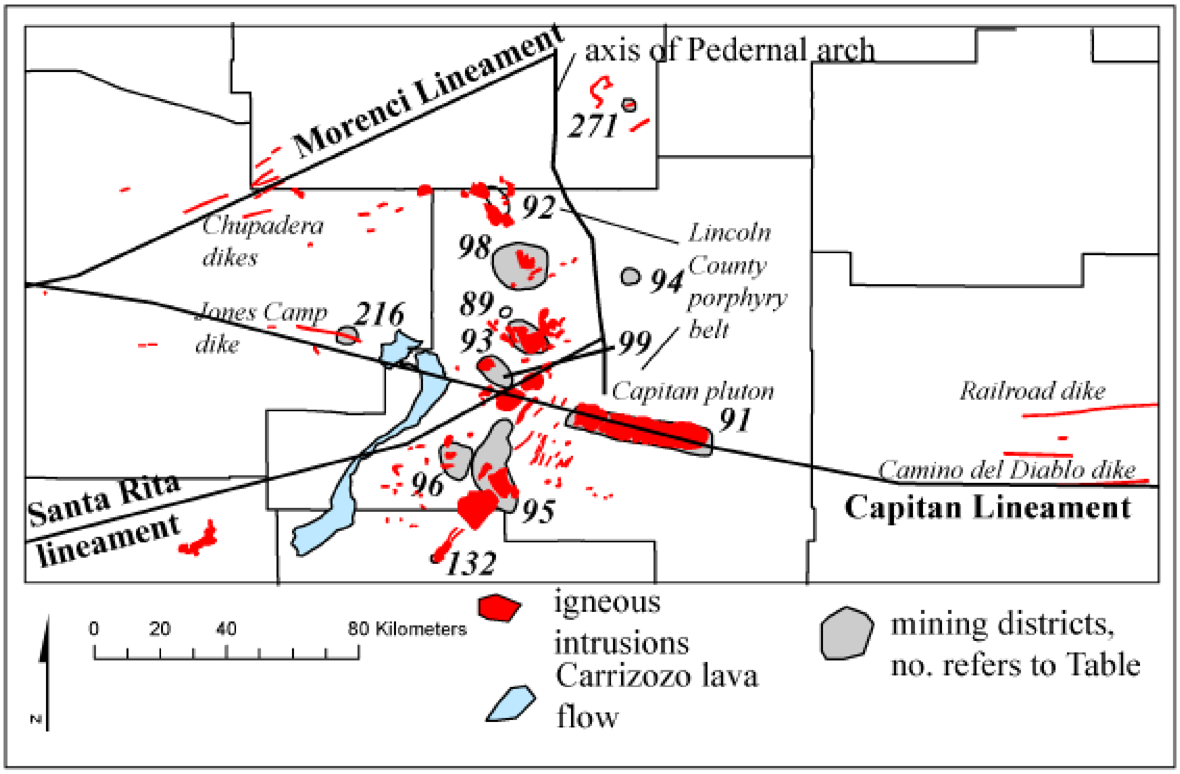


FIGURE 3. Mining districts and igneous intrusions forming the Lincoln County porphyry belt (LCPB; McLemore and Zimmerer, 2009). The mining district identification numbers are from the New Mexico Mines Database, are prefaced with DIS, and are defined in Table 5.

It has not been proven that the mineral deposits associated with this belt are genetically related to the igneous rocks; however, it is likely that they are. Supporting evidence for a magmatic origin includes: 1) fluid inclusion, stable isotope, and age data from the Capitan quartz-REE-Th veins (Phillips, 1990; Phillips et al., 1991; Campbell et al., 1995; Dunbar et al., 1996), 2) nature of stockwork molybdenum deposits at Sierra Blanca (Thompson, 1968, 1973), 3) close spatial association with igneous rocks (Table 4), 4) presence of skarn deposits along the contacts of igneous rocks (Table 4, 5), and 5) similarity to other deposits at Cripple Creek, Colorado and elsewhere where a magmatic origin is favored (Thompson et al., 1985; Porter and Ripley, 1985; Thompson, 1992; Maynard et al., 1989, 1990; Kelley and Luddington, 2002). It is likely that the co-occurrence of Au, Cu, Fe, Mo, F, W, and other elements is the result of several complex magmatic fractionation and differentiation events and tectonic subenvironments, which overlap near the Great Plains Margin. The association of lineaments and other major structures with igneous rocks and mineral deposits in New Mexico suggests that near vertical deep-seated fracture systems probably channeled the magmas and resulting fluids. Once the magmas and fluids reached shallow levels, local structures and wall rock compositions determined the final character and distribution of intrusions and mineralization. Figure 5 summarizes the formation of GPM deposits in New Mexico.

Evidence suggests that complex, multiple intrusions are needed to generate the fluids necessary to produce GPM mineral deposits. The more productive districts, such as Nogal and White Oaks occur in areas of complex magmatism that lasted for more than 5 Ma and resulted in intrusions of different ages. Many of these areas have older calc-alkaline rocks followed by younger alkaline rocks (Table 4; Fig. 4; Allen and Foord, 1991). In areas such as the Capitan Mountains, where intrusive activity occurred in less than 5 Ma, only localized minor Au, Ag, and REE occurrences are found (McLemore and Phillips, 1991). Additional age determinations are required to confirm these observations, especially in the Gallinas, Sierra Blanca, and Tecolote districts.

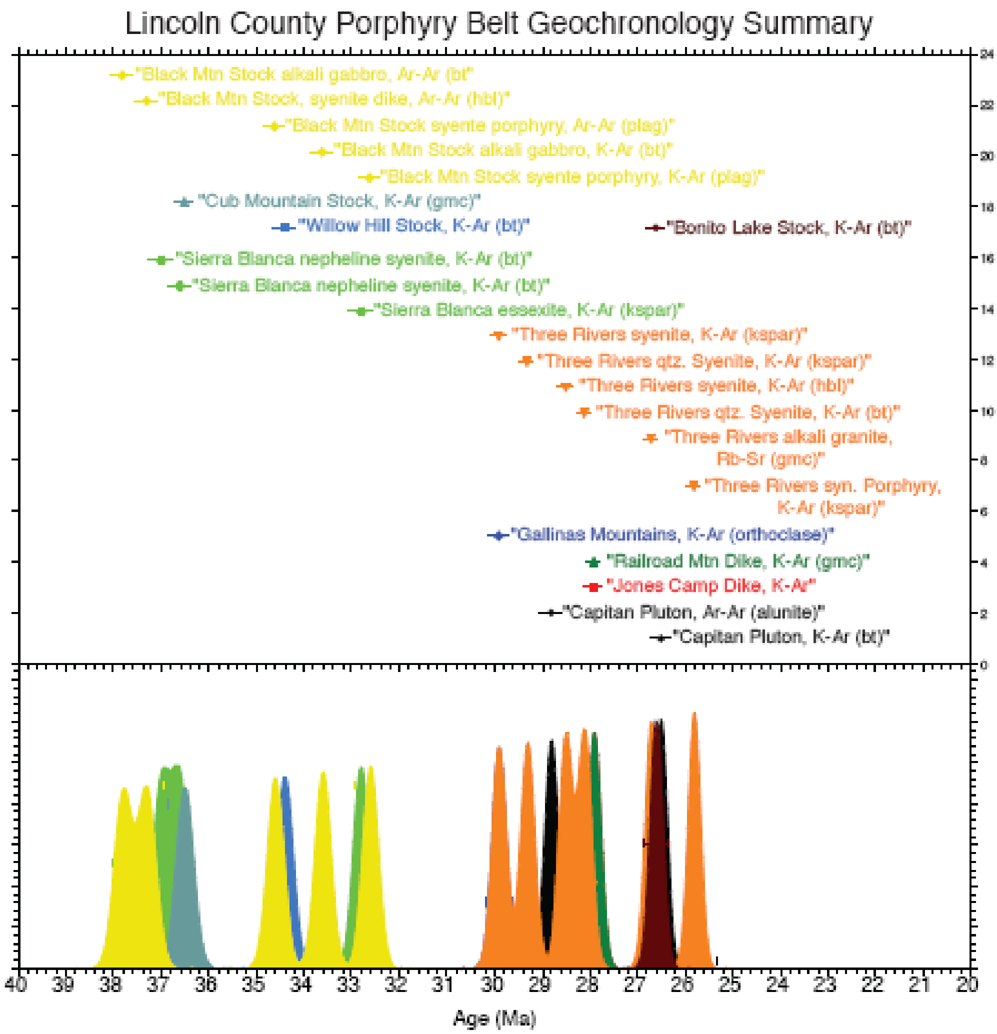


FIGURE 4. Ideogram of K/Ar, Rb/Sr, and $Ar^{40}/Ar^{39}$ ages of igneous rocks in the LCPB area. $^{40}Ar/^{39}Ar$ ages have been recalculated using the new decay constant (modified from McLemore

and Zimmerer, 2009). References are cited in Table 4. The Gallinas Mountains trachyte/syenite was dated by K/Ar methods as 29.9 Ma (Perhac, 1970).

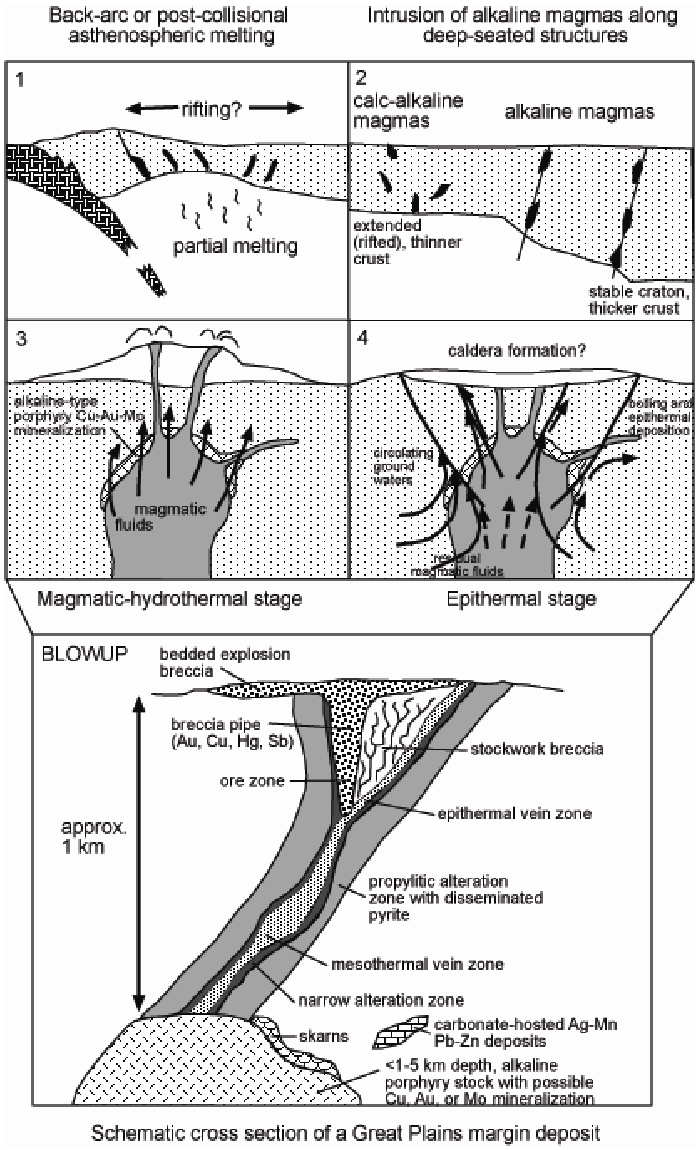


FIGURE 5. Schematic model for formation of Great Plains Margin deposits (modified from Richards, 1995).

TABLE 4. Major intrusions along the eastern Capitan lineament and Lincoln County porphyry belt.

| Intrusive Complex | Lithology | Age (million years) | Mineral | Method | Reference |
|---|---|---|---|---|---|
| Capitan Pluton | granite | 28.8 | adularia | Ar/Ar | Campbell et al. (1994, 1995) |
| Carrizo Mountain | granite | | | | |
| Lone Mountain | syenite | | | | |
| Patos Mountain | monzonite | | | | |

| Intrusive Complex | Lithology | Age (million years) | Mineral | Method | Reference |
|---|---|---|---|---|---|
| Vera Cruz | monzonite | | | | |
| Jones Camp Dike | | 27.9 | ? | K/Ar | Aldrich et al. (1986) |
| Railroad Mountain Dike | gabbro | 27.9 | gmc | K/Ar | Aldrich et al. (1986) |
| Camino del Diablo | diabase | | | | |
| Jicarilla Mountains | monzonite | 38.2 | biotite | K/Ar | Bachman and Mehnert (1978) |
| Gallinas Mountains | trachyte/syenite | 29.9 | orthoclase | K/Ar | Perhac (1970) |
| Tecolote Hills | syenite-diorite | | | | |
| **Sierra Blanca Complex** | | | | | |
| Three Rivers (alkali granite) | | 26.7 | gmc | Rb/Sr | Allen and Foord (1991) |
| Three Rivers (quartz. Syenite) | | 28.1 | biotite | K/Ar | Allen and Foord (1991) |
| Three Rivers (quartz. Syenite) | | 29.3 | K-feldspar | K/Ar | Allen and Foord (1991) |
| Three Rivers (Porphyry) | | 25.8 | K-feldspar | K/Ar | Thompson (1973) |
| Three Rivers (syenite) | | 28.5 | amphibole | K/Ar | Allen and Foord (1991) |
| Three Rivers (syenite) | | 29.9 | K-feldspar | K/Ar | Allen and Foord (1991) |
| Rialto | monzonite | | | | |
| **Older Sierra Blanca Intrusions** | | | | | |
| Older S.B. (essexite) | | 32.8 | K-feldspar | K/Ar | Allen and Foord (1991) |
| Older S.B. (nepheline syenite) | | 36.6 | biotite | K/Ar | Allen and Foord (1991) |
| Older S.B. (essexite) | | 36.6-37 | inferred | | |
| Older S.B. (nepheline syenite) | | 37 | biotite | K/Ar | Allen and Foord (1991) |
| Hollow Hill | rhyolite | | | | |
| Bonito Lake Stock | syenite | 26.6 | biotite | K/Ar | Weber (1971) |
| Willow Hill Stock | syenite | 34.4 | biotite | K/Ar | Weber (1971) |
| Cub Mountain Stock | syenite | 36.5 | gmc | K/Ar | Aldrich et al. (1986) |
| Black Mountain Stock | | | | | |
| Alkali Gabbro | | 17.5 | apatite | fission-track | Thompson (1973) |
| Alkali Gabbro | | 33.6 | biotite | K/Ar | Weber (1971) |
| Alkali Gabbro | | 37.8 | biotite | Ar/Ar | Allen and Foord (1991) |
| Hornblende syenite Porphyry | | 22.6 | apatite | fission-track | Allen and Foord (1991) |
| Hornblende syenite Porphyry | | 32.6 | Plagioclase | K/Ar | Allen and Foord (1991) |
| Hornblende syenite Porphyry | | 34.6 | Plagioclase | Ar/Ar | Allen and Foord (1991) |
| Hornblende syenite Porphyry | | 36.3 | zircon | fission-track | Allen and Foord (1991) |
| Hornblende syenite Dike | | 37.3 | hornblende | Ar/Ar | Allen and Foord (1991) |

| Intrusive Complex | Lithology | Age (million years) | Mineral | Method | Reference |
|---|---|---|---|---|---|
| Hornblende syenite Dike | | 47.7 | hornblende | K/Ar | Allen and Foord (1991) |
| Baxter Mountain | syenite | | | | |
| Carrizozo lava flows | basalt | 5200 yrs | | $^{36}Cl$ | Dunbar (1999) |

TABLE 5. Mining districts along the Lincoln County porphyry belt (LCPB) and Capitan lineament, central New Mexico. Names of districts are after File and Northrop (1966), wherever practical, but some districts have been added. Estimated value of production is in original cumulative dollars and includes all commodities in the district. Production data modified from Lindgren et al. (1910), Anderson (1957), U.S. Geological Survey (1903-1927) and U.S. Bureau of Mines Mineral Yearbooks (1927-1990), New Mexico State Inspector of Mines Annual Reports, and Energy, Minerals and Natural Resources Department (1994). *majority of production is due to clay.

| District no. | District | Types of deposits | Years of Production | Estimated Cumulative Production | Reference |
|---|---|---|---|---|---|
| DIS271 | Duran | GPM-iron replacement | | none | Kelley (1972), McLemore (1984) |
| DIS092 | Gallinas Mountains | GPM-REE-Th- U veins, sedimentary copper, placer gold | 1909-1955 | $261,000 | Perhac (1970), Griswold (1959), Schreiner (1993), McLemore (1991b) |
| DIS098 | Tecolote Iron | GPM | 1915-1919 | $24,000 | Rawson (1957), Allen and Foord (1991), Korzeb and Kness (1992) |
| DIS089 | Ancho | sedimentary | 1902-1922 | $10,000* | McLemore (1991a) |
| DIS093 | Jicarilla | GPM, placer gold | 1850-1957 | $165,000 | Seagerstrom and Ryberg (1974), McLemore et al. (1991), Marvin and Dobson (1979), Griswold (1959) |
| DIS099 | White Oaks | GPM, placer gold | 1850-1953 | $3,100,000 | Thompson (1991b,c), Ronkos (1991), Griswold (1959), Grainger (1974), Weber (1971) |
| DIS091 | Capitan | GPM-REE-Th- U veins, Fe skarn | 1960-2000 | $500,000 | Allen and McLemore (1991), Campbell et al. (1994, 1995), McLemore and Phillips (1991), Phillips (1990) |
| DIS096 | Schelerville | GPM | | $10,000 | Griswold (1959), Korzeb and Kness (1992) |
| DIS095 | Nogal (Nogal-Bonito) | GPM, placer gold | 1865-1942 | $300,000 | Thompson (1968, 1973, 1991b,c), Moore et al. (1991), Allen and Foord (1991), Weber (1971), Aldrich et al. (1986), Douglass and Campbell (1995), Douglass (1992), Korzeb and Kness (1992) |

| District no. | District | Types of deposits | Years of Production | Estimated Cumulative Production | Reference |
|---|---|---|---|---|---|
| DIS132 | Three Rivers (Apache No. 1, White Mtn) | replacement iron | 1911-1943 | $160 | McLemore (1991a) |
| DIS216 | Jones (Jones Camp) | iron replacement | 1942-1943 | $1000 | Aldrich et al. (1986, #312), Gibbons (1981) |
| DIS241 | Chupadera Mesa | iron replacement | | $1000 | Aldrich et al. (1986, #322), McLemore (1984) |
| DIS211 | Chupadero | Precambrian vein and replacements, sedimentary copper, RGR | | $1000 | McLemore (1984) |

## LOCAL STRATIGRAPHY

The oldest rocks in the Gallinas Mountains are altered Proterozoic gneisses and granites (exposed in Red Cloud Canyon) that are overlain by arkoses, quartz sandstones, siltstones, shales and limestones of the Permian Abo, Yeso and Glorieta Formations. The mineralized area of the Gallinas Mountains lies in a magnetic low surrounded by magnetic high anomalies (Fig. 6). Similar magnetic anomalies are characteristic of some alkaline complexes associated with mineral deposits (Woolley, 1987).

### Proterozoic rocks

Proterozoic granite and granitic gneiss are exposed by faulting in three places in the Gallinas Mountains (Fig. 7). The granite is light gray to pink, foliated, fine- to medium-grained and equigranular, and consists of quartz, microcline, oligoclase, biotite, and trace hornblende, zircon, titanite, and apatite (Perhac, 1970; Schreiner, 1993). The granitic gneiss is medium- to coarse-grained, strongly foliated and consists of bands of plagioclase, orthoclase, quartz, biotite and trace zircon, titanite, and apatite. Quartz diorite was found in drill core by Molycorp, Inc. (Schreiner, 1993) and is fine- to medium-grained, consisting of plagioclase, microcline, hornblende, and trace quartz, biotite, titanite, rutile, pyrite, chalcopyrite, magnetite, and apatite.

### Permian sedimentary rocks

### Abo Formation

Permian Abo Formation consists of a basal arkosic conglomerate, a middle arkose, siltstone, and shale sequence, and an upper shale unit. Most of the Abo rocks are a distinctive brick-red color. In the Gallinas Mountains, the Abo Formation ranges in thickness from 100 to 200 ft and unconformably overlie the Proterozoic rocks (Perhac, 1970). The conglomerates and sandstones are poorly sorted, and consist of subrounded to angular grains of quartz, feldspar, rock fragments of granite, mica schist, quartzite and minor accessory minerals.

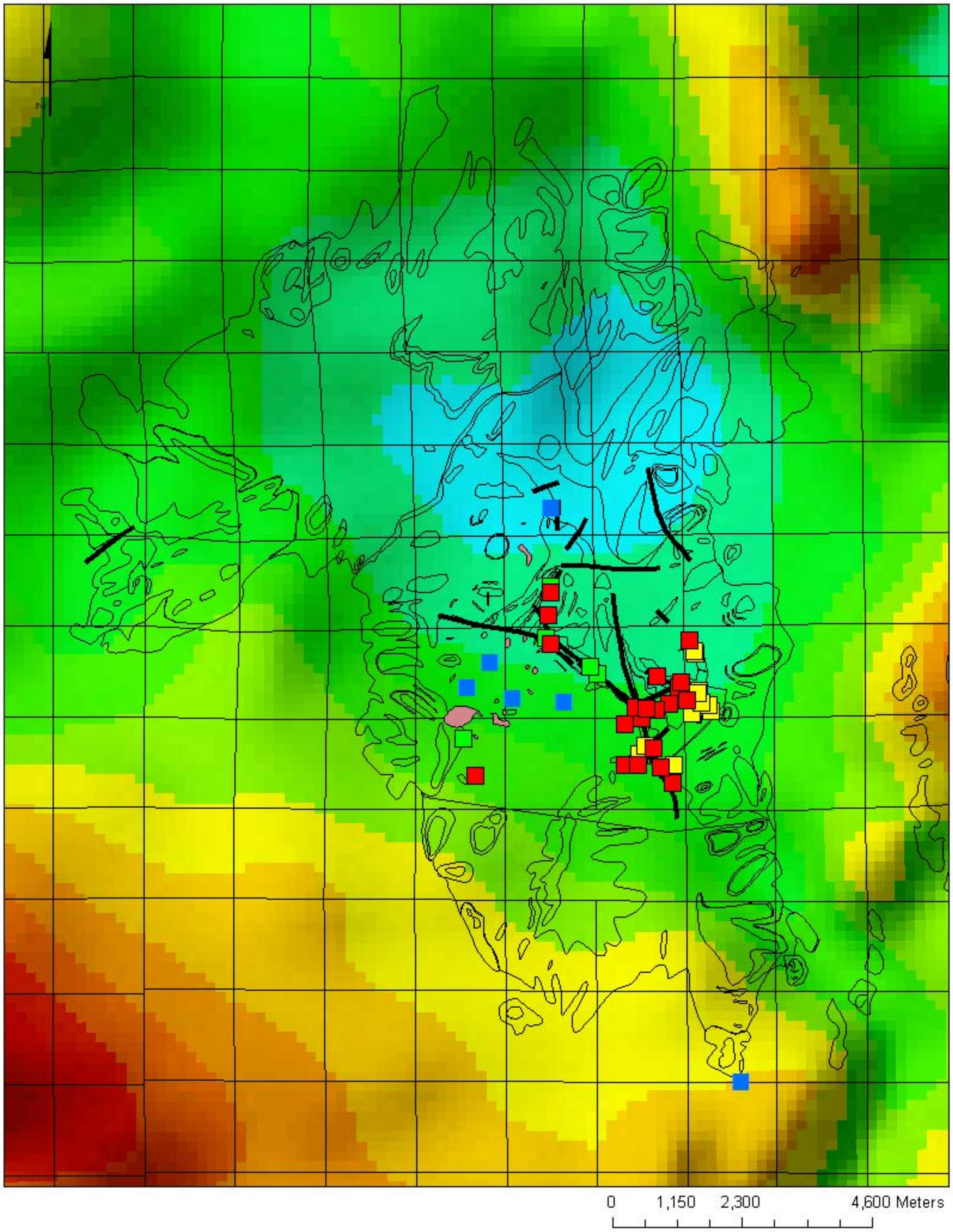


FIGURE 6. Aeromagnetic map of the Gallinas Mountains area, from Kucks et al. (2001). Note the aeromagnetic high (red) southeast of the Gallinas Mountains, which could be indicative of an intrusion in the subsurface. The blue in the center of the Gallinas Mountains is a magnetic low anomaly. The magnetic high anomaly in the northeastern portion of the map could be indicative of subsurface continuation of the latite. See Figure 7 for the geologic map.

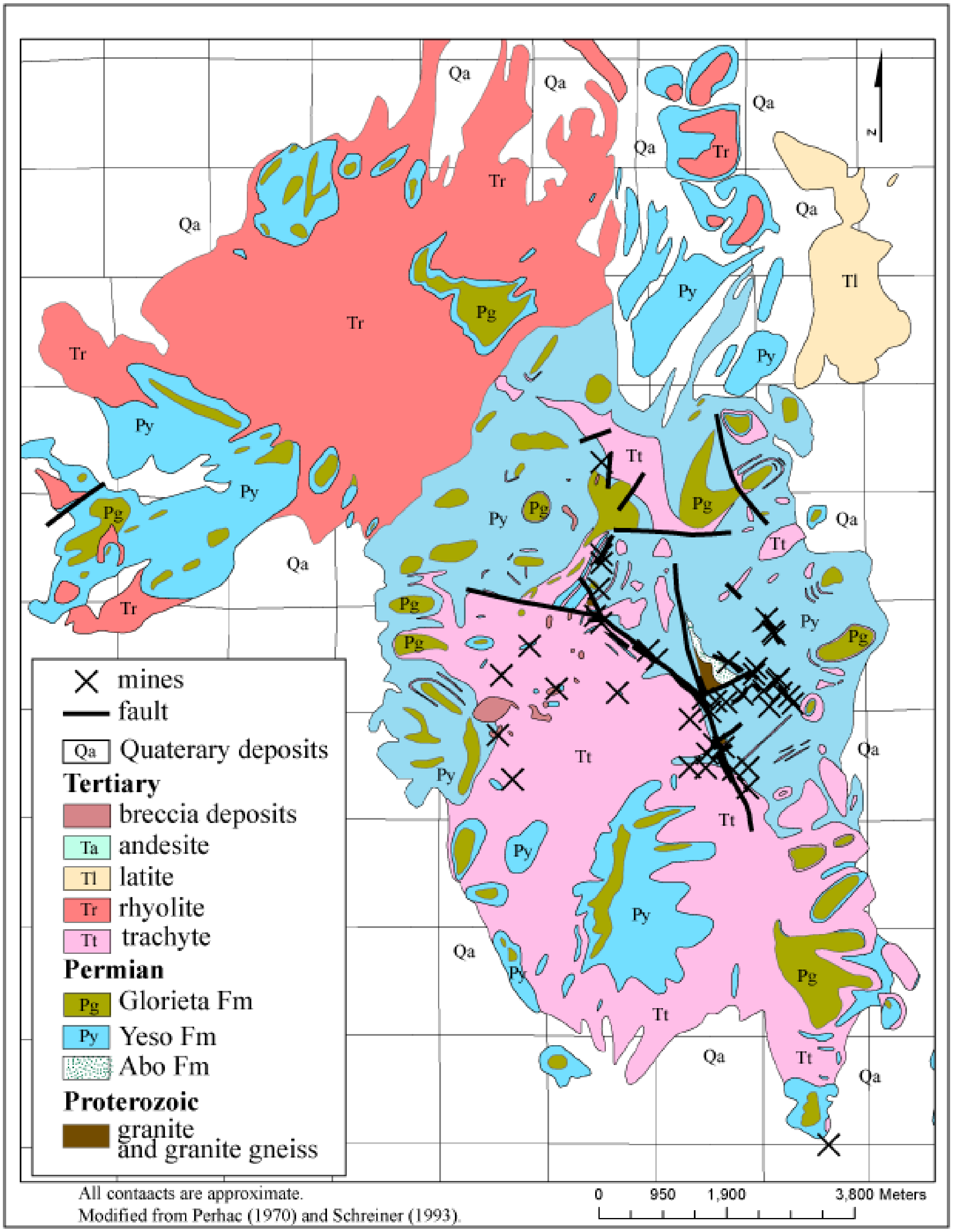


FIGURE 7. Geologic map of the Gallinas Mountains, Lincoln and Torrance Counties, New Mexico (modified from Kelley et al., 1946; Kelley, 1949, 1971; Perhac, 1961, 1970; Woodward and Fulp, 1991; Schreiner, 1993; field reconnaissance by the author).

### Yeso Formation

The Yeso Formation unconformably overlies the Abo Formation and consists of 1500 ft of tan to orange, thinly-bedded sandstone, siltstone, shale, limestone, and dolomite. The gypsum facies, commonly found in the Yeso Formation elsewhere in central New Mexico, is absent in the Gallinas Mountains (Kelley, 1949; Perhac, 1961, 1970).

### Glorieta Sandstone

The more resistant Glorieta Sandstone, is as much as 250 ft thick, overlies the Yeso Formation, and caps many of the mesas and ridges in the Gallinas Mountains. The unit is tan to light gray, massive, medium-bedded, well- to moderately-sorted, locally cross-bedded, quartz sandstone. The quartz sandstone consists predominantly of well- to moderately-rounded quartz grains and few rock fragments cemented by silica and containing few accessory minerals, including feldspar, zircon, apatite, muscovite, and magnetite. The Glorieta Sandstone caps many of the mesas and ridges in the area (Fig. 7).

## Tertiary igneous rocks

The nomenclature of igneous rocks in this report conforms to the International classification proposed by LeMaitre (1989), where the primary classification of igneous rocks is based upon mineralogy and, if too fine-grained to determine mineralogy, by the use of whole-rock geochemical analyses using the TAS (Le Bas et al., 1986) and R1-R2 (de la Roche et al., 1980) diagrams. According to the definition of volcanic and plutonic rocks proposed by LeMaitre (1989), the igneous rocks in the Gallinas Mountains are mostly volcanic (i.e. aphanitic texture) and not plutonic (i.e. coarse-grained rock), except for portions of the trachyte/syenite. Kelley et al. (1946), Poe (1965), Perhac (1961, 1970), and Schreiner (1993) used the volcanic terminology, which is used in this report. Allen and Foord (1991) and Williams-Jones et al. (2000) used the plutonic terminology for these rocks; i.e. syenogabbro, quartz syenite, syenodiorite, and alkali rhyolite. The volcanic rocks are mostly extrusive or shallow intrusive as interpreted from their texture.

The igneous rocks are generally poorly exposed and the contacts are generally covered and not exposed. Cougar Mountain, in the northeastern portion of the Gallinas Mountains, consists of a porphyritic latite stock (Kelley et al., 1946; Poe, 1965; Perhac, 1970). The northern portion of the Gallinas Mountains consists of a rhyolite stock. The southern portion of the Gallinas Mountains consists of porphyritic trachyte (trachytic texture) to syenite (equigranular texture). These igneous rocks have intruded Permian Yeso and Abo Formations. Poe (1965) determined from thermal states of feldspar that the latite is the oldest, followed by the trachyte/syenite, and the youngest is the rhyolite. This requires confirmation by isotopic age dating.

The age of the igneous rocks is mid-Tertiary and likely similar in age to other igneous rocks in the LCPB. A sample of trachyte/syenite has been dated as 29.2 Ma by K-Ar dating methods on feldspar (Perhac, 1970), but Allen and Foord (1991) believed the igneous rocks in the Gallinas Mountains are older than 32 Ma on the basis of chemical data. Additional age dating is required.

### Latite

The latite is in the northern Gallinas Mountains (Fig. 7) and ranges in lithology from latite to trachydacite to trachyandesite, according to the classification by LeMaitre (1989). The latite is light to medium gray, holocrystalline to porphyritic, matrix supported (Fig. 8) and consists of euhedral plagioclase and hornblende phenocrysts in a medium- to fine-grained matrix of plagioclase, orthoclase, hornblende, titanite (sphene), apatite, magnetite, and quartz (Poe, 1965; Perhac, 1961, 1970). The porphyritic texture is produced by large plagioclase and hornblende phenocrysts surrounded by a fine-grained matrix. The nearby Yeso sedimentary rocks are nearly flat lying, suggesting that the latite is a stock. An aeromagnetic high anomaly to the northeast could indicate additional latite in the subsurface (Fig. 6).

FIGURE 8. Photograph of the porphyritic latite (sample GM10-6).

**Trachyte/syenite**

The trachyte/syenite (called syenite by some workers) is found in the southern Gallinas Mountains (Fig. 7) and is associated with the mineral deposits. The trachyte/syenite consists of tan to buff to light gray holocrystalline-porphyritic trachyte with trachytic texture (Fig. 9) to porphyritic-holocrystalline syenite with equigranular texture. It consists of albite and K-feldspar phenocrysts in an aphanitic groundmass consisting of albite, K-feldspar, biotite or hornblende (now altered to hematite and limonite) and trace amounts of apatite, quartz, zircon, and hematite.


FIGURE 9. Photograph of the trachyte (sample GM10-9).

**Rhyolite**

The rhyolite is found in the northwestern Gallinas Mountains (Fig. 7) and is more than 500 ft thick at Gallinas Peak. The rhyolite is tan to pinkish gray to white, fine-grained to aphanitic to porphyritic (Fig. 10) and contains small miarolitic cavities (few millimeters in diameter) containing small crystals of quartz and feldspar. The groundmass consists of orthoclase, quartz, albite, and trace biotite, aegirine-augite, apatite, titanite, magnetite, ilmenite, zircon, and muscovite. Albite phenocrysts form the local porphyritic texture.


FIGURE 10. Photograph of the rhyolite (sample GM10-7).

### Andesite

An altered andesite dike intruded the Yeso sandstone near the Sky High prospect. The andesite is dark gray to dark brown, porphyritic and consists of hornblende, pyroxene, plagioclase, K-feldspar, and trace amounts of sericite, calcite, apatite, and biotite.

### Magmatic-hydrothermal breccia pipes

Several breccia pipes are hosted in the trachyte/syenite and Yeso Formation and consist of angular to subrounded fragments of sandstone, shale, limestone, granite, granitic gneiss, and trachyte/syenite that are as much as 1 m in diameter. The contacts are covered and not exposed, but the pipes appear to be roughly elliptical in shape. Most of the breccia pipes are matrix-supported and are cemented by quartz, feldspar, fluorite, and hematite along with small crystals of other minerals and rock fragments. The matrix locally has a trachytic or porphyritic texture (Schreiner, 1993). Two breccia pipes at the M and E No. 13 prospect are clast-supported. The magmatic-hydrothermal breccia pipes form a north-east-trending belt, approximately 2-3 miles long and 0.5 mile wide (Fig. 7). Most of the breccia pipes are strongly altered and weathered to hematite and locally carbonate. Fenitization of mineralized breccia pipes was identified by Schreiner (1993).

The classification of breccia pipes is primarily based upon the mechanism of brecciation and the involvement of water, magma, or tectonics (Sillitoe, 1985). Schreiner (1993) called these breccia pipes intrusive breccias. Intrusion breccias are formed directly from the subsurface movement of magmas (Sillitoe, 1985). Magmatic-hydrothermal breccias are formed by the release of hydrothermal fluids from the magma chamber and can include magmatic, meteoric, connate, or ocean waters (Sillitoe, 1985). In the Gallinas breccia pipes, the breccia cement consists of hydrothermal minerals not magma and the texture is hydrothermal not magmatic; therefore, magmatic-hydrothermal breccia pipe is a better term (Sillitoe, 1985).

## PETROCHEMISTRY OF THE IGNEOUS ROCKS

The igneous rocks in the Gallinas Mountains are metaluminous to peraluminous, alkaline volcanic rocks (Fig. 11; Frost et al., 2001), and have chemical compositions similar to A-type granitoids (Appendix 3; Whalen et al., 1987). A-type (anorogenic or anhydrous) granitoids typically are found along rift zones and within stable continental blocks and the identification of A-type granitoids is based upon both tectonic setting and chemical characteristics. Many ore deposits are associated with A-type granitoids (Lindgren, 1933; Mutschler et al., 1985, 1991; McLemore, 1996). The trachyte/syenite and latite samples plot within the within-plate granite tectonic field of Pearce et al. (1984; WPG, Fig. 11), whereas the rhyolite sample plots within the volcanic-arc granite field (VAG, Fig. 11). Trachyte/syenite and latite are possibly related, but the rhyolite could be a separate magmatic event (Appendix 3). Detailed dating and geochemical analyses are required to confirm this hypothesis. The geochemical characteristics of the Gallinas Mountains are consistent with a crustal source for the igneous rocks.

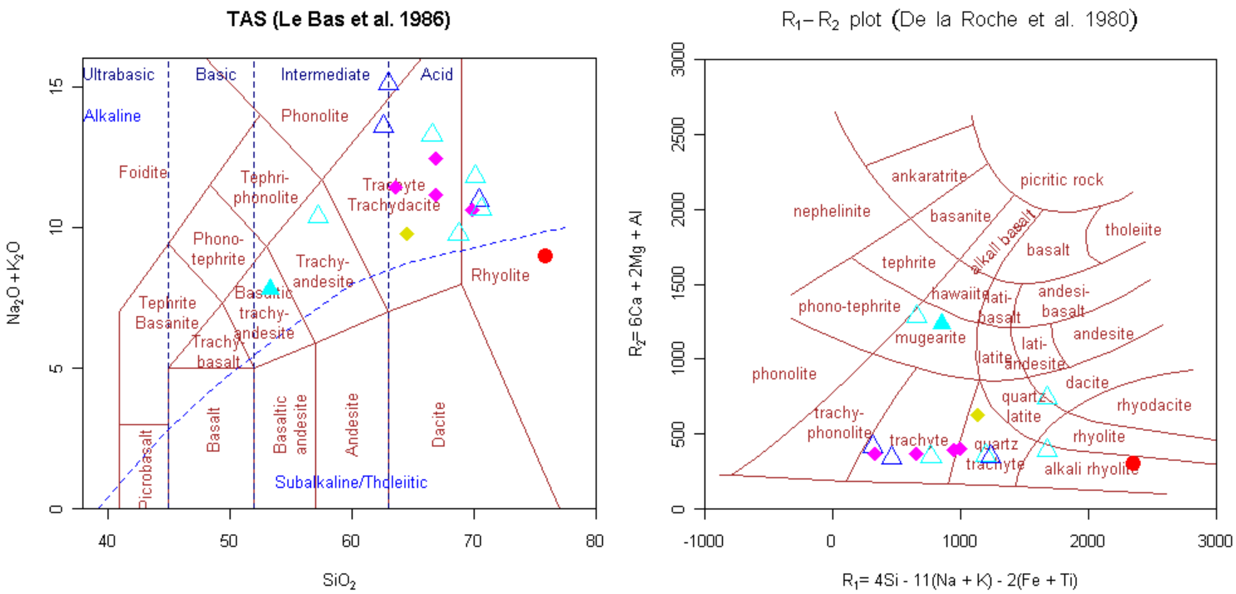


a) Geochemical plots showing the lithology and chemical composition, i.e. alkaline, of the igneous rocks from the Gallinas Mountains. Key is below.

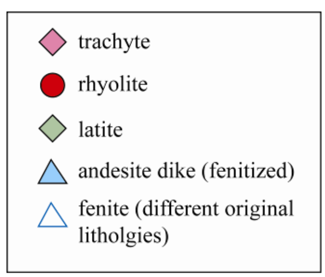


KEY

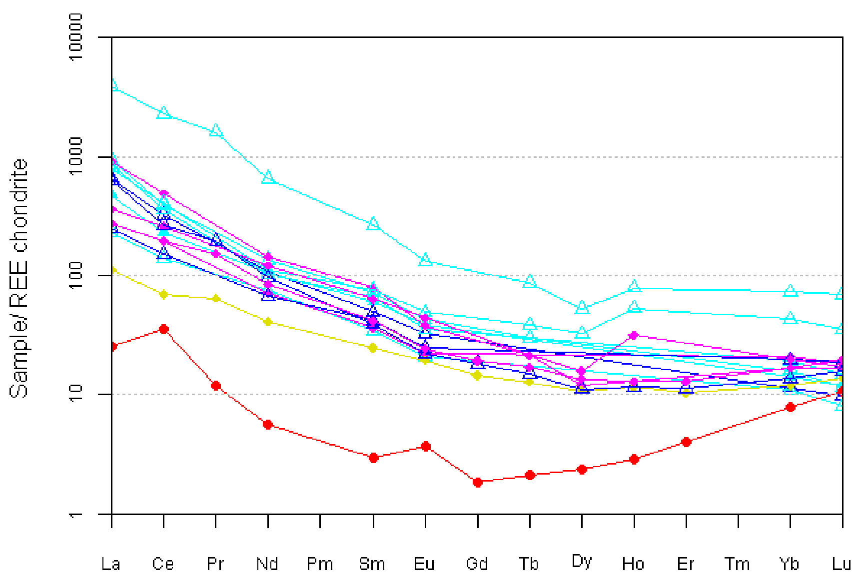


b) Enriched light-REE chondrite-normalized patterns (with no Eu anomaly) of igneous rocks in the Gallinas Mountains. Key is above.

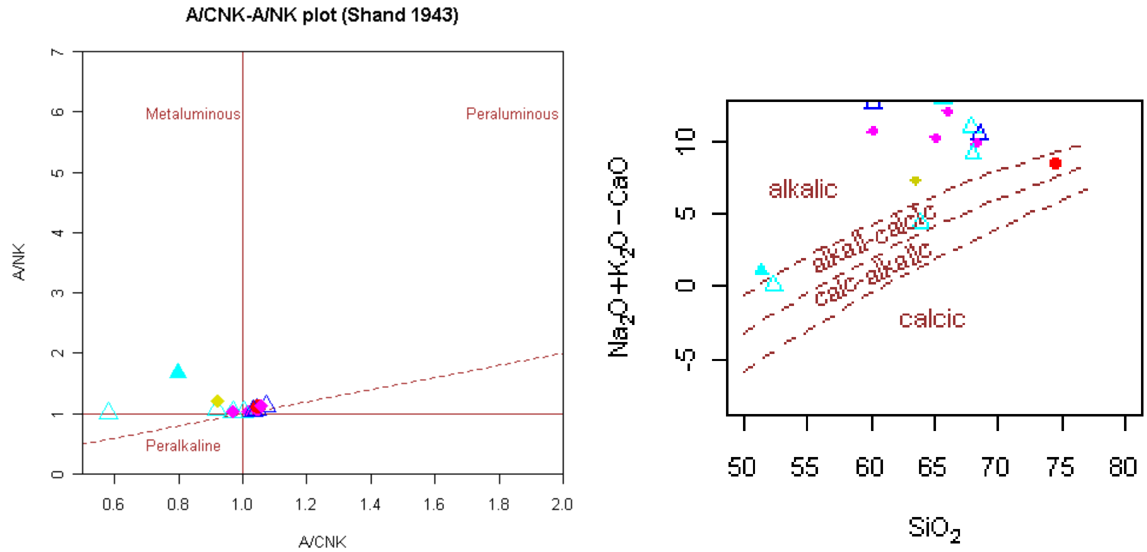


c) Geochemical plots showing the chemical characteristics of the igneous rocks from the Gallinas Mountains, i.e. peraluminous to metaluminous and alkalic to alkalic-calcic. Key is above.

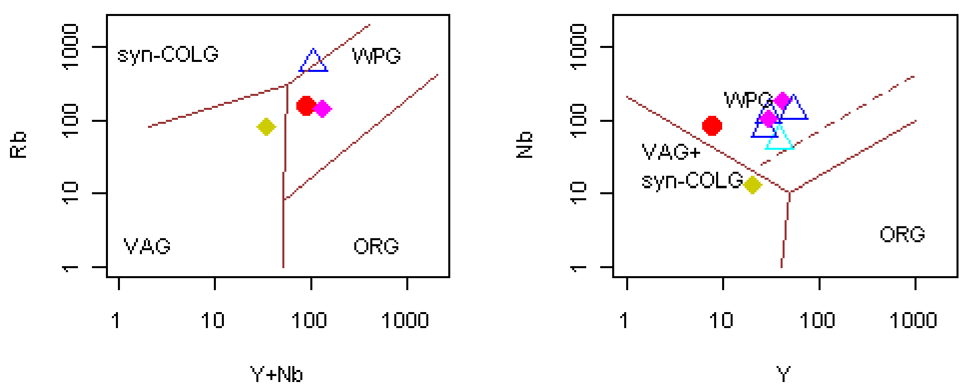


d) Tectonic classification of igneous rocks from the Gallinas Mountains, i.e. within plate granites. Key is above.

FIGURE 11. Geochemical plots characterizing the igneous rocks in the Gallinas Mountains. Additional plots are in Appendix 2. Turquoise triangles are breccia pipes and fenite samples, red circle is rhyolite, pink diamond is latite, blue diamond is trachyte/syenite, and open blue triangle is fenitized trachyte/syenite. Chemical analyses are from Schreiner (1993) and this report. Geochemical plots by Pearce et al. (1984), Le Bas et al. (1986), de la Roche et al. (1980), and Frost et al. (2001).

## DESCRIPTION OF MINERAL DEPOSITS

### Introduction

Four types of deposits have been identified in the Gallinas Mountains (Table 6; Fig. 12; McLemore et al., 1991a), as defined by McLemore (1996) and the U.S. Geological Survey (Cox and Singer, 1983):

1. GPM iron skarn deposits (U.S. Geological Survey classification, iron skarn, 18d)
2. GPM breccia pipe deposits
3. GPM REE-F hydrothermal veins (U.S. Geological Survey classification, thorium-rare-earth veins, 10b)
4. GPM Cu-REE-F (±Pb, Zn, Ag) hydrothermal veins (U.S. Geological Survey classification, thorium-rare-earth veins, 10b)

A fifth type of deposit, carbonatites (Cox and Singer, 1986), could be in the subsurface as suggested by previous drilling, but no samples have been obtained for precise determination of the lithology.

The mineralogy in the Gallinas Mountains is diverse and includes fluorite, quartz, barite, pyrite, iron oxides and accessory bastnaesite, calcite, chalcedony, galena, bornite, chalcocite, pyromorphite, anglesite, chrysocolla, malachite, and azurite and rare agardite (yttrium-arsenic oxide), mimetite, wulfenite, vanadinite, mottramite, cerusite, among others (Table 7; Perhac, 1964, 1968, 1970; Perhac and Heinrich, 1964; McAnulty, 1978; DeMark, 1980). Geothermometric fluid-inclusion studies indicate a temperature of formation of 250-400°C with salinities of approximately 15 NaCl eq. wt% at pressures of 1-2 kbar (Perhac, 1970; Williams-Jones et al., 2000). $Nb_2O_5$ ranges from 8-148 ppm (Moore, 1965; Schreiner, 1993).

The following selected descriptions are from cited references, especially Johnson (1928), Rothrock et al. (1946), Williams (1966), Perhac (1970), Schreiner (1993) and field reconnaissance by the author. More detailed descriptions can be found in Schreiner (1993) and earlier references.

TABLE 6. Mines and prospects in the Gallinas Mountains. Mine identification numbers are from the New Mexico Mines Database (McLemore et al., 2005a, b). Mine locations are shown in Figure 9. UTM are in meters and NAD 27.

| Mine id | Mine name | UTM easting | UTM northing | Type of Deposit | Commodities produced | Commodities present not produced |
|---|---|---|---|---|---|---|
| NMLI0002 | All American | 430160 | 3785872 | REE-F veins | F | U, Th, REE, Cu, Fe |
| NMLI0003 | American | 429093 | 3785541 | Iron skarn | Fe | U, Th, REE |
| NMLI0210 | Big Ben | 430175 | 3786768 | REE-F veins | none | U, Th, REE |
| NMLI0009 | Bottleneck | 432430 | 3785090 | REE-F veins | None | U, Th, REE, F |
| NMLI0302 | Buckhorn | 432736 | 3785671 | Cu-REE-F veins | None | REE, U, Th |
| NMLI0011 | Congress | 432463 | 3785172 | REE-F veins | None | U, Th, REE, F |
| NMLI0328 | Conqueror Apex | 431857 | 3784696 | REE-F veins | None | REE, fluorite |

| Mine id | Mine name | UTM easting | UTM northing | Type of Deposit | Commodities produced | Commodities present not produced |
|---|---|---|---|---|---|---|
| NMLI0318 | Conqueror No. 10 | 432098 | 3783663 | REE-F veins | None | REE, F, Au, fluorite |
| NMLI0315 | Conqueror No. 4 | 432012 | 3784675 | REE-F veins | None | REE, F, Au, fluorite |
| NMLI0319 | Deadwood | 431720 | 3783910 | Cu-REE-F veins | Cu | REE, F, Au, fluorite |
| NMLI0014 | Eagle Nest | 432051 | 3785272 | REE-F veins | None | U, Th, REE, F, Cu, Ag |
| NMLI0317 | Eureka | 432948 | 3784751 | Cu-REE-F veins | None | REE, F, Au, fluorite |
| NMLI0299 | Gallinas | 433468 | 3778071 | REE-F veins | Fe | |
| NMLI0327 | Helen S | 431665 | 3784733 | REE-F veins | None | REE, fluorite |
| NMLI0314 | Hilltop | 432256 | 3784791 | REE-F veins | None | REE, F, Au, fluorite |
| NMLI0316 | Hoosier Boy | 432832 | 3784809 | Cu-REE-F veins | None | REE, F, Au, fluorite |
| NMLI0329 | Hoosier Girl North | 432762 | 3784974 | Cu-REE-F veins | None | REE, fluorite |
| NMLI0021 | Hoosier Girl South | 432566 | 3784839 | REE-F veins | None | F, REE, U, Th |
| NMLI0311 | Iron Box | 430190 | 3788260 | REE-F veins | Fe | |
| NMLI0313 | Iron Lamp | 430390 | 3784833 | Iron skarn | None | Fe, REE |
| NMLI0027 | Last Chance | 432624 | 3785909 | REE-F veins | None | F, Th, REE, U, V |
| NMLI0320 | Little Jack | 431695 | 3783700 | REE-F veins | None | REE, F, Au, fluorite |
| NMLI0029 | Little Wonder | 432716 | 3785718 | Cu-REE-F veins | None | F, Th, U, REE, Cu, V |
| NMLI0301 | M and E No. 13 | 428605 | 3784217 | Breccia pipe | None | REE, U, Th |
| NMLI0323 | North All American | 430073 | 3785979 | Breccia pipe | None | REE, fluorite |
| NMLI0308 | Old Hickory | 432789 | 3785014 | Cu-REE-F veins | F | Cu, Pb, REE |
| NMLI0310 | Park | 430979 | 3785321 | Breccia pipe | None | REE, F, Au |
| NMLI0037 | Pride | 428818 | 3783554 | REE-F veins | None | U, Th, REE |
| NMLI0039 | Rare Metals | 428668 | 3785107 | Iron skarn | None | Fe, U, REE |
| NMLI0040 | Red Cloud | 431825 | 3784047 | Cu-REE-F veins | F, bastnaesite, Cu, Pb, Ag | REE, Th, U, Zn |
| NMLI0330 | Red Cloud fluorite | 431966 | 3784008 | REE-F veins | F | REE |

| Mine id | Mine name | UTM easting | UTM northing | Type of Deposit | Commodities produced | Commodities present not produced |
|---|---|---|---|---|---|---|
| NMLI0042 | Rio Tinto | 432323 | 3783697 | Cu-REE-F veins | F, Cu, Pb, bastnaesite | U, Th, REE |
| NMLI0322 | Seventeen No. 2 | 430856 | 3785452 | Breccia pipe | None | REE, fluorite |
| NMLI0045 | Sky High | 430175 | 3786882 | Breccia pipe | None | F, U, Th, REE |
| NMLI0048 | Summit | 432648 | 3784602 | Cu-REE-F veins | None | F, U, Th, REE |
| NMLI0300 | unknown | 431454 | 3783709 | REE-F veins | None | REE, U, Th |
| NMLI0309 | unknown | 432314 | 3783392 | REE-F veins | None | REE, F |
| NMLI0312 | unknown | 429484 | 3784900 | Iron skarn | None | Fe |
| NMLI0321 | unknown | 430131 | 3786384 | REE-F veins | None | REE, fluorite |
| NMLI0324 | unknown | 431469 | 3784427 | REE-F veins | None | REE, fluorite |
| NMLI0325 | unknown | 431768 | 3784537 | REE-F veins | None | REE, fluorite |
| NMLI0326 | White Oaks | 433003 | 3784642 | Cu-REE-F veins | None | REE, fluorite |

TABLE 7. Minerals found in the Gallinas Mountains (Kelley et al., 1946; Perhac, 1970; Modreski, 1979, 1983; DeMark, 1980; Schreiner, 1993; Modreski and Schreiner, 1993; DeMark and Hlava, 1993; Northrop, 1996; VTM field notes).

| Mineral | Formula | Occurrence |
|---|---|---|
| **All 4 types of mineral deposits** | | |
| quartz | $SiO_2$ | Cement, crystals |
| fluorite | $CaF_2$ | Massive, purple to clear, cementing breccias, 2-3 stages |
| barite | $BaSO_4$ | White bladed crystals |
| calcite | $CaCO_3$ | |
| pyrite | $FeS_2$ | Mostly as pseudomorphs in fluorite matrix, replaced by goethite and hematite |
| **Iron skarn deposits** | | |
| hematite | $Fe_2O_3$ | |
| magnetite | $Fe_3O_4$ | |
| **GPM REE-F and Cu-REE-F vein and breccias deposits** | | |
| bastnaesite | $[Ce, La, (CO_3)]F$ | Yellow hexagonal crystals, inclusions in fluorite |
| agardite | $(Ce,Ca,La)Cu6(AsO_4)_3(OH)_6 \cdot 3H_2O$ | Fluorite matrix, acicular crystals |
| parisite | $Ca(Nd,Ce,La)_2(CO_3)_3F_2$ | |
| xenotime | $(Yb,Y,Er)PO_4$ | |
| monazite | $(Sm,Gd,Ce,Th,Ca)(PO_4)$ | |
| **GPM Cu-REE-F vein deposits** | | |
| mimetite | $Pb_5(AsO_4)_3Cl$ | Trace as prisms with chrysocolla |
| chalcopyrite | $CuFeS_2$ | trace |
| chrysocolla | $CuSiO_3 \cdot H_2O$ | botryoidal crusts and vein fillings |
| conichalcite | $CaCu^{+2}(AsO_4)(OH)$ | Rounded and botryoidal crusts and coatings in |

| Mineral | Formula | Occurrence |
|---|---|---|
| | | brecciated sandstones |
| wulfenite | $(Fe, Mn)WO_4$ | Fracture coatings and small orange tabular crystals |
| tenorite | $CuO$ | trace |
| descloisite | $PbZn(VO_4)(OH)$ | trace |
| vanadinite | $Pb_5(VO_4)_3Cl$ | Prisms typically associated with mottramite |
| mottramite | $(Pb,Bi,Ca)Cu(VO_4)(OH,O)$ | Small black crystals |
| cerussite | $PbCO_3$ | Gray crystals associated with chrysocolla and mimetite, Red Cloud and Buckhorn |
| galena | $PbS$ | trace |
| sphalerite | $(Zn, Fe)S$ | trace |
| bornite | $Cu_5FeS_4$ | trace |
| chalcocite | $Cu_2S$ | trace |
| pyromophite | $Pb_5(PO_4)_3Cl$ | trace |
| anglesite | $PbSO_4$ | trace |
| argentite | $Ag_2S$ | Buckhorn mine |
| malachite | $Cu_2 (CO_3)(OH)_2$ | Trace to minor |
| azurite | $Cu_2(CO_3)_2 (OH)_2$ | Trace to minor |
| linarite | PbCu(SO4)(OH)2 | Buckhorn mine |
| smithsonite | $ZnCO_3$ | trace |
| adamite | Zn2(AsO4)(OH) | Buckhorn mine |
| tennantite | Cu10(Fe,Zn)2As4S13 | Buckhorn mine |
| proustite | Ag3AsS3 | Buckhorn mine |
| covellite | CuS | Buckhorn mine |
| digenite | Cu9S5 | Buckhorn mine |
| shattuckite | Cu5(SiO3)4(OH)2 | Buckhorn mine |
| brochantite | Cu4(SO4)(OH)6 | Buckhorn mine |
| cyanotrichite | Cu4Al2(SO4)(OH)12.2H2O | Buckhorn mine |
| spangolite | Cu6Al(SO4)(OH)12Cl.3H2O | Buckhorn mine |
| cornubite | Cu5(AsO4)2(OH)4 | Buckhorn mine |
| duftite | PbCu(AsO4)(OH) | Buckhorn mine |
| iodargyrite | AgI | Buckhorn mine |
| freibergite | $(Ag,Cu)_6(Cu,Ag)_4(Fe,Zn)2Sb_4S_{12-13}$ | Buckhorn mine |

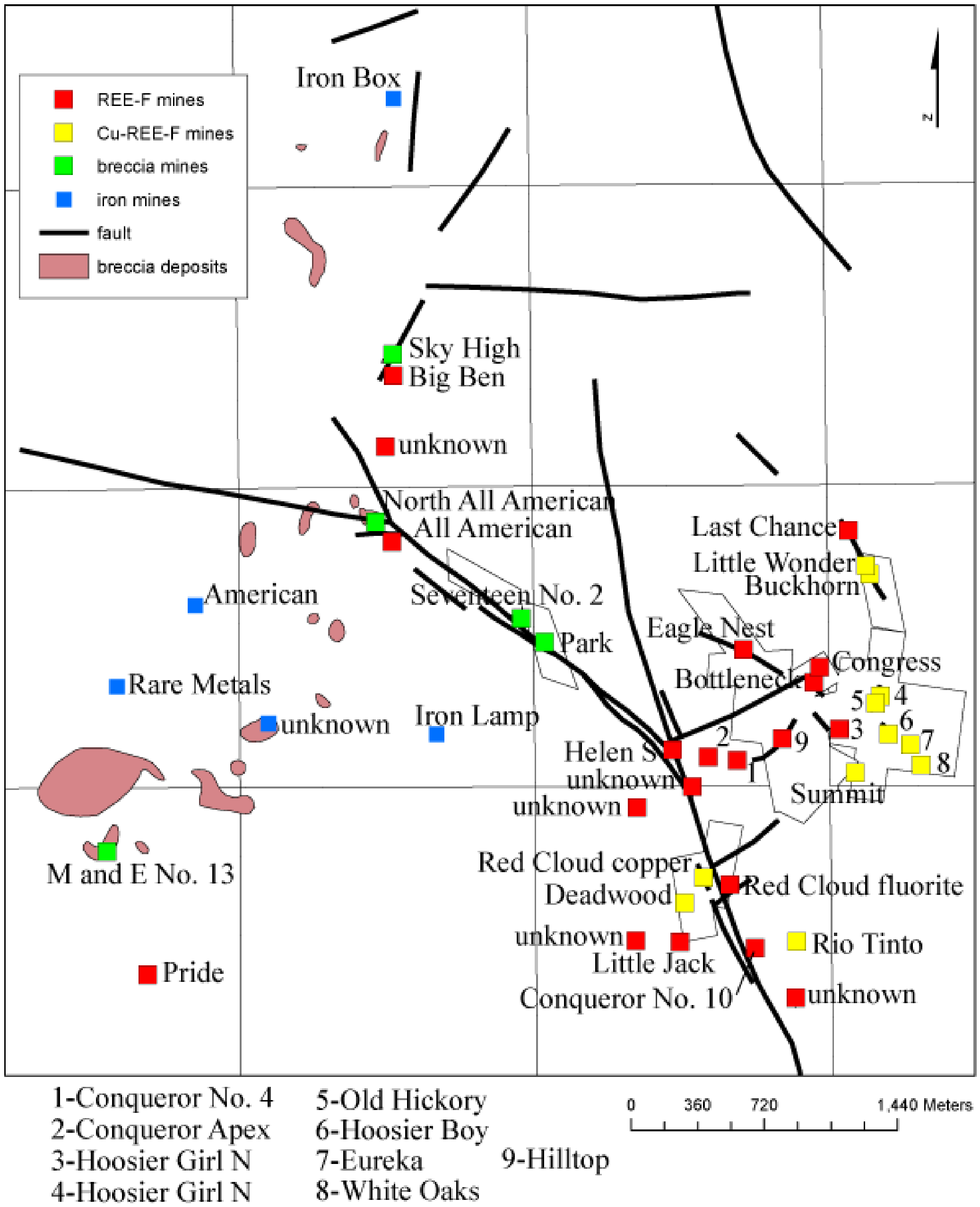


FIGURE 12. Mines and prospects in the Gallinas Mountains, Lincoln County.

### Great Plains Margin-iron skarn (or pyrometasomatic iron) deposits

The GPM iron skarn deposits are found throughout the Gallinas Mountains replacing Yeso limestone, sandstone, and siltstone and are spatially associated with the igneous rocks (Kelley et al., 1946; Kelley, 1949; Harrer and Kelly, 1963). These deposits typically consist of magnetite, hematite, limonite, and martite in a gangue of calcite, quartz, fluorite, tremolite, actinolite, pyrite, fluorite, phlogopite, and locally bastnaesite (Table 7). The iron ore grade is typically less than 50%.

**American (NMLI0003)**

The American (Iron Hammer) mine was mined by the Lincoln Ore and Metals Co. in 1942. In 1943, the mine was leased to A.F. Denison who mined approximately 806 short tons. In 1943, the Mineral Materials Co. continued stripping. Total production from the mine in 1942-1943 is 3,944 short tons of 54.5-56.2% Fe (Kelley, 1949). The deposit was approximately 400 ft long and 5 ft wide and contained magnetite, hematite, epidote, diopside, allanite, and tremolite (Kelley, 1949; Schreiner, 1993). Iron mineralization extended only to the 170 ft crosscut, approximately 65 ft below the main bench. Ore shipments averaged 55.7% Fe and 0.033% P (Kelley, 1949). Sample no. 58 contained 34.2% Fe and 1090 ppm REE; the REE mineral is allanite (Appendix 2; Schreiner, 1993). The iron mineralization replaced limestone and sandstone along the contact with the trachyte/syenite, which is either a roof pendent on top of the trachyte/syenite or a xenolith within the trachyte/syenite.

**Rare Metals (NMLI0039)**

The Rare Metals (Little Marie) mine was prospected by the Lincoln Ore and Metals Co. and the U.S. Bureau of Mines in 1943, but there was no production (Kelley, 1949). The deposit is developed by a 10 ft adit and several pits and trenches. The iron mineralization replaced limestone and consists of magnetite, hematite, fluorite, galena, epidote, tremolite, and phlogopite. Two separate deposits are approximately 350 ft long and 10-15 ft thick and averages 40-50% Fe. Sample 59 contained 47.1% Fe and 209 ppm REE (Appendix 2; Schreiner, 1993) and is slightly radioactive due to U and Th (McLemore, 1983). The iron mineralization replaced either a roof pendent on top of the trachyte/syenite or a xenolith within the trachyte/syenite.

**Gallinas (NMLI0299)**

The Gallinas (Red Cliff) mine was mined by open pit by Dudley Cornell, Paul Teas and Vincent Moore in 1942. Total production from the mine in 1942 was 6410 short tons of 48.7% Fe (Kelley, 1949). The deposit was approximately 125 ft long, 7-10 ft thick, consisted of magnetite, hematite, and gypsum, and replaced limestone and sandstone. Sample 260 contained 44.8% Fe and 216 ppm REE (Appendix 2; Schreiner, 1993).

**Iron Lamp (NMLI0313)**

The Iron Lamp deposit was developed by an 18-ft-deep shaft and trenches, and contained magnetite and hematite (Kelley, 1949; Schreiner, 1993). The deposit is 100 ft long and 2-4 ft thick (Kelley, 1949). Sample no. 96 contained 50.3% Fe and 125 ppm REE (Appendix 2; Schreiner, 1993). The iron mineralization replaced limestone in either a roof pendent on top of the trachyte/syenite or in a xenolith within the trachyte/syenite. There was no reported production.

**Iron Box (NMLI0311)**

The Iron Box deposit is 4-6 ft thick and 100 ft long (Sheridan, 1947). The deposit is in limestone and sandstone and overlain by a trachyte/syenite sill.

**Unknown (NMLI0312)**

A small skarn is found in Yeso limestone in section 23, T1S, R11E and contained magnetite, hematite, diopside, and tremolite (Schreiner, 1993). Sample 61 contained 627 ppm REE (Appendix 2; Schreiner, 1993).

## Great Plains Margin-breccia pipes

Many GPM breccia deposits are circular or oval in plan view and possibly formed by intrusion, gaseous explosions, or collapse (Griswold, 1959). Schreiner (1993) calls the Gallinas breccia pipes intrusive breccias, but they are better described as magmatic-hydrothermal breccias pipes (Sillitoe, 1985). Typical mineralogy is listed in Table 7 and they are described above in the description of igneous rocks.

**Sky High (NMLI0045)**

The Sky High prospect consists of a breccia pipe developed by shafts (up to 100 ft deep), pits, trenches, and road cuts. The breccia consists of angular to subrounded trachyte/syenite, sandstone, and less common granite rock fragments cemented by quartz, hematite, fluorite, barite, and calcite. Chryscolla, malachite, azurite, wulfenite, mimetite, pyrite, and iron and manganese oxides are locally found. Twenty samples ranged from 0.08% to 1.04% REE, less than 254 ppm Y, and minor Au, Ag, and Cu (Appendix 2; Schreiner, 1993).

**M and E No. 13 (NMLI0301)**

The M and E No. 13 (Pinatosa) prospect consists of 2 shafts, 3 pits and a bull dozed area on the edge of the M and E intrusive breccia pipe. The breccia pipe is approximately 350-700 ft long, 150-350 ft wide, clast-supported, and is hosted by trachyte/syenite (Perhac, 1970; Schreiner, 1993; Williams-Jones et al., 2000). Fluorite, barite, quartz, pyrite, bastnaesite, and calcite cement the breccia pipe. Xenotime, monazite, malachite, and azurite are found in vugs locally.

**Seventeen No. 2 (NMLI0322)**

The Seventeen No. 2 prospect consists of a 30-ft adit in a fenitized breccia pipe that consists of angular to subrounded rock fragments of sandstone, siltstone, granite, trachyte/syenite, and limestone. Quartz, calcite, bastnaesite, apatite, and zircon are found. Samples contained as much as 0.06% REE and 23 ppb Au (Appendix 2; Schreiner, 1993).

**Breccia pipes in Sawmill Canyon**

Three small mineralized breccia pipes were mapped in the Sawmill Canyon area in the northern portion of the mineralized area in the Gallinas Mountains by Woodward and Fulp (1991; Fig. 7). The pipes are predominantly composed of trachyte/syenite and Yeso sandstone, silicified, iron-oxide stained, and argillized, and fractured. Gold assays of rock chips range from 10 to 183 ppm Au (Woodward and Fulp, 1991).

## Great Plains Margin REE-F hydrothermal vein deposits

### Cu-REE-F (±Pb, Zn, Ag) hydrothermal vein deposits

The Cu-REE-F (±Pb, Zn, Ag) hydrothermal vein deposits were first developed and mined in the Gallinas Mountains and consist of fissure and fracture filling brecciated hydrothermal veins. Fluorite, barite, and quartz are major minerals along with many copper and lead minerals (Table 7).

*Buckhorn (NMLI0302)*

The Buckhorn consists of an adit, three shafts, and pits along a northwest-trending brecciated vein containing fluorite, barite, quartz, calcite, pyrite and trace amounts of galena, tennantite, argentian tennantite/freibergite, proustite, xeotime, and zircon. Oxidation has produced covellite, digenite, chrysocolla, shattuckite, malachite, azurite, cerusite, brochantite, cyanotrichite, spangolite, adamite, cornubite, dufite, mimetite, iodargyrite, perroudite or capgaronnite (Table 7; Modreski and Schreiner, 1993; DeMark and Hlava, 1993).

*Hoosier Boy (NMLI0316)*

The Hoosier Boy prospect consists of a 30-ft shaft along a brecciated vein, 2-5 ft thick, trending N25°E, and consisting of fluorite, calcite, and hematite.

*Old Hickory (NMLI0308)*

The Old Hickory mine consists of a 200-ft-deep shaft and adit along a brecciated vein, approximately 13 ft thick, 180 ft long, trending N20ºE and consisting of fluorite, calcite, quartz, and trace amounts of galena, malachite, chrysocolla, pyrite and dolomite. The vein pinches out with depth (Rothrock et al., 1946). A sample contained 60.9% $CaF_2$, 25.2% $SiO_2$, 3.6% $CaCO_3$, 0.44% CuO, and 0.14% PbO (NMBMMR files, 1943).

**REE-F hydrothermal vein deposits**

The REE-F hydrothermal vein deposits were developed and mined for fluorite and consist of fissure and fracture filling brecciated hydrothermal veins, similar to the Cu-REE-F (±Pb, Zn, Ag) hydrothermal vein deposits. Fluorite, barite, and quartz are major minerals; only trace amounts, if any, base and precious metals are found (Table 7).

*All American (NMLI0002)*

The All American prospect consists of 2 shafts (85 ft deep), pits, and trenches at the intersection of major faults, striking N30°W, N0°, and N80°W in fractured and brecciated sandstone and trachyte/syenite in Red Cloud Canyon. Fluorite, barite, calcite and trace bastnaesite are found. In the 85-ft level of the shaft, copper oxides in limestone and sandstone are reported by Griswold (1959). In 1949-1951, 129 tons of fluorspar ore was produced (Rothrock et al., 1946). Five samples contained 0.03% to 0.33% REE and trace amounts of Au, Ag, and Cu (Appendix 2; Schreiner, 1993).

*Big Ben (NMLI0210)*

The Big Ben prospect consists of a 100-ft shaft, adit and pits along brecciated veins of fluorite, barite, quartz, and calcite.

*Bottleneck (NMLI0009)*

The Bottleneck prospect consists of a 25-ft shaft, 30-ft adit, and pits along a brecciated vein 2-4 ft thick. Veins of fluorite cut older fluorite-barite matrix (Rothrock et al., 1946).

*Congress (NMLI0011)*

The Congress prospect consists of pits along a N20°E trending brecciated vein that is approximately 4 ft wide.

***Pride (NMLI0037)***

The Pride prospect consists of shafts, pits, and a trench in brecciated fault zone, trending N10°E, in trachyte/syenite. Fluorite, galena, malachite, and chrysocolla are found. Samples contained as much as 2.14% REE, 6.2% Pb, 0.5% Cu, 71 ppb Au and 2.9 ppm Ag (Appendix 2; Schreiner, 1993).

## Potential carbonatite deposits

A fifth type of deposit, carbonatites (Cox and Singer, 1986), could be in the subsurface as suggested by previous drilling, but no samples have been obtained for precise determination of the lithology. Carbonatites are inferred at depth by the presence of fenitization, carbonatization of the breccias, presence of REE, and similarity of the intrusive rocks and mineralization to areas with carbonatites. Carbonatites are carbonate-rich rocks of apparent magmatic derivation (Fig. 13) and typically contain REE, U, Th, Nb, Ta, Zr, Hf, Fe, Ti, V, Cu, apatite, vermiculite, and barite. Some of the world's largest REE deposits are associated with carbonatites, such as Mountain Pass, California and Bayan Obo, Inner Mongolia, China (Castor and Hedrick, 2006).

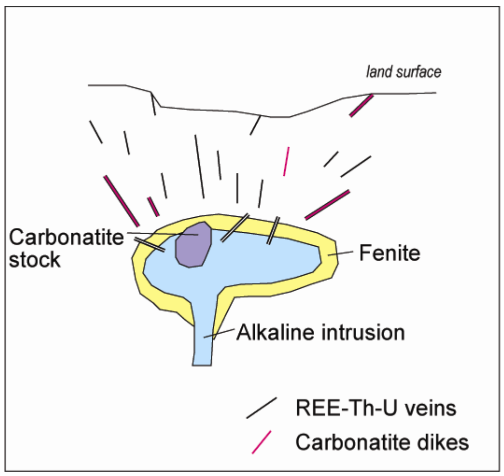


FIGURE 13. Relationship of REE-Th-U veins to alkaline rocks and carbonatites (modified from Staatz, 1992).

## ALTERATION

Schreiner (1993) described the alteration associated with the mineralization in the Gallinas Mountains in detail, which is only summarized in this report. The trachyte/syenite, Proterozoic granite and granitic gneiss, and magmatic-hydrothermal breccia have been altered locally by two separate periods of fenitization; sodic followed by potassic fenitization. Sodic fenitization is characterized by replacement of feldspars and other minerals by albite. Potassic fenitization is characterized by replacement of feldspars, including older albite, and other minerals by K-feldspar. Temperatures ranging from 400 to 700°C are estimated for fenitization (Eckerman, 1966; Kresten and Morgan, 1986; Haggerty and Mariano, 1983; Le Bas, 1987).

## EVALUATION OF THE NURE STREAM-SEDIMENT DATA

### Description

A regional geochemical database, including stream-sediment and water samples, exists for the state of New Mexico that was generated from reconnaissance surveys as part of the U.S. Department of Energy's National Uranium Resource Evaluation (NURE) program during 1974-

1984 (McLemore and Chamberlin, 1986; McLemore, 2010b). Field sampling techniques are detailed in Sharp and Aamodt (1978). The NURE data is typically arranged by 1x2-degree quadrangles, although a few areas were sampled and evaluated in greater detail (Estancia Basin, Grants uranium district, and San Andres and Oscura Mountains area). Total number of stream-sediment samples in the state analyzed was 27,798 and 12,383 water samples were analyzed. Chemical analyses for New Mexico were performed at two national laboratories (Los Alamos and Oak Ridge) and each laboratory utilized different analytical techniques and analyzed sediments for different elements (Hansel and Martell, 1977; Cagle 1977; Aredt et al., 1979). Only the stream sediments were examined for this report.

Some of the NURE data are problematic (Haxel, 2002; McLemore, 2010a, b) and the entire data set should be used with caution. Some of the recognized problems of the NURE data include inconsistent sampling techniques, variability in density of sampling, different size fractions used for analysis, different laboratories and different analytical techniques and analytical errors, and different analytical detection limits. These issues and concerns encountered with the NURE data are described by McLemore (2010b). Normal distributions of geochemical data should not be assumed (Rollinson, 1993) and can be determined by histograms or other statistical methods. However, regional geochemical data such as the NURE data typically are not normal or log-normal distributions, especially if the data consists of large number of samples because the data are characterized by a variety of factors. Methods of evaluating if the validity of NURE data in New Mexico, include examining histograms, comparing the NURE data with average upper crustal values, comparing data for pairs of statistically similar elements, such as Zr-Hf, Th-U, and La-Ce (Haxel, 2002), comparing descriptive statistics and histograms for different laboratories, and examining the descriptive statistics between the 1x2-degree quadrangles. In addition, there are several areas in New Mexico where subsequent stream-sediment surveys have been completed and show similar geochemical patterns as the with the NURE data (Ellinger, 1988; Ellinger and Cepeda, 1991; Watrus, 1998; New Mexico Bureau of Mines and Minerals Resources et al., 1998). Some NURE samples have been re-analyzed by the U.S. Geological Survey and most samples compare well.

The main purposes of the NURE program were to provide an assessment of the nation's uranium resources and to identify areas favorable for uranium mineralization. The NURE data were not designed to reveal uranium or other mineral deposits, but if the NURE data are used with caution, the data can be used to identify areas of potential geochemical interest for further study. Ultimately, field examination of these identified areas must be conducted.

Elemental geochemical patterns in stream-sediment and water samples can be used in environmental studies to detect areas of anomalously high concentrations of elements and perhaps to distinguish between natural background and possible contamination from mining and other anthropogenic inputs (Schreck et al., 2005; McLemore, 2010b), as well as identify areas for potential economic mineral resources. Numerous studies have utilized the NURE data for New Mexico to evaluate mineral resource potential (Laughlin et al., 1985; Bartsch-Winkler and Donatich, 1995; Bartsch-Winkler, 1997; New Mexico Bureau of Mines and Mineral Resources et al., 1998; McLemore et al., 2001). Zumlot (2006) presented an evaluation of the NURE data for the entire state and used slightly different statistical techniques then used in this report and presented much of the data analysis on a web site (https://webspace.utexas.edu/howarifm/www/NURE/1nm.htm/). Different approaches to evaluating the NURE data is another method of validating the data set.

## Methods of study

The NURE data for New Mexico were downloaded from Smith (1997) and the data from samples in the vicinity of the Gallinas Mountains (Fig. 14) were entered in to a spreadsheet. Below detection values (i.e. concentrations of 0 and negative values) were eliminated from the data set to form a processed data set. Statistical analysis was performed on the processed data. The processed NURE data were entered into GIS ArcMap, along with mines from the New Mexico Mines Database (McLemore et al., 2005a, b), and the state geologic map (New Mexico Bureau of Geology and Mineral Resources, 2003). Single element maps were plotted for selected elements using ArcMap. Descriptive statistics, histograms, box plots, scatter plots, and cumulative frequency plots were created using data for the entire state and for the selected area (Table 8). Outliers were identified, located (using search in ArcMap), and determined if they were due to analytical error or atypical abundance (i.e. geochemical anomalies). Since the sample density is not very detailed, single outliers could have geochemical significance.

TABLE 8. Descriptive statistics of processed NURE data for New Mexico using WinStat@. Data are in parts per million (ppm). Upper crustal abundance is from Rudnick and Gao (2005). Note the difference in the mean for Sc, Y, and Hf values and the upper crustal abundance for Sc, Y and Hf which suggests that Sc, Y, and Hf NURE chemical analyses could be problematic. The other elements have mean values similar to the upper crustal abundance and are likely valid chemical analyses.

| | U | Th | La | Ce | Sm | Eu | Dy | Yb | Lu | Y | Hf | Zr | Sc |
|---|---|---|---|---|---|---|---|---|---|---|---|---|---|
| Number of samples | 27351 | 25033 | 24985 | 24952 | 11487 | 11526 | 11516 | 11475 | 11516 | 13495 | 12256 | 18369 | 25008 |
| Mean | 3.35 | 8.11 | 26.62 | 54.47 | 5.03 | 1.17 | 4.62 | 3.97 | 0.45 | 14.23 | 13.70 | 123.96 | 5.87 |
| Variance | 14.25 | 68.11 | 293.22 | 1073.02 | 7.67 | 0.21 | 4.99 | 5.12 | 6.40E-02 | 97.58 | 138.41 | 34518 | 8.55 |
| Standard deviation | 3.78 | 8.25 | 17.12 | 32.78 | 2.77 | 0.45 | 2.23 | 2.26 | 0.25 | 9.88 | 11.76 | 185.79 | 2.92 |
| Minimum | 0.1 | 0.2 | 1 | 1 | 0.1 | 0.1 | 1 | 0.1 | 0.1 | 1 | 0.7 | 1 | 0.1 |
| Maximum | 445.1 | 332.5 | 467 | 722 | 63.6 | 8.1 | 78 | 69.4 | 6.9 | 165 | 261.4 | 4689 | 48.8 |
| 5th Percentile | 1.72 | 1.3 | 3 | 6 | 1.9 | 0.6 | 2 | 1.6 | 0.2 | 1 | 1.6 | 7 | 1.9 |
| 25th Percentile | 2.4 | 4 | 18 | 37 | 3.7 | 0.9 | 4 | 2.9 | 0.3 | 9 | 7.2 | 48 | 4 |
| Median | 2.9 | 7 | 26 | 54 | 4.8 | 1.1 | 4 | 3.7 | 0.4 | 13 | 11.9 | 66 | 5.5 |
| 75th Percentile | 3.59 | 9.9 | 34 | 68 | 5.8 | 1.4 | 5 | 4.5 | 0.5 | 17 | 16.9 | 112 | 7.1 |
| Geometric mean | 3.00 | 6.02 | 21.00 | 42.84 | 4.52 | 1.10 | 4.24 | 3.50 | 0.40 | 10.72 | 10.11 | 68.87 | 5.17 |
| Geometric Standard Deviation | 1.50 | 2.22 | 2.27 | 2.31 | 1.60 | 1.45 | 1.521 | 1.70 | 1.58 | 2.43 | 2.33 | 3.04 | 1.71 |
| Abundance in the upper crust (ppm) | 2.7 | 10.5 | 31 | 63 | 4.7 | 1.0 | 3.9 | 2.0 | 0.31 | 21 | 5.3 | 193 | 14 |

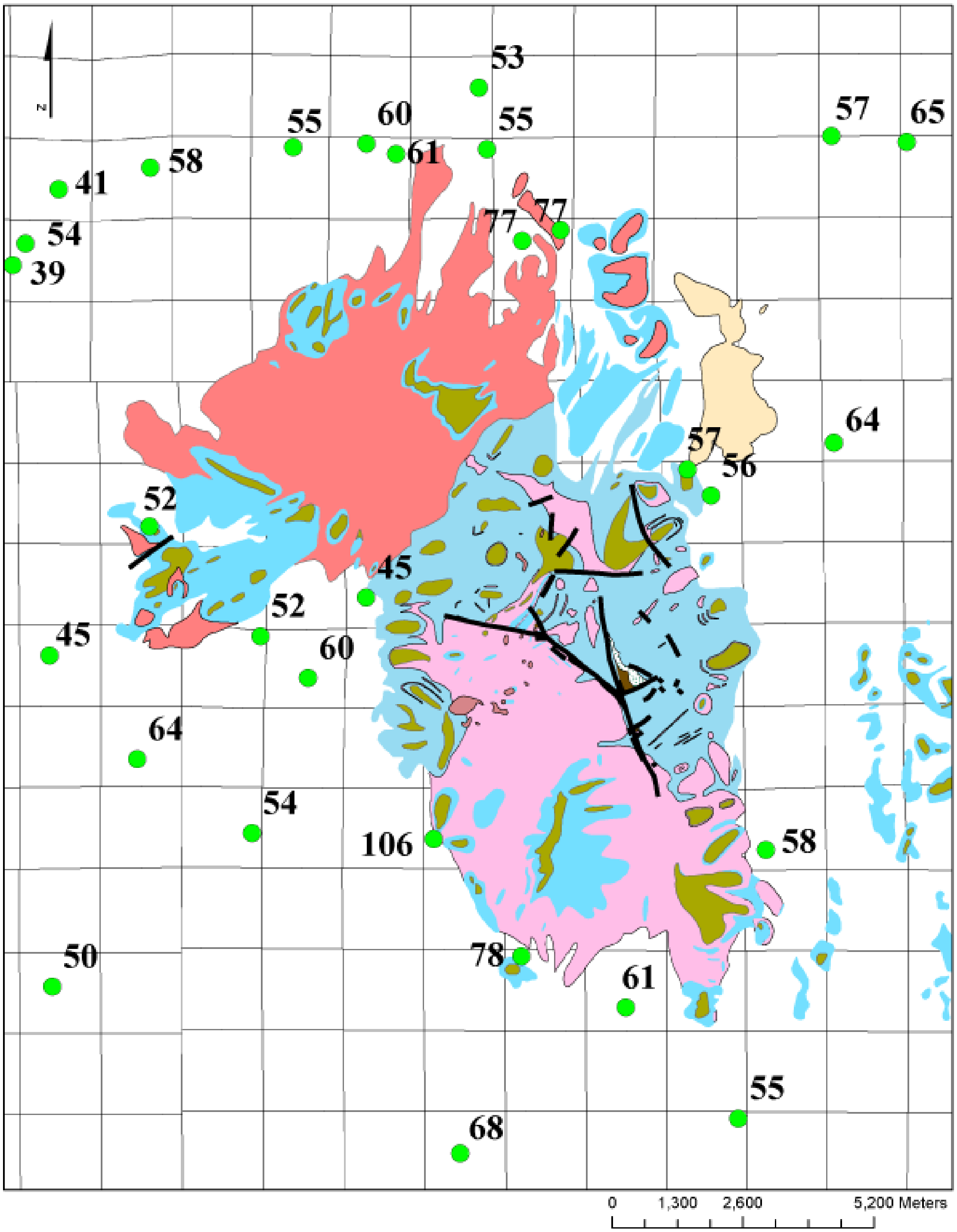


FIGURE 14. Distribution of Ce (in ppm) analyses in the NURE stream-sediment samples in the Gallinas Mountains area (data from Smith, 1997). Green circles are location of NURE samples. Note the high values of 106 and 78 ppm from drainages near the mineralized area in the Gallinas Mountains.

## Geochemical anomaly maps

There are several ways to display geochemical element maps. Point maps of the raw data are used to display absolute concentrations of individual samples (used in this report). Symbols for specific ranges of concentration can be used (Chamberlin, 2009). The point data can be krigged (Laughlin et al, 1985) or contoured. Other techniques can be employed.

Identification of geochemical anomalies (i.e. outliers) and background concentration is not always simple. An orientation or analog study can be performed in a non-mineralized or uncontaminated site to define a local threshold against which anomalies can be judged. Anomalies can be determined by statistical methods such as selecting the upper 2.5% of the data or the mean plus 2σ (standard deviation) as geochemical anomalies (Hawkes and Webb, 1962). However, these statistical methods do not always account for different geochemical processes that form the anomalies nor do they always account for two or more overlapping populations. The geochemical threshold also can be determined by plotting a cumulative frequency plot and the threshold value is at the break in slope (Matschullat et al., 2000). The box plot also can be used to define the upper and lower threshold (Bounessah and Atkin, 2003; Reimann et al., 2005). These later two techniques begin to account for different geochemical processes and for two or more overlapping populations. The data also can be compared to average crustal abundance or other averaged data. Table 9 summarizes the upper threshold for REE and other elements using these techniques.

TABLE 9. Upper concentration thresholds (i.e. outliers) for REE calculated by different methods.

| Method | La ppm | Ce ppm | Sc ppm | Y ppm | U ppm | Th ppm | Reference |
|---|---|---|---|---|---|---|---|
| Upper crustal abundance | 31 | 63 | 14 | 21 | 2.7 | 10.5 | Rudnick and Gao (2005) |
| Mean (entire state) | 29.4 | 61.9 | 6.2 | 15.8 | 3.4 | 9.5 | NURE data |
| Median (entire state) | 27.0 | 58.0 | 6.0 | 13.0 | 2.9 | 8.5 | NURE data |
| Mean + 2σ | 45.6 | 92.6 | 9.1 | 25.6 | 7.4 | 18.0 | Hawkes and Webb (1962) |
| Box plot | 34.0 | 72.0 | 7.6 | 18.0 | 3.6 | 11.0 | Bounessah and Atkin (2003) |
| Cumulative frequency plot | 55 | 100 | 12 | 25 | 7 | 20 | |

## NURE Results in the Gallinas Mountains

Approximately 30 stream-sediment samples were collected and analyzed for the NURE program in the Gallinas Mountains area and only two samples are anomalous for Ce and La (78, 106 ppm Ce, Fig. 15; 63 ppm La). Most samples are within normal crustal abundance for Ce (40-106 ppm), La (18-63 ppm), Y (8-14 ppm), Sc (3-6 ppm), Th (3-13 ppm), and U (2-4 ppm).

## GEOCHEMISTRY OF THE GALLINAS REE DEPOSITS

Another set of geochemical data for this area consists of 279 rock and mineralized samples that were collected and analyzed for various elements by Schreiner (1993) and the author for this report. Geochemical anomaly maps were constructed using ARCMAP@ and indicate that the higher concentrations of REE, Cu, Pb, and Au are found along faults filled with Cu-REE-F and REE-F veins and the M and E breccia deposit (Figs. 15-18). Descriptive statistics are in Table 10.

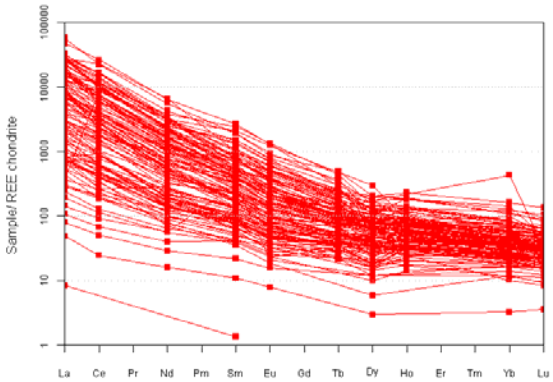


a) REE-F veins (131 samples)

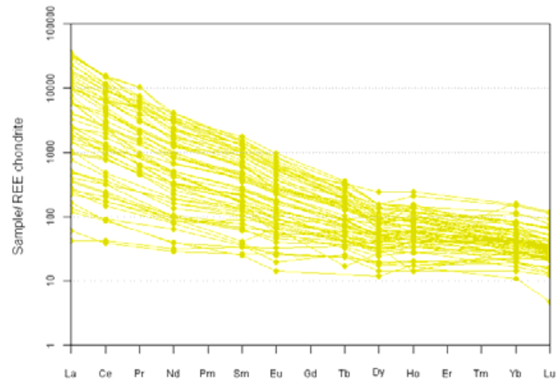


b) Cu-REE-F veins (65 samples)

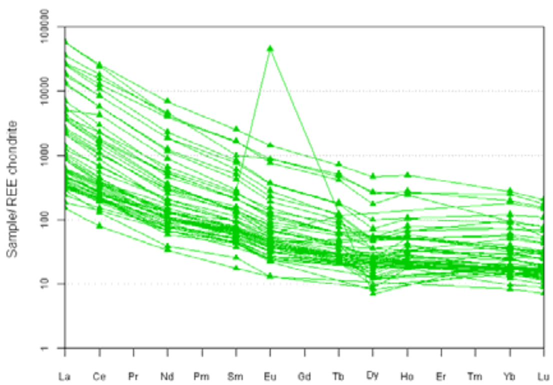


c) Breccia pipe deposits (58 samples)

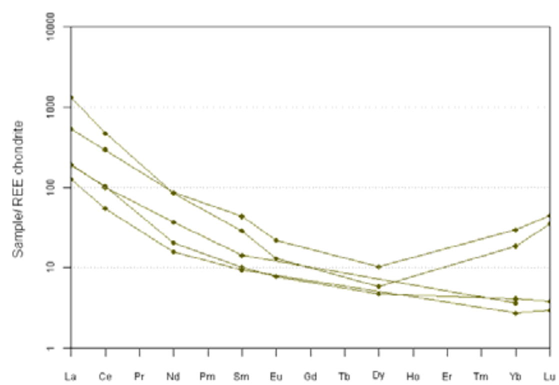


d) iron skarns (6 samples)

FIGURE 15. Chondrite-normalized REE plots of mineralized samples from the Gallinas Mountains. Data from Schreiner (1993) and this report (Appendix 2). Chondrite values from Nakamura (1974). Note the similarity in REE patterns between the different deposit types.

TABLE 10. Descriptive statistics of chemical analyses of samples from the Gallinas Mountains. Chemical analyses are from Schreiner (1993) and this report (Appendix 2).

| | La | Ce | Sm | Eu | Yb | Lu | Y | Total REE | Sc | Th |
|---|---|---|---|---|---|---|---|---|---|---|
| Cases | 273 | 278 | 272 | 270 | 271 | 264 | 273 | 278 | 260 | 266 |
| Mean | 2716.59 | 3367.5 | 75.8733 | 29.4215 | 9.90258 | 1.16511 | 179.608 | 7758.78 | 5.16838 | 37.6868 |
| Std.error | 234.304 | 281.46 | 5.84276 | 12.748 | 0.65587 | 6.40E-02 | 12.9061 | 626.476 | 0.26241 | 2.7719 |
| Std.deviation | 3871.34 | 4692.88 | 96.3612 | 209.471 | 10.797 | 1.03964 | 213.244 | 10445.4 | 4.23127 | 45.2084 |
| Minimum | 2.7 | 21 | 0.27 | 0.6 | 0.6 | 0.1 | 3 | 7 | 0.13 | 1.8 |
| Maximum | 19101 | 22702 | 539 | 3440 | 95 | 7 | 752 | 56697 | 33 | 277 |
| Range | 19098.3 | 22681 | 538.73 | 3439.4 | 94.4 | 6.9 | 749 | 56690 | 32.87 | 275.2 |
| Sum | 7.42E+05 | 9.36E+05 | 20637.5 | 7943.8 | 2683.6 | 307.59 | 49033 | 2.16E+06 | 1343.78 | 10024.7 |
| 10th Percentile | 81.82 | 125.4 | 7.43 | 1.8 | 3.1 | 0.435 | 33.4 | 362.5 | 1.404 | 6.9 |
| 25th Percentile | 167.5 | 257.75 | 13.425 | 3.3 | 4.5 | 0.6 | 55.5 | 707.75 | 2.5625 | 12 |
| Median | 799 | 1130 | 33.45 | 7.3 | 7.3 | 0.92 | 95 | 2683 | 4.275 | 25 |

| | La | Ce | Sm | Eu | Yb | Lu | Y | Total REE | Sc | Th |
|---|---|---|---|---|---|---|---|---|---|---|
| 75th Percentile | 3930 | 5215 | 102.75 | 21.025 | 11 | 1.2975 | 178 | 12171.1 | 6.635 | 47.325 |
| 90th Percentile | 9000 | 9871 | 200 | 46.2 | 18.08 | 2.14 | 725.6 | 23261.1 | 9.332 | 77.09 |
| 95th Percentile | 10360 | 13400 | 295.2 | 65.81 | 26.64 | 3.1 | 735.3 | 31272.3 | 12.95 | 116.5 |
| 99th Percentile | 19100.3 | 22700.2 | 495.75 | 111.29 | 69.952 | 6.9805 | 741 | 51665.9 | 21.673 | 276 |
| Geom. mean | 786.915 | 1101.94 | 35.9083 | 8.39467 | 7.2976 | 0.90952 | 104.758 | 2724.18 | 3.85947 | 23.9027 |
| Geom. Std.Dev. | 6.0954 | 5.33654 | 3.67389 | 3.57712 | 2.10913 | 1.97389 | 2.81045 | 5.04863 | 2.27045 | 2.60099 |

| | U | Au | Ag | Cu | Pb | Zn | Mo | Nb | Fe | Ba |
|---|---|---|---|---|---|---|---|---|---|---|
| Cases | 267 | 263 | 263 | 278 | 278 | 271 | 266 | 27 | 260 | 260 |
| Mean | 18.7326 | 216.205 | 5.5349 | 2122.75 | 5511.6 | 589.173 | 104.132 | 97.1111 | 2.83415 | 5105.25 |
| Std.error | 2.93341 | 19.7947 | 0.45515 | 530.204 | 1824.2 | 96.0582 | 17.9655 | 10.3444 | 0.403 | 501.313 |
| Std.deviation | 47.9323 | 321.016 | 7.38134 | 8840.27 | 30415.5 | 1581.32 | 293.008 | 53.7511 | 6.49827 | 8083.42 |
| Minimum | 1.2 | 5 | 0.2 | 2 | 2 | 2 | 1 | 3 | 5.00E-02 | 2 |
| Maximum | 700 | 1711 | 42 | 89200 | 3.71E+05 | 10202 | 1319 | 184 | 56 | 79000 |
| Range | 698.8 | 1706 | 41.8 | 89198 | 3.71E+05 | 10200 | 1318 | 181 | 55.95 | 78998 |
| Sum | 5001.6 | 56862 | 1455.68 | 5.90E+05 | 1.53E+06 | 1.60E+05 | 27699 | 2622 | 736.88 | 1.33E+06 |
| 10th Percentile | 3.6 | 11 | 0.7 | 8.9 | 18 | 25.2 | 2.7 | 12.2 | 0.651 | 2 |
| 25th Percentile | 5.1 | 21 | 4 | 16.75 | 35.75 | 51 | 5.75 | 57 | 1.0225 | 125 |
| Median | 8.6 | 54 | 4 | 73 | 95 | 113 | 13 | 94 | 1.545 | 2200 |
| 75th Percentile | 17 | 329 | 4 | 438.25 | 503.75 | 323 | 40.25 | 135 | 2.69 | 7250 |
| 90th Percentile | 37.68 | 611 | 9.32 | 4263.7 | 6625.7 | 1144.6 | 182.8 | 182.2 | 4.398 | 15590 |
| 95th Percentile | 69.6 | 611 | 27.86 | 10478.8 | 21440 | 3371.8 | 1196.6 | 183.6 | 4.859 | 18065 |
| 99th Percentile | 195.32 | 1709.36 | 40.36 | 54267 | 2.14E+05 | 10201 | 1317.33 | ****** | 50.3224 | 39458 |
| Geom. mean | 9.92846 | 71.7888 | 3.40207 | 107.592 | 174.628 | 141.048 | 16.9083 | 73.3424 | 1.65995 | 583.646 |
| Geom. Std.Dev. | 2.59338 | 4.72707 | 2.75504 | 10.2459 | 9.60548 | 4.65031 | 5.32604 | 2.64873 | 2.33774 | 29.0815 |

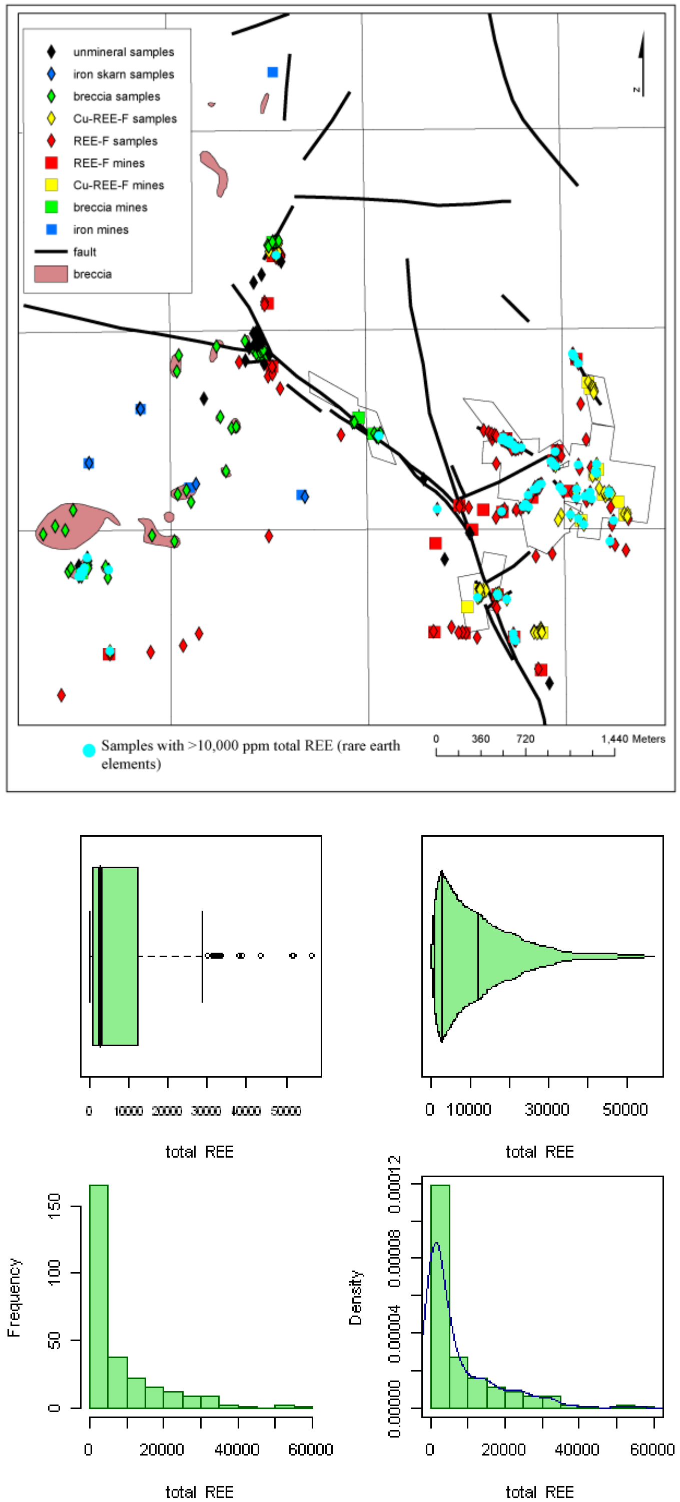


FIGURE 16. Geochemical anomaly map and statistical plots (box plots, histogram, cumulative frequency distribution plot for all samples) of total REE (rare earth elements, ppm) of samples from the Gallinas Mountains. Chemical analyses are from Schreiner (1993) and this report (Appendix 2). Mines identified in Figure 12.

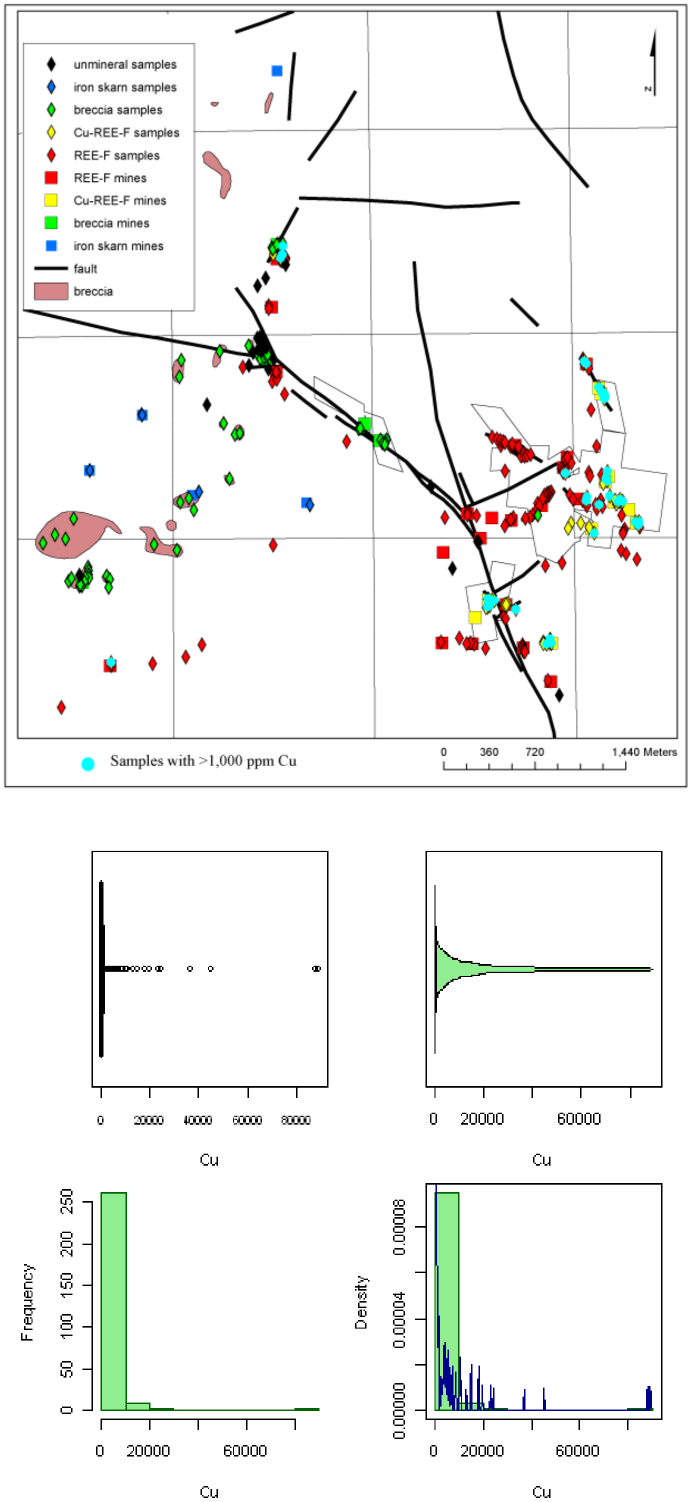


FIGURE 17. Geochemical anomaly map and statistical plots (box plots, histogram, cumulative frequency distribution plot for all samples) of copper (ppm) of samples from the Gallinas Mountains. Chemical analyses are from Schreiner (1993) and this report (Appendix 2). Mines identified in Figure 12.

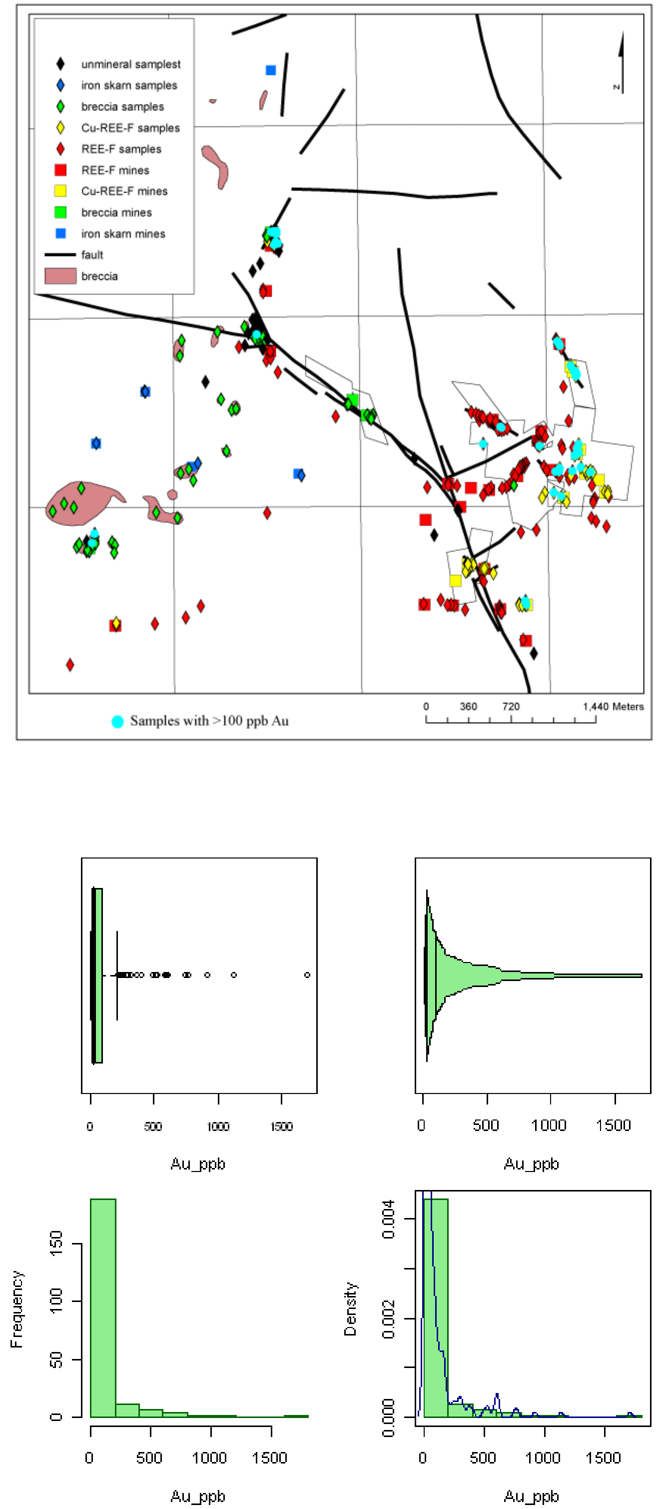


FIGURE 18. Geochemical anomaly map and statistical plots (box plots, histogram, cumulative frequency distribution plot for all samples) of gold (ppb) of samples from the Gallinas Mountains. Chemical analyses are from Schreiner (1993) and this report (Appendix 2). Mines identified in Figure 12.

Trace-element composition of fluorites from the Gallinas Mountains are characterized by relatively flat to LREE-enriched chondrite-normalized REE patterns, with no Eu anomaly (Fig. 19; Gagnon et al., 2003). The earliest generation of fluorite is similar to the composition of the trachyte/syenite. The fluorite samples plot in the hydrothermal and pegmatitic field according to the classification of Möller et al. (1976; Gagnon et al., 2003), which is consistent with a magmatic-hydrothermal origin.

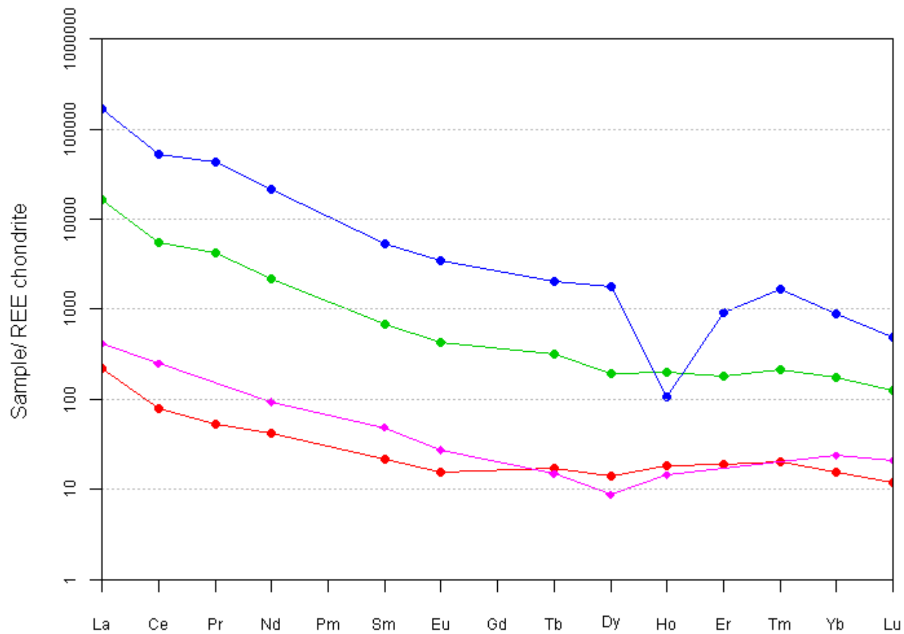


FIGURE 19. Chondrite-normalized REE plot of average fluorite from the Gallinas Mountains (from Gagnon et al., 2003). Red is P1 (1st stage, early), green is P2 (2nd stage), and blue is P3 (3rd stage; late). Purple is trachyte/syenite (Schreiner, 1993).

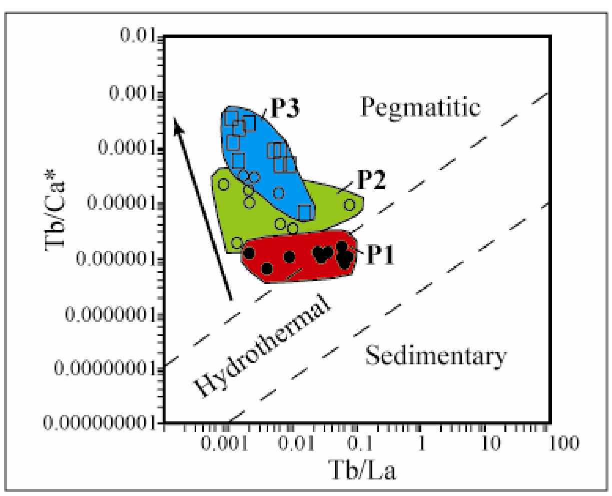


FIGURE 20. Log Tb/Ca verses log Tb/La plot of fluorite samples from the Gallinas Mountains (from Gagnon et al., 2003). Pegmatitic, hydrothermal, and sedimentary fields are from Möller et

al. (1976). The arrow indicates the compositional trend from earliest (P1) to latest (P3). See Gagnon et al. (2003) for more detailed discussion.

## DISCUSSION

### Mineral zonation, sequence of events and paragenesis of the mineral deposits

The mineral zonation for the Gallinas Mountains was determined by mineralogy and chemistry of the individual deposits (Figs. 15-18) and is shown in Figure 21. The sequence of events in the Gallinas Mountains is summarized as:

- Emplacement of the trachyte/syenite about 30 Ma
- Sodic fenitization
- Deposition of the iron skarns
- Faulting and brecciation
- Formation of the magmatic-hydrothermal breccia pipes
- Potassic fenitization
- Additional brecciation
- Deposition of the REE-F and Cu-REE-F veins
- Late stage deposition of quartz and calcite

The paragenesis as determined from petrographic studies by Schreiner (1993), Williams-Jones et al. (2000) and field observations by the author is summarized in Figure 22. A schematic model showing the formation of the deposits in the Gallinas Mountains is shown in Figure 23.

### Relationship of the mineral deposits in the Gallinas Mountains to other REE deposits in New Mexico and elsewhere

The REE deposits in the Gallinas Mountains are among the highest potential for REE in New Mexico. Chemically, samples from the Gallinas Mountains are similar in REE chemistry to Bayan Obo, Lemhi Pass, and Olympic Dam deposits and are different from Capitan deposits (Fig. 24). The Gallinas Mountains deposits are similar in size and grade to small- to medium size deposits found elsewhere in the world (Fig. 25). Estimated resources amount to at least 537,000 short tons of 2.95% total REE (not NI-43-101 compliant; Jackson and Christiansen, 1993; Schreiner, 1993). Drilling is required identify a better resource estimate. However, the Gallinas Mountains has not been extensively drilled and future exploration could identify additional resources.

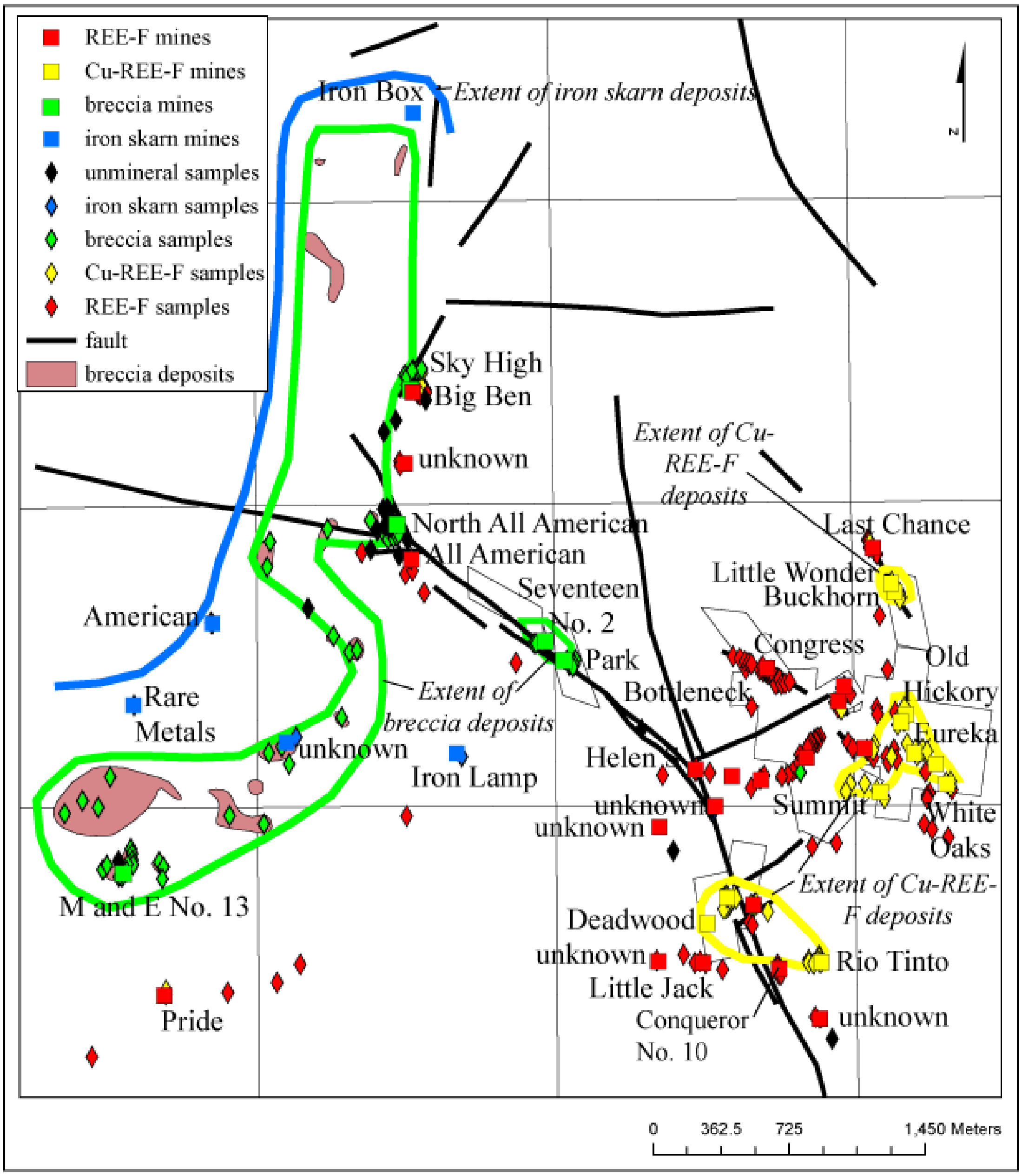


FIGURE 21. Mineral zoning in the Gallinas Mountains, Lincoln County, New Mexico, based upon predominant mineralogy and chemistry of the known deposits.

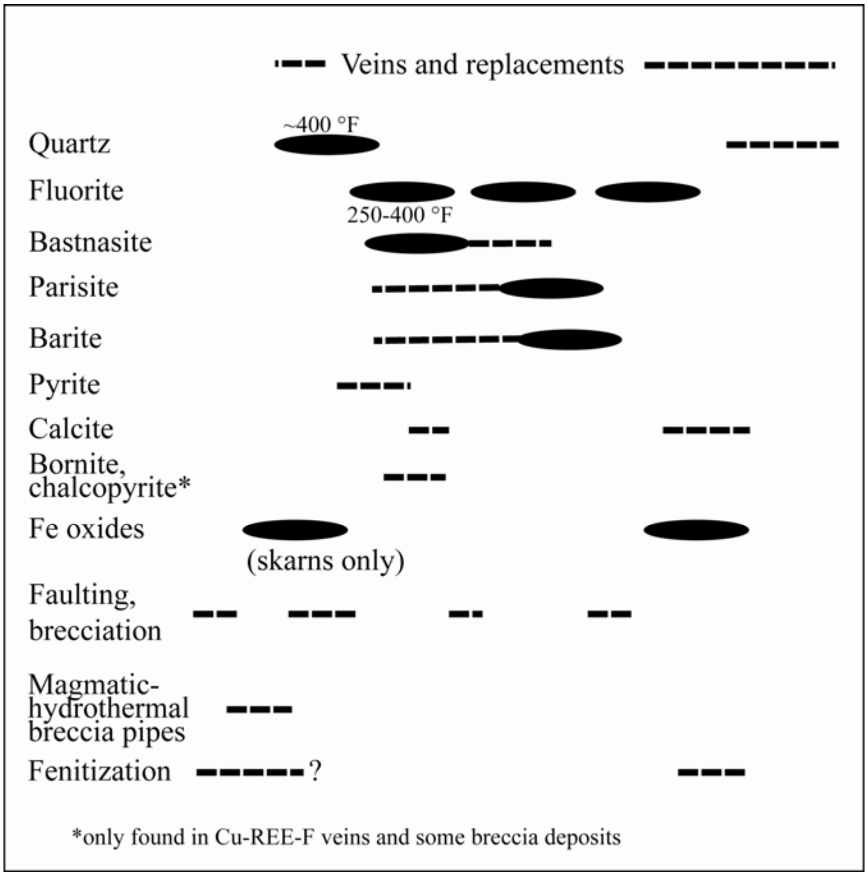


FIGURE 22. Simplified paragenesis of the REE deposits in the Gallinas Mountains (modified from Perhac, 1970, Schreiner, 1993, William-Jones et al., 2000, and field observations by the author). Temperature estimates are from Williams-Jones et al. (2000).

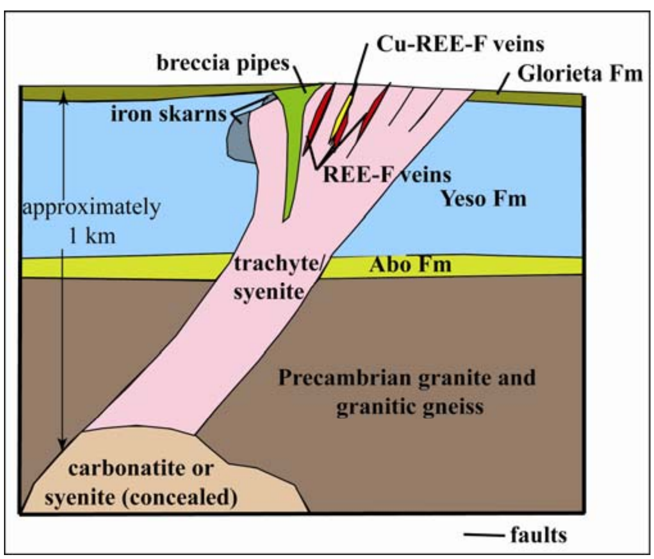


FIGURE 23. Schematic model of formation of the mineral deposits in the Gallinas Mountains, Lincoln County, New Mexico (modified in part from Schreiner, 1993; Richards, 1995; Williams-Jones et al., 2000).

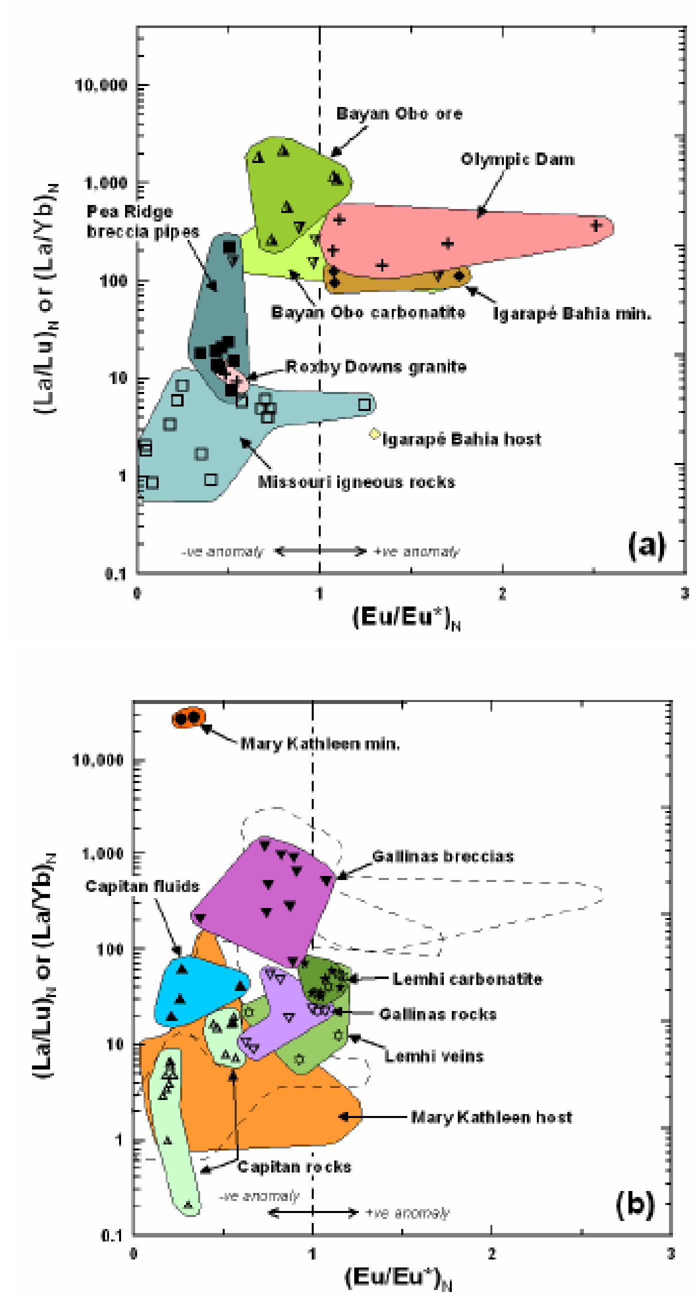


FIGURE 24. Differentiation of different types of REE deposits by La/Lu or La/Yb verses normalized Eu/Eu* (from Samson and Wood, 2005; Castor and Hedrick, 2006; Gillerman, 2008). Samples from Gallinas Mountains are similar in REE chemistry to Bayan Obo, Lemhi Pass, and Olympic Dam deposits and different from Capitan deposits. Note also that there are different compositions within some districts (i.e. Lemhi Mountains, Gallinas, Capitan).

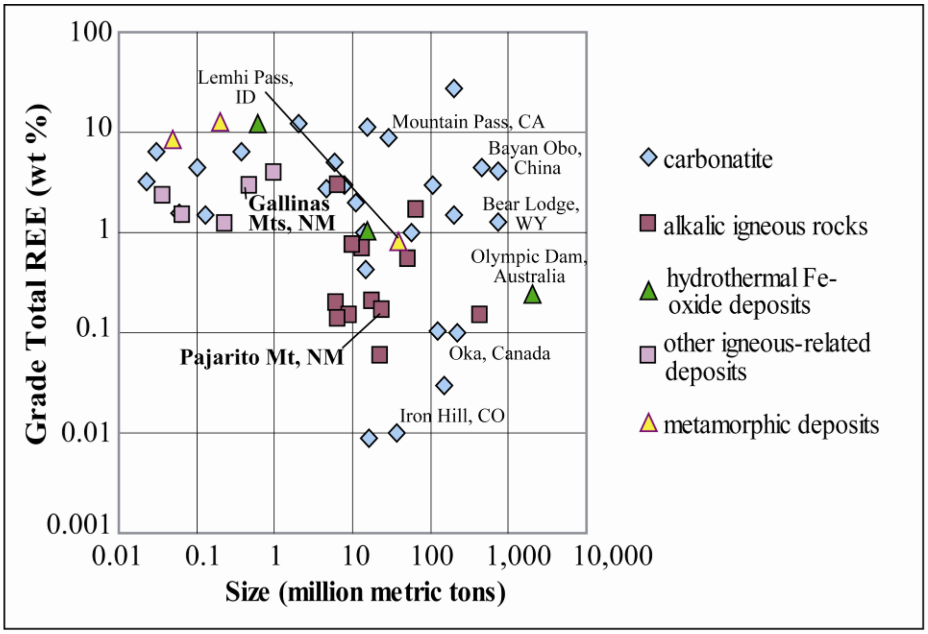


FIGURE 25. Grade and size (tonnage) of selected REE deposits, using data from Oris and Grauch (2002) and resources data from Schreiner (1993) and Jackson and Christiansen (1993) for the Gallinas Mountains. Deposits in bold are located in New Mexico. Additional exploration could identify additional resources in most of these areas.

## PRELIMINARY CONCLUSIONS

- The igneous rocks in the Gallinas Mountains are metaluminous to peraluminous, alkaline volcanic rocks, and have chemical compositions similar to A-type granitoids (Fig. 11, Appendix 3). Trachyte/syenite and latite are possibly related, but the rhyolite could be a separate magmatic event. Detailed dating and geochemical analyses are required to confirm this hypothesis. These data suggest a crustal source for the igneous rocks.
- Resources amount to at least 537,000 short tons of 2.95% total REE (not NI-43-101 compliant; Jackson and Christiansen, 1993; Schreiner, 1993). Drilling is required identify a better resource estimate.
- District zonation is defined by Cu-REE-F (±Pb, Zn, Ag) hydrothermal veins that form center of the district, surrounded by REE-F hydrothermal veins (Fig. 21). The magmatic-hydrothermal breccia pipe deposits form a belt partially surrounding the veins. Iron skarns formed at the top and edge of the trachyte/syenite body and are likely the earliest stage of mineralization. The iron skarns are probably related to the REE-F and REE-F-Cu veins and breccias because they typically contain bastnaesite and fluorite and are similar in trace element geochemistry (Fig. 15).
- Most fenites are more enriched in REE than unaltered igneous rocks (Appendices 1, 2).
- Sequence of events
    - Emplacement of the trachyte/syenite about 30 Ma
    - Sodic fenitization
    - Deposition of the iron skarns
    - Faulting and brecciation
    - Formation of the magmatic-hydrothermal breccia pipes
    - Potassic fenitization

- Additional brecciation
- Deposition of the REE-F and Cu-REE-F veins
- Late stage deposition of quartz and calcite

- The paragenesis is defined by four stages of brecciation and faulting with three stages of fluorite deposition. REE minerals were deposited during the 1st and 2nd stage of fluorite deposition (Fig. 22).
- A genetic model is summarized by intrusion/extrusion of crustal-derived igneous source rock in an extensional terrain possibly related to alkaline-carbonatite complex with mineralization related to mixing of magmatic-hydrothermal and formation fluids (Fig. 23).

## RECOMMENDATIONS FOR FUTURE STUDIES

The most important future research activity needed is the precise dating of the igneous rocks in the Gallinas Mountains to fully understand the temporal relationships and to better delineate the timing of igneous activity and associated mineralization and alteration. Additional detailed outcrop geologic mapping along with geochemical analyses are needed in the Gallinas Mountains to better define the local structural framework and to establish the framework for interpretations of the temporal relationships. Any additional geologic mapping also should be focused on defining the extent of the alteration and defining any alteration zonation. Highly altered areas could be indicative of higher grades of mineralization. Additional geochemical studies, including isotopic studies, of igneous rocks, mineralization, and alteration will aid in a better understanding of the systematics of igneous intrusion and mineralization in the Gallinas Mountains. REE and radiometric isotope analyses are invaluable in differentiating between mantle and crustal sources.

## ACKNOWLEDGEMENTS

This work is part of ongoing research of the economic geology of mineral resources in New Mexico at NMBGMR, Peter Scholle, Director and State Geologist. Mark Mansell and Charles Knowles provided technical assistance. Charles Knowles and Malcomb Bucholtz reviewed an earlier version of this manuscript. This work was funded by the NMBGMR. Some geochemical analyses were funded by Strategic Resources, Inc. (http://www.strategicresourcesinc.ca/, accessed 5/14/2010). Matt Zimmerer provided the geochronology summary. Finally, I would like to thank Russ Schreiner for his prior work in the area and sharing his insights and information over the years.

## REFERENCES

Adams, J.W., 1965, Rare earths; in Mineral and water resources of New Mexico: New Mexico Bureau of Mines and Mineral Resources, Bulletin 87, p. 234-237.

Aldrich, M.J., Jr., Chapin, C.E., and Laughlin, A.W., 1986, Stress history and tectonic development of the Rio Grande Rift, New Mexico: Journal of Geophysical Research, v. 91, no. B6, p. 6199-9211.

Allen, M.S. and Foord, E.E., 1991, Geological, geochemical and isotopic characteristics of the Lincoln County porphyry belt, New Mexico: implications for regional tectonics and mineral deposits: New Mexico Geological Society, Guidebook 42, p. 97-113.

Allen, M.S. and McLemore, V.T., 1991, The geology and petrogenesis of the Capitan pluton, New Mexico: New Mexico Geological Society, Socorro, Guidebook 42, p. 115-127.

Anderson, E.C., 1957, The metal resources of New Mexico and their economic features through 1954: New Mexico Bureau of Mines and Mineral Resources, Bulletin 39, 183 p.

Aredt, J.W., Butz, T.R., Cagle, G.W., Kane, V.E. and Nicols, C.E., 1979, Hydrogeochemical and stream sediment reconnaissance procedures of the National Uranium Resource Evaluation project: Oak Ridge Gaseous Diffusion Plant, Report GJBX-32(80), 56 p.

Bachman, G.O. and Mehnert, H.H., 1978, New K-Ar dates and the late Pliocene to Holocene geomorphic history of the central Rio Grande region, New Mexico: Geological Society of America, Bulletin, v. 89, p. 283-292.

Bartsch-Winkler, S.B., ed., 1997, Geology, mineral and energy resources, Mimbres Resource Area, New Mexico: U.S. Geological Survey, Open-file Report 97-521, CD-ROM

Bartsch-Winkler, S.B. and Donatich, A.J., ed., 1995, Mineral and Energy Resources of the Roswell Resource Area, East-Central New Mexico: U.S. Geological Survey, Bulletin 2063, 145 p.

Bonham, H.F., Jr., 1988, Models for volcanic-hosted epithermal precious metal deposits; *in* Bulk mineable precious metal deposits of the western United States: Geological Society of Nevada, Symposium Proceedings, p. 259-271.

Bounessah, M. and Atkin, B.P., 2003, An application of exploratory data analysis (EDA) as a robust non-parametric technique for geochemical mapping in a semi-arid climate: Applied Geochemistry, v. 18, p. 1185-1195.

Cagle, G.W., 1977, The Oak Ridge analytical program; in Symposium on hydrogeochemical and stream sediment reconnaissance for uranium in the United States: U.S. Department of Energy, Report GJBX-77(77), p. 133-156.

Campbell, A.R., Banks, D.A., Phillips, R.S., and Yardley, B.W.D., 1995, Geochemistry of the Th-U-REE mineralizing fluid, Capitan Mountains, New Mexico, USA: Economic Geology, v. 90, p. 1273-1289.

Campbell, A.R., Heizler, M.T., and Dunbar, N.W., 1994, $^{40}Ar/^{39}Ar$ dating of fluid inclusions in quartz from the Capitan pluton, New Mexico: Proceedings, Pan-American Conference on Research on Fluid Inclusions, v. 5, p. 11.

Castor, S.B. and Hedrick, L.B., 2006, Rare earth elements; in Kogel, J.E, Trivedi, N.C., Barker, J.M., and Krukowski, S.T., ed., Industrial Minerals volume, 7th edition: Society for Mining, Metallurgy, and Exploration, Littleton, Colorado, p. 769-792.

Chamberlin, R.M, 2009, Rare-earth geochemical anomaly at Sierra Larga, New Mexico: NURE stream-sediment data suggest a monazite placer deposit in the Permian Gloria Sandstone: New Mexico Geological Society Guidebook 60, p. 71-73.

Clark, K.F., 1989, Metallogenic provinces and epochs in Mexico: 28th International Geological Congress, Abstracts, v. 1, p. 1-300.

Clark, K.F., Foster, C.T., and Damon, P.E., 1982, Cenozoic mineral deposits and subduction-related magmatic arcs in Mexico: Geological Society of America Bulletin, v. 93, p. 533-544.

Committee on Critical Mineral Impacts of the U.S. Economy, 2008, Minerals, Critical Minerals, and the U.S. Economy: Committee on Earth Resources, National Research Council, ISBN: 0-309-11283-4, 264 p., http://www.nap.edu/catalog/12034.html

Cox, D.P., and Singer, D.A., 1986, Mineral deposit models, U.S. Geological Survey, Bulletin 1693, 379 p.

Dean, R.S., 1944, Bastnaesite at Corona, New Mexico: American Mineralogist, v. 29, p. 157.

De la Roche, H., Leterrier, J., Grandclaude, P. and Marchal, M., 1980, A classification of volcanic and plutonic rocks using R1, R2-diagrams and major element analysis—its relationships with current nomenclature: Chemical Geology, v. 29, p. 183-210.

DeMark, R.S., 1980, The Red Cloud mines, Gallinas Mountains, New Mexico: Mineralogical Record, v. 11, no.2, p. 69-72.

DeMark, R.S. and Hlava, P.F., 1993, Spangolite and other secondary minerals from the Buckhorn mine, Lincoln County, New Mexico (abstr.): New Mexico Geology, v. 15, p. 19.

Douglass, S.E., 1992, Characterization of alkaline rock-hosted precious and base metal mineralization in the Nogal mining district, Lincoln County, New Mexico (M.S. thesis): New Mexico Institute of Mining and Technology, Socorro, 122 p.

Douglass, S.E. and Campbell, A.R., 1995, Characterization of alkaline rock-related mineralization in the Nogal mining district, Lincoln County, New Mexico: Economic Geology, v. 89, p. 1306-1321.

Dunbar, N.W., 1999, Cosmogenic $^{36}$Cl-determined age of the Carrizozo lava flows, north-central New Mexico: New Mexico Geology, v. 21, p. 25-29.

Dunbar, N.W., Campbell, A.R., and Candela, P.A., 1996, Physical, chemical, and mineralogical evidence for magmatic fluid migration within the Capitan pluton, southeastern New Mexico: Geological Society of America Bulletin, v. 108, p. 318-333.

Eaton, G.P., 1980, Geophysical and geological characteristics of the crust of the Basin and Range Province; *in* Burchfield, C., Silver, E., and Oliver, J., eds., Continental tectonics, National Research Council Studies in Geophysics: Washington, D.C., National Academy of Sciences, p. 96-113.

Eckerman, H.V., 1966, Progress of research on the Alno carbonatite; in O.F. Tuttle and J. Gittins, eds., Carbonatites: New York, John Wiley and Sons, p. 3-31.

Ellinger, S., 1988, Stream sediment geochemical survey of the eastern half of the Capitan Mountains, Lincoln County, New Mexico: M.S. thesis, West Texas State University, Canyon, Texas, 108 p. 108.

Ellinger, S. and Cepeda, J.C., 1991, A geochemical survey of ferrous and selected base metals in the eastern half of the Capitan Mountains, Lincoln County, New Mexico: New Mexico Geological Society, Guidebook 42, p. 299-304.

File, L., and Northrop, S.A., 1966, County township, and range locations of New Mexico's mining districts: New Mexico Bureau of Mines and Mineral Resources, Circular 84, 66 p.

Frost, B.D., Barnes, C.G., Collins, W.J., Arculus, R.J., Ellis, D.J., and Frost, C.D., 2001, A geochemical classification for granitic rocks: Journal of Petrology, v. 42, no. 11, p. 2033-2048.

Fulp, M.S. and Woodward, L.A., 1991, Mineral deposits of the New Mexico alkalic province (abstr.): Geological Society of America, Abstracts with Programs, v. 23, p. 23.

Gagnon, J.E., Samson, I.M., Fryer, B.J., and Williams-Jones, A.E., 2003, Compositional heterogeneity in fluorite and the genesis of fluorite deposits: insights from LA-ICP-Ms analysis: Canadian Mineralogist, v. 41, p. 365-382.

Gibbons, T.L., 1981, Geochemical and petrographic investigation of the Jones Camp magnetite ores and associated intrusives, Socorro County, New Mexico (M.S. thesis): Socorro, New Mexico Institute of Mining and Technology, 156 p.

Gillerman, V.S. 2008, Geochronology of Iron Oxide-Copper-Thorium-REE Mineralization in Proterozoic Rocks at Lemhi Pass, Idaho, and a Comparison to Copper-Cobalt Ores, Blackbird Mining District, Idaho: final report, U.S. Geological Survey, Mineral Resources External Research Program, report 06HQGR0170, 148 p., http://minerals.usgs.gov/mrerp/Gillerman-06HQGR0170.pdf

Glass, J.J. and Smalley, R.G., 1945, Bastnaesite {Gallinas Mountains, New Mexico]: American Mineralogist, v. 30, p. 601-615.

Grainger, J.R., 1974, Geology of the White Oaks mining district, Lincoln County, New Mexico (M.S. thesis): Albuquerque, University of New Mexico, 69 p.

Griswold, G.B., 1959, Mineral deposits of Lincoln County, New Mexico: New Mexico Bureau of Mines and Mineral Resources, Bulletin 67, 117 p.

Haggerty, S.E. and Mariano, A.N., 1983, Strontian-loparite and stronio-chevkinite: Two new minerals in rheomorphic fenities from the Parana Basin carbonatites, South America: Contributions to Mineralogy and Petrology, v. 84, p. 365-381.

Hansel, J.M. and Martell, C.J., 1977, Automated energy-dispersive X-ray determination of trace elements in streams: U.S. Department of Energy Report GJBX-52(77), 8 p.

Harrer, C.M. and Kelly, F.J., 1963, Reconnaissance of iron resources in New Mexico, U.S. Bureau Mines, Information Circular 08190, 112 p.

Hawkes, H.E. and Webb, J.S., 1962, Geochemistry in mineral exploration: Harper, New York.

Haxel, G.B., 2002, Geochemical evaluation of the NURE data for the southwest United States (abstr.): Geological Society of America, Abstracts with Programs, v. 34, no. 6, p. 340.

Haxel, G.B., Hedrick, J.B., and Orris, G.J., 2002, Rare earth elements—critical resources for high technology: U.S. Geological Survey, Fact Sheet 087-02, 4 p., http://pubs.usgs.gov/fs/2002/fs087-02/fs087-02.pdf

Hedrick, J.B., 2009, Rare earths (advanced release): U.S. Geological Survey, 2007 Minerals Yearbook, 20 p.

Jackson, W.D. and Christiansen, G., 1993, International strategic minerals inventory summary report—rare-earth oxides: U.S. Geological Survey, Circular 930-N, 76 p.

Johnston, W.D., Jr., 1928, Fluorspar in New Mexico: New Mexico Bureau of Mines and Mineral Resources, Bulletin 4, 128 p.

Jones, F.A., 1904, New Mexico mines and minerals: Santa Fe, New Mexican Printing Company, 349 p.

Kelley, K.D. and Luddington, S., 2002, Cripple Creek and other alkaline-related gold deposits in the southern Rocky Mountains, USA: influence of regional tectonics: Mineralium Deposita, v. 37, p. 38-60.

Kelley, V.C., 1949, Geology and economics of New Mexico iron ore deposits: University of New Mexico, Publications in Geology, no. 2, 246 p.

Kelley, V.C., 1971, Geology of the Pecos country, southeastern New Mexico: New Mexico Bureau Mines Mineral Resources, Memoir 24, 75 p.

Kelley, V.C., Rothrock, H.E., and Smalley, R.G., 1946, Geology and mineral deposits of the Gallinas district, Lincoln County, New Mexico: U.S. Geological Survey, Strategic Minerals Investigation Preliminary Map 3-211, scale 1:62,500.

Kelley, V.C. and Thompson, T.B., 1964, Tectonics and general geology of the Ruidoso—Carrizozo region, central New Mexico: New Mexico Geological Society, Guidebook 15, p. 110-121.

Korzeb, S.L., and Kness, R.F., 1992, Mineral resource investigation of the Roswell Resource Area, Chaves, Curry, De Baca, Guadalupe, Lincoln, Quay, and Roosevelt Counties, New Mexico: U. S. Bureau of Mines, Open-file Report MLA 12-92, 220 p.

Kresten, P. and Morgan, V., 1986, Fenitization at the Fen complex, southern Norway: Lithos, v. 19, p. 27-42.

Kucks, R.P., Hill, P.L., and Heywood, C.E., 2001, New Mexico magnetic and gravity maps and data; a web site for distribution of data: U.S. Geological Survey, Open-file Report 01-0061, http://greenwood.cr.usgs.gov/pub/open-file-reports/ofr-01-0061/ (January 2009).

Laughlin, A.W., Cole, G.L., Freeman, S.H., Aldrich, M.J., and Maassen, L.W., 1985, A computer assisted mineral resource assessment of Socorro and Catron Counties, New Mexico: Geology and Geochemistry Group, Earth and Space Sciences Division, Los Alamos National Laboratory, Los Alamos, New Mexico, unclassified report LA-UR-85-375.

Le Bas, M.J., 1987, Nephelinites and carbonatites; in J.G. Fitton and B.G.J. Upton, eds., Alkaline igneous rocks: Geological Society, Special Publication No. 3, p. 53-83.

Le Bas, M.J., LeMaitre, R.W., Streckusen, A., and Zanettin, B., 1986, A chemical classification of volcanic rocks based on the total alkali-silica diagram: Journal of Petrology, v. 27, p. 745-750.

LeMaitre, R.W., ed., 1989, A classification of igneous rocks and glossary of terms: Blackwell Scientific Publications, Oxford, Great Britain, 193 p.

Lindgren, W., 1915, The igneous history of the Cordilleras and its problems: Yale University, p. 284-286.

Lindgren, W., 1933, Mineral deposits: 4th edition, New York, McGraw-Hill, 930 p.

Lindgren, W., Graton, L.C., and Gordon, C.H., 1910, The ore deposits of New Mexico: U.S. Geological Survey, Professional Paper 68, 361 p.

Marvin, R.F. and Dobson, S.W., 1979, Radiometric ages: Compilation B, U.S. Geological Survey: Isochron/West, no. 26, p. 3-32.

Mason, G.T., Jr. and Arndt, R.E., 1996, Mineral resources data system (MRDS): U.S. Geological Survey, Digital Data Series DDS-20, CD-ROM.

Matschullat, J., Ottenstein, R., and Reimann, C., 2000, Geochemical background—can we calculate it?: Environmental Geology, v. 39, no. 9, p. 990-1000.

Maynard, S.R., Martin, K.W., Nelson, C.J., and Schutz, J.L., 1989, Geology and gold mineralization of the Ortiz Mountains, Santa Fe County, New Mexico: Society of Mining Engineers, Preprint No. 89-43, 9 p.

Maynard, S.R., Nelson, C.J., Martin, K.W., and Schutz, J.L., 1990, Geology and gold mineralization of the Ortiz Mountains, Santa Fe County, New Mexico: Mining Engineering, August, p. 1007-1011.

McAnulty, W.N., 1978, Fluorspar in New Mexico: New Mexico Bureau of Mines and Mineral Resources, Memoir 34, 64 p.

McLemore, V.T., 1983, Uranium and thorium occurrences in New Mexico—distribution, geology, production, and resources; with selected bibliography: New Mexico Bureau of Mines and Mineral Resources, Open file Report 182, 950 p., also; U.S. Department of Energy Report GJBX11 (83).

McLemore, V.T., 1984, Preliminary report on the geology and mineral resource potential of Torrance County, New Mexico: New Mexico Bureau of Mines and Mineral Resources, Open-file Report 192, 202 p.

McLemore, V.T., 1991a, Base-and precious-metal deposits in Lincoln and Otero Counties, New Mexico: New Mexico Geological Society, Guidebook 42, p. 305-309.

McLemore, V.T., 1991b, Gallinas Mountains mining district, New Mexico: New Mexico Geological Society, Guidebook 42, p. 62-63.

McLemore, V.T., 1996, Great Plains margin (alkaline-related) gold deposits in New Mexico; in Coyner, A.R. and Fahey, P.L., eds, Geology and ore deposits of the American Cordillera, Symposium Proceedings: Geological Society of Nevada, Reno, p. 935-950.

McLemore, V.T., 2001, Silver and gold resources in New Mexico: New Mexico Bureau of Mines and Mineral Resources, Resource Map 21, 60 p.

McLemore, V.T., 2010a, Rare earth elements (REE) deposits in New Mexico, including evaluation of the NURE stream sediment data: New Mexico Bureau of Geology and Mineral Resources, Open-file Report, in press.

McLemore, V.T., 2010b, Use of the New Mexico Mines Database and ArcMap in Uranium Reclamation Studies: Society of Mining, Metallurgy and Exploration Annual Convention, Phoenix, Feb 2010, Preprint 10-125

McLemore, V.T. and Chamberlin, R.M., 1986, National Uranium Resource Evaluation (NURE) data available through New Mexico Bureau of Mines and Mineral Resources: New Mexico Bureau of Mines and Mineral Resources, pamphlet, 11 p.

McLemore, V.T., Donahue, K., Breese, M., Jackson, M.L., Arbuckle, J., and, Jones, G., 2001, Mineral-resource assessment of Luna County, New Mexico: New Mexico Bureau of Mines and Mineral Resources, Open file Report 459, 153 pp., CD-ROM, http://geoinfo.nmt.edu/publications/openfile/downloads/OFR400-499/451-475/471/ofr_471.pdf

McLemore, V.T., Hoffman, G., Smith, M., Mansell, M., and Wilks, M., 2005a, Mining districts of New Mexico: New Mexico Bureau of Geology and Mineral Resources, Open-file Report 494, CD-ROM.

McLemore, V. T., Krueger, C. B., Johnson, P., Raugust, J. S., Jones, G.E., Hoffman, G.K. and Wilks, M., 2005b, New Mexico Mines Database: Society of Mining, Exploration, and Metallurgy, Mining Engineering, February, p. 42-47.

McLemore, V.T., North, R.M., and Leppert, S., 1988a, Rare-earth elements (REE), niobium and thorium districts and occurrences in New Mexico: New Mexico Bureau of Mines and Mineral Resources, Open-file Report OF-324, 28 p.

McLemore, V.T., North, R.M., and Leppert, S., 1988b, Rare-earth elements (REE) in New Mexico: New Mexico Geology, v. 10, p. 33-38.

McLemore, V.T., Ouimette, M., and Eveleth, R.W., 1991, Preliminary observations on the mining history, geology, and mineralization of the Jicarilla mining district, Lincoln County, New Mexico: New Mexico Geological Society, Socorro, Guidebook 42, p. 311-316.

McLemore, V.T. and Phillips, R.S., 1991, Geology of mineralization and associated alteration in the Capitan Mountains, Lincoln County, New Mexico: New Mexico Geological Society, Guidebook 42, p. 291-298.

McLemore, V.T. and Zimmerer, M., 2009, Magmatic Activity and Mineralization Along The Capitan, Santa Rita, And Morenci Lineaments In The Chupadera Mesa Area, Central New Mexico: New Mexico Geological Society Guidebook 60, p. 375-386.

Modreski, P.J., 1979, Rare earth elements in agardite and in other minerals from the Red Cloud district, New Mexico (abstr.): New Mexico Minerals Symposium, University of New Mexico, Albuquerque, New Mexico.

Modreski, P.J., 1983, Agardite-(La), a chemically complex rare-earth arsenate from the Gallinas district, Lincoln County, New Mexico (abstr.); in Oxidation mineralogy of base metal deposits: 5th Joint Mineralogical Society of America, Friends of Mineralogy Symposium, Tucson, Arizona.

Modreski, P.J. and Schreiner, R.A., 1993, Silver and copper mineralization at the Buckhorn mine, Gallinas Mountains, New Mexico (abstr.): New Mexico Geology, v. 15, p. 20.

Möller, P., Parekh, P.P. and Schneider, H.J., 1976, The application of Tb/Ca-Tb/La abundance ratios to problems of fluorspar genesis: Mineralium Deposita, v. 11, p. 111-116.

Moore, D.G., Jr., 1965, The niobium and tantalum content of some alkali igneous rocks: M.S. thesis, New Mexico Institute of Mining and Technology, Socorro, 100 p.

Moore, S.L., Thompson, T.B., and Foord, E.E., 1991, Structure and igneous rocks of the Ruidoso region, New Mexico: New Mexico Geological Society, Socorro, Guidebook 42, p. 137-145.

Mutschler, F.E., Griffin, M.E., Stevens, D.S., and Shannon, S.S., Jr., 1985, Precious metal deposits related to alkaline rocks in the North American Cordillera-an interpretive review: Transactions Geological Society of South Africa, v. 88, p. 355-377.

Mutschler, F.E., Mooney, T.C., and Johnson, D.C., 1991, Precious metal deposits related to alkaline igneous rocks-a space-time trip through the Cordillera: Mining Engineering, v. 43, p. 304-309.

Nakamura, N., 1974, Determination of REE, Ba, Fe, Mg, Na and K I carbonaceous and ordinary chondrites: Geochimica et Cosmochimica Acta, v. 38, p. 757-775.

Naumov, A.V., 2008, Review of the world market of rare-earth metals: Russian Journal of Non-ferrous Metals, v. 49, p. 14-22.

New Mexico Bureau of Geology and Mineral Resources, 2003, Geologic map of New Mexico: New Mexico Bureau of Geology and Mineral Resources, scale 1:500,000.

New Mexico Bureau of Mines and Mineral Resources, New Mexico State University Southwest Technology Institute, and TRC Mariah Associates, Inc., 1998, Mineral and energy resource assessment of the McGregor Range (Fort Bliss), Otero County, New Mexico: New Mexico Bureau of Mines and Mineral Resources Open-file report 456, 543 p., http://geoinfo.nmt.edu/publications/openfile/downloads/OFR400-499/451-475/456/ofr-456.pdf

North, R.M., and McLemore, V.T., 1986, Silver and gold occurrences in New Mexico: New Mexico Bureau of Mines and Mineral Resources, Resource Map 15, 32 p., scale 1:1,000,000.

North, R.M., and McLemore, V.T., 1988, A classification of the precious metal deposits of New Mexico; *in* Bulk mineable precious metal deposits of the western United States Symposium Volume: Geological Society of Neva, Reno, Symposium proceedings, p. 625-659.

Northrop, S.A., 1996, Minerals of New Mexico: University of New Mexico Press, Albuquerque, New Mexico, 356 p.

Oris, G.J. and Grauch, R.I., 2002, Rare earth elements mines, deposits, and occurrences: U.S. Geological Survey, Open-file Report 02-189, 174 p.

Pearce, J.A., Harris, N.B.W. and Tindle, A.G., 1984, Trace element discrimination diagrams for the tectonic interpretation of granitic rocks: Journal of Petrology, v. 24, p. 956–983.

Perhac, R.M., 1961, Geology and mineral deposits of the Gallinas Mountains, New Mexico: Unpublished Ph.D. thesis, Ann Arbor, University of Michigan, 224 p.

Perhac, R.M., 1968, Notes on the mineral deposits of the Gallinas Mountains, New Mexico: New Mexico Geological Society, Guidebook 15, p. 152-154.

Perhac, R.M., 1970, Geology and mineral deposits of the Gallinas Mountains, Lincoln and Torrance Counties, New Mexico: New Mexico Bureau of Mines and Mineral Resources, Bulletin 95, 51 p.

Perhac, R.M., and Heinrich, E.W., 1964, Fluorite-bastnaesite deposits of the Gallinas Mountains, New Mexico and bastnaesite paragenesis: Economic Geology, v. 59, p. 226–239.

Phillips, R.S., 1990, Geochemistry of hydrothermal Th-U-REE quartz/fluorite veins from the Capitan pluton (M.S. thesis): Socorro, New Mexico Institute of Mining and Technology, 202 p.

Phillips, R.S., Campbell, A.R., and McLemore, V.T., 1991, Th-U-REE quartz/fluorite veins, Capitan pluton, New Mexico: evidence for a magmatic/hydrothermal origin: New Mexico Geological Society, Guidebook 42, p. 129-136.

Poe, T.I., III, 1965, The intrusive sequence of igneous rocks in the Gallinas Mountains, New Mexico: M.S. thesis, New Mexico Institute of Mining and Technology, Socorro, 41 p.

Porter, E.W. and Ripley, E.M., 1985, Petrologic and stable isotope study of the gold-bearing breccia pipe at the Golden Sunlight deposit, Montana: Economic Geology, v. 80, p. 1689-1706.

Prodehl, C. and Lipman, P.W., 1989, Crustal structure of the Rocky Mountain region; *in* Pakiser, L.C. and Mooney, W.D., eds., Geophysical framework of the continental United States: Boulder, Colorado, Geological Society of America Memoir 172, p. 249-284.

Rawson, D.E., 1957, The geology of the Tecolote Hills area, Lincoln County, New Mexico (M.S. thesis): Albuquerque, University of New Mexico, 77 p.

Reimann, C., Filzmoser, P. and Garrett, R.G., 2005, Background and threshold: critical comparison of methods of determination: Science of the Total Environment, v. 346, p. 1-16.

Richards, J.P., 1995, Alkalic-type epithermal gold deposits—a review; *in* Thompson, J.F.H., ed., Magmas, fluids, and ore deposits: Mineralogical Association of Canada, Short Course Series, v. 23, p. 367-400.

Rollinson, H., 1993, Using geochemical data: evaluation, presentation, interpretation: Pearson Education Ltd., Essex, England, 352 p.

Ronkos, C.J., 1991, Geology, alteration, and gold mineralization in the White Oaks mining district, Lincoln County, New Mexico (abstr.): Geological Society of America, Programs with Abstracts, v. 23, p. 88.

Rothrock, H.E., Johnson, C.H., and Hahn, A.D., 1946, Fluorspar resources of New Mexico: New Mexico Bureau of Mines and Mineral Resources, Bulletin 21, 245 p.

Rudnick, R.L. and Gao, C., 2005, Composition of the continental crust; in R.L. Rudnick, ed., The Crust: Treatise on Geochemistry, v. 3, Elsevier, San Diego, California, p. 1-64.

Salvi, S. and Williams-Jones, A.E., 2005, Alkaline granite-syenite deposits; *in* Linnen, R.L. and Samson, I.M., eds., Rare-element geochemistry and mineral deposits: Geological Association of Canada, GAC Short Course Notes 17, p. 315-341.

Samson, I.M. and Wood, S., 2005, The rare-earth elements: behavior in hydrothermal fluids and concentration in hydrothermal mineral deposits, exclusive of alkaline settings; *in* Linnen, R.L. and Samson, I.M., eds., Rare-element geochemistry and mineral deposits: Geological Association of Canada, GAC Short Course Notes 17, p. 269-297.

Schreck, P., Schubert, M., Freyer, K., Treutler, H. and Weiss, H., 2005, Multi-metal contaminated stream sediment in the Mansfeld mining district: metal provenance and source detection: Geochemistry: Exploration, Environment, Analysis, v. 5, p. 51-57.

Schreiner, R.A., 1993, Mineral investigation of the rare-earth-element-bearing deposits, Red Cloud Mining district, Gallinas Mountains, Lincoln County, New Mexico: U.S. Bureau of Mines, MLA 99-93, 189 p.

Seagerstrom, K. and Ryberg, G.E., 1974, Geology and placer-gold deposits of the Jicarilla Mountains, Lincoln County, New Mexico: U.S. Geological Survey, Bulletin 1308, 25 p..

Sharp, R.R., Jr. and Aamodt, P.L., 1978, Field procedures for the uranium hydrogeochemical and stream sediment reconnaissance by the Los Alamos Scientific Laboratory: U.S. Department of energy, Report GJBZ-68(78), 64 p.

Sheridan, M.J., 1947, Lincoln County iron deposits, New Mexico: U.S. Bureau of Mines, Report of Investigation 3988

Sillitoe, R.H. 1985, Ore-related breccias in volcanoplutonic arcs: Economic Geology, v. 80, p. 1467-1515.

Smith, S.M., 1997, National geochemical database: reformatted data from the National Uranium Resource Evaluation (NURE) Hydrogeochemical and Stream Sediment Reconnaissance (HSSR) Program, version 1.4 (2006): U.S. Geological Survey Open-file Report 97-492. http://pubs.usgs.gov/of/1997/ofr-97-0492/

Soulé, J.H., 1943, Gallinas fluorspar deposits, Lincoln County, New Mexico: U.S. Bureau of Mines, War Minerals Report 125, 14 p.

Soulé, J.H., 1946, Exploration of Gallinas fluorspar deposits, Lincoln County, New Mexico: U.S. Bureau of Mines, Report of Investigations 3854, 25 p.

Staatz, M.H., 1992, Descriptive model of thorium-rare-earth veins; *in* Bliss, J.D., ed., Developments in mineral deposit modeling: U.S. Geological Survey, Bulletin 2004, p. 13-15.

Taylor, S.R., and McClennan, S.M., 1985, The Continental Crust; its composition and evolution: Blackwell Science Publishers, Oxford, 312 p.

Thompson, T.B., 1968, Hydrothermal alteration and mineralization of the Rialto Stock, Lincoln County, New Mexico: Economic Geology, v. 63, p. 943-949.

Thompson, T.B., 1973, Mineral deposits of Nogal and Bonito mining districts, New Mexico: New Mexico Bureau of Mines and Mineral Resources, Circular 123, 29 p.

Thompson, T.B, 1991a, Genesis of gold associated with alkaline igneous rocks (abstr.): Geological Society of America, Abstracts with Programs, v. 23, p. 99-100.

Thompson, T.B., 1991b, The Bonito-Nogal district, Lincoln County, New Mexico (abstr.): Geological Society of America, Abstracts with Programs, v. 23, p. 99.

Thompson, T.B., 1991c, The Lincoln County porphyry belt, New Mexico (abstr.): Geological Society of America, Abstracts with Programs, v. 23, p. 99.

Thompson, T.B., 1992, Mineral deposits of the Cripple Creek district, Colorado: Mining Engineering, v. 44, p. 135-138.

Thompson, T.B., Trippel, A.D., and Dwelley, P.C., 1985, Mineralized veins and breccias of the Cripple Creek district, Colorado: Economic Geology, v. 80, p. 1669-1688.

U.S. Bureau of Mines, 1927-1990, Mineral yearbook: Washington, D.C., U.S. Government Printing Office, variously paginated.

U.S. Bureau of Mines, 1995, MAS/MILS CD-ROM: U.S. Bureau of Mines, Special Publication 12-95, CD-ROM.

U.S. Geological Survey, 1902-1927, Mineral resources of the United States (1901-1923): Washington, D.C., U.S. Government Printing Office, variously paginated.

Van Alstine, R.E., 1976, Continental rifts and lineaments associated with major fluorspar districts: Economic Geology, v. 71, p. 977-987.

Watrus, J.M., 1998, A regional geochemical atlas for part of Socorro County, New Mexico: M.S. thesis, New Mexico Institute of Mining and Technology, Socorro, NM, 176 p., also New Mexico Bureau of Geology and Mineral Resources, Open-file Report OF-445, http://geoinfo.nmt.edu/ publications/openfile/details.cfml?Volume=445

Weber, R.H., 1971, K-Ar ages of Tertiary igneous rocks in central and western New Mexico: Isochron/West, no. 1, p. 33-45.

Whalen, J.B., Currie, K.L., and Chappell, B.W., 1987, A-type granites: geochemical characteristics, discrimination and petrogenesis: Contributions to Mineralogy and Petrology, v. 95, p. 40-418.

Williams-Jones, A.E., Samson, I.M., and Olivo, G.R., 2000, The genesis of hydrothermal fluorite-REE deposits in the Gallinas Mountains, New Mexico: Economic Geology, v. 95, p. 327-342.

Williams, F.E., 1966, Fluorspar deposits of New Mexico: U.S. Bureau of Mines, Information Circular 8307, 143 p.

Woodward, L.A. and Fulp, M.S., 1991, Gold mineralization associated with alkali trachyte breccias in the Gallinas mining district, Lincoln County, New Mexico: New Mexico Geological Society, Guidebook 42, p. 323-325.

Woolley, A.R., 1987, Alkaline rocks and carbonatites of the world, Part 1: North and South America: University of Texas Press, Austin.

Zandra, J.B., Engel, A.L., and Shedd, E.S., 1952, Concentration of bastnaesite and other cerium ores, with analytical methods: U.S. Bureau of Mines, Report of Investigations RI-4919, 15 p.

Zumlot, T.Y., 2006, Environmental evaluation of New Mexico stream sediment chemistry using the National Uranium Resource evaluation (NURE) program: Ph.D. dissertation, University of Texas at El Paso, El Paso, 252 p.

## APPENDIX 1. GEOCHEMICAL ANALYSES OF IGNEOUS ROCKS

TABLE A1-1. Geochemical analyses of igneous rocks from the Gallinas Mountains from Schreiner (1993) and this study. Major elements are in percent and trace elements are in parts per million (ppm). UTM locations are in meters in NAD 27.

| Sample | $SiO_2$ | $TiO_2$ | $Al_2O_3$ | $Fe_2O_3T$ | MnO | MgO | CaO | $Na_2O$ | $K_2O$ |
|---|---|---|---|---|---|---|---|---|---|
| 21 | 51.4 | 1.1 | 18 | 8.17 | 0.18 | 3.77 | 6.45 | 4.84 | 2.64 |
| 23 | 60.2 | 0.36 | 18.7 | 3.11 | 0.17 | 0.15 | 0.38 | 4.6 | 8.46 |
| 29 | 67.9 | 0.16 | 15.5 | 1.19 | 0.03 | 0.08 | 0.41 | 5.16 | 6.25 |
| 36 | 63.9 | 0.34 | 11.7 | 2.63 | 0.34 | 0.17 | 4.7 | 3.17 | 5.88 |
| 38 | 52.4 | 0.73 | 13.2 | 5.08 | 0.46 | 0.32 | 9.42 | 3.86 | 5.62 |
| 54 | 66.1 | 0.2 | 17.7 | 2.11 | 0.09 | 0.06 | 0.16 | 6.75 | 5.52 |
| 72 | 65.6 | 0.28 | 16.8 | 1.86 | 0.52 | 0.06 | 0.16 | 4.01 | 9.08 |
| 85 | 68.5 | 0.23 | 16.3 | 1.04 | 0.13 | 0.05 | 0.21 | 6.62 | 4.03 |
| 95 | 68.34 | 0.28 | 17.01 | 0.84 | 0.16 | 0.05 | 0.55 | 9.41 | 0.98 |
| 239 | 68 | 0.14 | 13.7 | 2.32 | 0.55 | 0.13 | 1.1 | 3.28 | 6.95 |
| 258 | 60.25 | 0.61 | 17.39 | 5.07 | 0.13 | 0.21 | 0.13 | 8.35 | 2.45 |
| GM10-6 | 63.55 | 0.409 | 16.54 | 4.76 | 0.103 | 1.12 | 2.32 | 5.9 | 3.72 |
| GM10-7 | 74.55 | 0.081 | 13.24 | 1.1 | 0.014 | 0.02 | 0.38 | 4.29 | 4.53 |
| GM10-8 | 61.26 | 0.441 | 16.91 | 3.86 | 0.007 | 0.04 | 0.05 | 0.67 | 14.02 |
| GM10-9 | 65.16 | 0.302 | 17.05 | 3.26 | 0.042 | 0.09 | 0.58 | 5.88 | 4.97 |

| Sample | $P_2O_5$ | LOI | total | La | Ce | Pr | Nd | Sm | Eu |
|---|---|---|---|---|---|---|---|---|---|
| 21 | 0.21 | 2.67 | 99.43 | 155 | 200 | | 67 | 12.1 | 3 |
| 23 | 0.18 | 1.34 | 97.65 | 217 | 280 | | 69 | 10 | 2.5 |
| 29 | 0.15 | 0.69 | 97.52 | 76.4 | 120 | | 47 | 7 | 1.6 |
| 36 | 0.26 | 4.63 | 97.72 | 283 | 310 | | 64 | 13.4 | 2.7 |
| 38 | 0.69 | 8.5 | 100.28 | 310 | 340 | | 86 | 14.6 | 3.3 |
| 54 | 0.12 | 0.63 | 99.44 | 91.1 | 170 | | 45 | 7.4 | 1.7 |
| 72 | 0.22 | 1.24 | 99.83 | 1290 | 1960 | 180 | 412 | 54.3 | 10.2 |
| 85 | 0.09 | 0.78 | 97.98 | 83.2 | 130 | | 42 | 8.4 | 1.9 |
| 95 | 0.1 | 0.83 | 98.55 | 297 | 422 | <70 | 91 | 16.1 | 2.9 |
| 239 | 0.25 | 1.84 | 98.26 | 264 | 350 | <50 | 70 | 15.4 | 3.8 |
| 258 | 0.37 | 2.02 | 96.98 | 120 | 225 | <50 | 76 | 12.8 | 3.4 |
| GM10-6 | 0.27 | 0.97 | 99.66 | 36.9 | 60.1 | 7.19 | 25.9 | 5 | 1.48 |
| GM10-7 | 0.03 | 0.35 | 98.59 | 8.3 | 30.7 | 1.32 | 3.5 | 0.6 | 0.28 |
| GM10-8 | 0.14 | 1.1 | 98.5 | 206 | 229 | 21.9 | 60.6 | 7.9 | 1.7 |
| GM10-9 | 0.13 | 1.01 | 98.47 | 90.2 | 168 | 17.2 | 53.7 | 8.4 | 1.87 |

| Sample | Gd | Tb | Dy | Ho | Er | Tm | Yb | Lu | Y |
|---|---|---|---|---|---|---|---|---|---|
| 21 | | <1 | | | | <2 | 3.1 | 0.41 | 33 |
| 23 | | <1 | | | | <2 | 2.5 | 0.33 | 30 |
| 29 | | <1 | | | | <2 | 2.4 | 0.27 | 27 |
| 36 | | 1.4 | | | | <2 | 4.2 | 0.5 | 57 |
| 38 | | 1.4 | | | | <2 | 3.5 | 0.39 | 39 |
| 54 | | <1 | | | | <2 | 4.6 | 0.62 | 42 |
| 72 | <200 | 4.1 | 18 | 5.5 | <100 | 3 | 16 | 2.36 | 187 |
| 85 | | <1 | | | | <2 | 4.3 | 0.63 | 54 |
| 95 | <200 | 1 | 5.4 | 2.2 | <100 | <2 | 4.3 | 0.58 | 52 |

| Sample | Gd | Tb | Dy | Ho | Er | Tm | Yb | Lu | Y |
|---|---|---|---|---|---|---|---|---|---|
| 239 | <200 | 1.8 | 11.1 | 3.7 | <100 | <2 | 9.4 | 1.2 | 90 |
| 258 | <200 | 1 | 4.1 | <1 | <100 | <2 | 3.7 | 0.56 | 47 |
| GM10-6 | 4 | 0.6 | 3.7 | 0.8 | 2.3 | 0.36 | 2.6 | 0.46 | 21 |
| GM10-7 | 0.5 | 0.1 | 0.8 | 0.2 | 0.9 | 0.18 | 1.7 | 0.36 | 8 |
| GM10-8 | 5 | 0.7 | 3.8 | 0.8 | 2.5 | 0.41 | 3 | 0.53 | 27 |
| GM10-9 | 5.3 | 0.8 | 4.6 | 0.9 | 2.9 | 0.49 | 3.7 | 0.67 | 30 |

| Sample | Sc | Th | U | Au | Ag | Cu | Pb | Zn | Mo |
|---|---|---|---|---|---|---|---|---|---|
| 21 | 14.9 | 30 | 6.8 | <5 | <0.2 | 50 | 32 | 83 | 2 |
| 23 | 1 | 71.3 | 6.4 | 12 | <0.2 | 17 | 17 | 51 | <1 |
| 29 | 0.62 | 274 | 8.8 | <5 | <0.2 | 9 | 10 | 15 | 1 |
| 36 | 4.5 | 23 | 3.1 | 165 | <0.2 | 193 | 16 | 108 | 7 |
| 38 | 17.7 | 25 | 4.7 | 73 | <0.2 | 47 | 28 | 144 | 3 |
| 54 | 0.63 | 63.4 | 10 | 9 | <0.2 | 4 | 8 | 30 | 3 |
| 72 | 1.9 | 49 | 9.8 | 27 | <0.2 | 9 | 36 | 37 | 20 |
| 85 | 0.94 | 50.5 | 3.8 | <5 | <0.2 | 2 | 3 | 11 | 2 |
| 95 | 1.44 | 43.1 | 3.7 | 10 | <0.2 | 29 | 28 | 35 | 1 |
| 239 | 4.39 | 11.7 | 6.4 | 28 | 0.2 | 167 | 1057 | 148 | 5 |
| 258 | 8.37 | 33 | 6.1 | 94 | <0.2 | 10 | 6 | 30 | 2 |
| GM10-6 | 7 | | | | 0.7 | 10 | | 70 | < 2 |
| GM10-7 | < 1 | | | | < 0.5 | < 10 | | 90 | 3 |
| GM10-8 | 5 | | | | 1.7 | 10 | | 190 | 20 |
| GM10-9 | 2 | | | | 1.4 | < 10 | | < 30 | < 2 |

| Sample | Nb | Ni | Co | Ba | Cr | Sr | F | UTM E | UTM N |
|---|---|---|---|---|---|---|---|---|---|
| 21 | | 14 | 18 | 3700 | 16 | 1431 | | 432693.3007 | 3784760.697 |
| 23 | 118 | 1 | 4 | 1800 | 18 | 749 | | 432710.8095 | 3784792.531 |
| 29 | | 3 | 2 | 1800 | 28 | 508 | | 432503.8882 | 3784840.282 |
| 36 | | 19 | 10 | 1600 | 44 | 329 | 395 | 432223.7487 | 3784808.448 |
| 38 | 52 | 21 | 16 | 2800 | 41 | 1104 | 867 | 432269.9081 | 3784856.199 |
| 54 | 181 | 2 | 2 | 430 | 19 | 107 | 140 | 431907 | 3785324.159 |
| 72 | | 5 | 3 | 3300 | 28 | 352 | | 432145.7553 | 3785188.865 |
| 85 | 135 | 3 | 2 | 770 | 17 | 247 | 602 | 431014.8512 | 3785288.983 |
| 95 | | 3 | 2 | 1700 | 20 | 802 | | 430057.4107 | 3786085.98 |
| 239 | | 12 | 4 | 2600 | 40 | 267 | | 432301.8679 | 3784879.461 |
| 258 | | 7 | 8 | 1900 | 22 | 96 | | 432762.7246 | 3785632.565 |
| GM10-6 | 13 | < 20 | 6 | 2360 | 20 | 1134 | | 433776 | 3791906 |
| GM10-7 | 82 | < 20 | < 1 | 327 | < 20 | 77 | | 427451 | 3789638 |
| GM10-8 | 76 | < 20 | 3 | 2072 | < 20 | 755 | | 430001 | 3785737 |
| GM10-9 | 104 | < 20 | 3 | 1554 | < 20 | 491 | | 431629 | 3784695 |

## APPENDIX 2. SELECTED GEOCHEMICAL ANALYSES OF ORE SAMPLES

TABLE A2-1. Geochemical analyses of ore samples from the Gallinas Mountains from Schreiner (1993) and this study. Trace elements are in parts per million (ppm). UTM locations are in meters in NAD 27. opt=ounces per ton.

| Sample | Description | UTM E | UTM N |
|---|---|---|---|
| 21 | fragments of fenitized andesite porphyry dike | 430244.619 | 3786723.96 |
| 22 | fenitized trachyte dike | 430083.547 | 3786618.12 |
| 23 | fenitized syenite | 430020.269 | 3786554.84 |
| 26 | fenitized and fractured trachyte dike | 430012.588 | 3786142.01 |
| 27 | fenitized trachyte dike | 430032.962 | 3786148.12 |
| 28 | fenitized trachyte dike | 430048.242 | 3786128.76 |
| 29 | fenitized gneiss | 430057.411 | 3786085.98 |
| 30 | fragments of fenitized gneiss in tree roots | 430018.7 | 3786052.36 |
| 32 | variably fenitized banded gneiss | 429978.972 | 3786026.9 |
| 33 | fragments of fenitized gneiss in tree roots | 430040.093 | 3786040.14 |
| 34 | fenitized gneiss | 430084.915 | 3786068.66 |
| 42 | fenitized sandstone | 430140.943 | 3785971.89 |
| 47 | outcrop of brecciated sandstone | 429944.336 | 3785925.03 |
| 48 | fractured sandstone with minor breccia | 430097.14 | 3785895.48 |
| 54 | outcrop of trachyte | 429606.131 | 3785618.4 |
| 85 | fragments of fenitized trachyte in tree roots | 428581.33 | 3784275.77 |
| 104 | fragments of fractured sandstone from dump | 431378.555 | 3784950.11 |
| 259 | fractured sandstone | 432379.748 | 3783285.52 |
| GM-09-LC-1 | brecciated sandstone | 431744 | 3784512 |
| GM-09-LC-4 | brecciated sandstone | 431542 | 3784300 |
| 153 | brecciated sandstone | 432694.454 | 3785257 |
| 258 | trachyte dike | 432289.252 | 3783403.17 |
| 10 | brecciated sandstone | 430202.05 | 3786809.1 |
| 11 | fractured sandstone | 430199.749 | 3786795.3 |
| 13 | intrusive breccia | 430236.565 | 3786786.09 |
| 14 | intrusive breccia | 430245.769 | 3786775.74 |
| 15 | intrusive breccia | 430244.619 | 3786761.93 |
| 16 | brecciated limestone bed | 430214.706 | 3786787.24 |
| 17 | brecciated limestone bed | 430202.05 | 3786757.33 |
| 18 | intrusive breccia | 430218.157 | 3786749.28 |
| 19 | intrusive breccia | 430234.264 | 3786742.37 |
| 24 | brecciated trachyte dike in contact with brecciated limestone | 430104.257 | 3786397.22 |
| 25 | brecciated limestone in contact with brecciated sandstone and trachyte dike (sample 24) | 430104.257 | 3786375.36 |
| 46 | brecciated zone in trachyte | 429895.439 | 3785911.78 |
| 49 | fragments of brecciated sandstone and trachyte from dump | 430165.392 | 3785872.05 |
| 50 | fragments of brecciated sandstone from dump | 430154.186 | 3785843.53 |
| 51 | fragments of brecciated trachyte from dump | 430127.7 | 3785794.63 |
| 52 | fragments of brecciated sandstone from dump | 430165.392 | 3785810.93 |
| 53 | fragments of brecciated sandstone from dump | 430225.367 | 3785693.91 |
| 90 | fragments of brecciated trachyte from dump | 428826.834 | 3783556.57 |
| 91 | fragment of brecciated sandstone in float | 428429.866 | 3783228.64 |

| Sample | Description | UTM E | UTM N |
|---|---|---|---|
| 92 | outcrop of fractured trachyte with minor breccia | 429155.871 | 3783567.78 |
| 93 | outcrop of brecciated zone in trachyte | 429419.975 | 3783617.88 |
| 94 | outcrop of brecciated zone in trachyte | 429546.573 | 3783714.24 |
| 95 | fragments of trachyte from dump | 430121.111 | 3784499.66 |
| 105 | brecciated trachyte | 431666.653 | 3784743.19 |
| 106 | fractured and altered trachyte | 431665.061 | 3784722.5 |
| 107 | brecciated trachyte sandstone contact | 431739.871 | 3784716.13 |
| 108 | brecciated zone in sandstone | 431967.485 | 3785067.9 |
| 109 | brecciated zone in sandstone | 431936.438 | 3785267.43 |
| 110 | brecciated sandstone | 431868.799 | 3785338.48 |
| 111 | brecciated sandstone | 431907 | 3785324.16 |
| 112 | brecciated sandstone | 431932.467 | 3785309.83 |
| 113 | brecciated sandstone | 431954.751 | 3785301.88 |
| 114 | brecciated sandstone | 431969.076 | 3785293.92 |
| 115 | brecciated sandstone | 432013.644 | 3785262.08 |
| 116 | brecciated sandstone | 432031.153 | 3785254.12 |
| 117 | brecciated sandstone | 432045.478 | 3785247.76 |
| 118 | brecciated sandstone | 432058.212 | 3785239.8 |
| 119 | brecciated sandstone | 432069.354 | 3785235.02 |
| 120 | brecciated sandstone | 432077.312 | 3785230.25 |
| 121 | brecciated sandstone | 432088.454 | 3785225.47 |
| 122 | brecciated sandstone | 432104.371 | 3785219.11 |
| 123 | brecciated sandstone | 432115.513 | 3785211.15 |
| 124 | brecciated sandstone | 432117.105 | 3785207.97 |
| 125 | brecciated sandstone | 432110.738 | 3785201.6 |
| 126 | brecciated sandstone | 432105.963 | 3785190.46 |
| 127 | fractured sandstone | 432094.821 | 3785185.68 |
| 128 | brecciated sandstone | 432125.063 | 3785203.19 |
| 129 | fractured sandstone | 432117.105 | 3785209.56 |
| 130 | brecciated sandstone | 432126.655 | 3785184.09 |
| 131 | brecciated sandstone | 432145.755 | 3785188.86 |
| 132 | brecciated sandstone | 432027.174 | 3785282.62 |
| 133 | brecciated sandstone | 432075.561 | 3785258.42 |
| 134 | brecciated sandstone | 432172.337 | 3785196.03 |
| 135 | brecciated sandstone | 432594.004 | 3785952.59 |
| 136 | brecciated sandstone | 432600.196 | 3785943.31 |
| 138 | brecciated sandstone | 432613.353 | 3785923.96 |
| 140 | brecciated sandstone | 432624.188 | 3785902.29 |
| 141 | brecciated sandstone | 432629.606 | 3785893 |
| 142 | brecciated sandstone | 432635.797 | 3785882.94 |
| 143 | brecciated sandstone | 432640.441 | 3785874.42 |
| 144 | brecciated sandstone | 432602.517 | 3785912.35 |
| 152 | fractured sandstone with minor breccia | 432655.222 | 3785547.28 |
| 154 | brecciated limestone bed | 432446.109 | 3785160.37 |
| 155 | brecciated limestone bed | 432475.397 | 3785137.45 |
| 156 | brecciated zone in sandstone | 432493.224 | 3785127.27 |
| 157 | fragments of brecciated sandstone and limestone from dump | 432410.998 | 3785083.98 |

| Sample | Description | UTM E | UTM N |
|---|---|---|---|
| 158 | brecciated sandstone-limestone contact | 432424.57 | 3785070.41 |
| 159 | brecciated sandstone | 432429.094 | 3785054.12 |
| 161 | brecciated zone in sandstone | 432631.97 | 3785051.45 |
| 162 | fragments of brecciated sandstone from dump | 432639.528 | 3785021.22 |
| 163 | fragments of brecciated sandstone from dump | 432732.625 | 3785030.8 |
| 178 | brecciated sandstone | 432723.543 | 3784830.73 |
| 180 | brecciated sandstone | 432683.751 | 3784795.71 |
| 181 | brecciated sandstone | 432736.277 | 3784776.61 |
| 182 | fragments of brecciated limestone | 432693.301 | 3784760.7 |
| 185 | fractured sandstone with minor breccia | 432580.29 | 3784827.55 |
| 186 | brecciated sandstone | 432613.716 | 3784784.57 |
| 187 | brecciated sandstone | 432480.013 | 3784872.12 |
| 188 | brecciated sandstone | 432503.888 | 3784840.28 |
| 189 | fluorite, barite, quartz rich zone | 432331.984 | 3784899.17 |
| 190 | brecciated sandstone | 432317.659 | 3784894.4 |
| 191 | brecciated sandstone | 432301.742 | 3784888.03 |
| 192 | brecciated sandstone | 432314.476 | 3784870.52 |
| 193 | brecciated sandstone | 432301.868 | 3784879.46 |
| 194 | brecciated sandstone | 432293.784 | 3784859.38 |
| 195 | brecciated sandstone | 432287.008 | 3784863.98 |
| 196 | brecciated sandstone | 432279.458 | 3784873.71 |
| 197 | brecciated sandstone | 432269.908 | 3784856.2 |
| 198 | brecciated sandstone | 432260.358 | 3784841.87 |
| 199 | brecciated sandstone | 432223.749 | 3784808.45 |
| 200 | fragments of brecciated sandstone from dump | 432236.482 | 3784789.35 |
| 201 | brecciated sandstone | 432201.465 | 3784736.82 |
| 202 | brecciated sandstone | 432182.364 | 3784716.13 |
| 203 | brecciated sandstone | 432158.489 | 3784700.21 |
| 204 | brecciated sandstone | 432125.063 | 3784692.25 |
| 205 | brecciated sandstone | 432029.561 | 3784698.62 |
| 206 | brecciated sandstone and conglomeratic sandstone | 432008.869 | 3784679.52 |
| 207 | brecciated sandstone | 431961.118 | 3784631.77 |
| 213 | brecciated sandstone | 432889.08 | 3784708.17 |
| 217 | fragments of vuggy trachyte | 433030.742 | 3784611.08 |
| 218 | brecciated sandstone | 432912.956 | 3784596.75 |
| 219 | brecciated sandstone | 432900.222 | 3784582.43 |
| 220 | brecciated sandstone | 432897.039 | 3784563.33 |
| 221 | fragments of brecciated sandstone from dump | 432881.122 | 3784429.62 |
| 222 | fractured and brecciated siltstone | 432922.506 | 3784400.97 |
| 223 | brecciated siltstone and sandstone | 433008.458 | 3784356.4 |
| 224 | breccia zone in sandstone | 432411.57 | 3784334.12 |
| 225 | breccia zone in sandstone | 432281.05 | 3784315.02 |
| 239 | fenitized gneissic granite | 431945.367 | 3783914.47 |
| 240 | trachyte dike-gneissic granite contact | 431960.073 | 3783897.5 |
| 241 | calcite vein in sandstone | 431445.54 | 3783716.13 |
| 242 | fragments of sandstone | 431591.033 | 3783746.36 |
| 243 | fractured sandstone | 431706.861 | 3783697.05 |

| Sample | Description | UTM E | UTM N |
|---|---|---|---|
| 244 | fractured sandstone with minor breccia | 431679.652 | 3783709.14 |
| 245 | brecciated sandstone | 431649.419 | 3783701.58 |
| 246 | fractured sandstone with minor breccia | 431798.311 | 3783663.34 |
| 247 | brecciated sandstone | 432092.423 | 3783688.23 |
| 248 | brecciated sandstone | 432093.554 | 3783669 |
| 249 | brecciated sandstone | 432095.817 | 3783650.9 |
| 250 | brecciated sandstone | 432099.21 | 3783635.06 |
| 251 | brecciated sandstone | 432109.391 | 3783631.67 |
| GM-09-LC-3 | fluorite breccia | 431488 | 3784705 |
| 4088 | | 431825 | 3784047 |
| 4089 | | 431825 | 3784047 |
| 4090 | | 431825 | 3784047 |
| 4091 | | 430712 | 3785314 |
| 4092 | | 432463 | 3785172 |
| 4093 | | 430160 | 3785872 |
| 6 | carbonatized and fenitized intrusive breccia | 430223.91 | 3786868.93 |
| 9 | carbonatized and fenitized brecciated trachyte | 430144.524 | 3786805.65 |
| 12 | brecciated sandstone | 430219.308 | 3786802.2 |
| 20 | fragments of brecciated sandstone from stockpile | 430203.2 | 3786774.59 |
| 89 | fractured trachyte with minor breccia | 428827.853 | 3783580 |
| 137 | brecciated sandstone | 432605.613 | 3785932.47 |
| 139 | brecciated sandstone | 432620.318 | 3785911.57 |
| 145 | brecciated sandstone | 432719.384 | 3785725.44 |
| 146 | brecciated sandstone | 432742.602 | 3785683.65 |
| 147 | brecciated sandstone | 432748.02 | 3785672.04 |
| 148 | brecciated sandstone | 432752.663 | 3785679 |
| 149 | fragments of brecciated sandstone and a few fragments of limestone from dump | 432762.725 | 3785668.94 |
| 150 | fragments of brecciated sandstone and a few fragments of limestone from dump | 432768.142 | 3785645.72 |
| 151 | brecciated sandstone | 432762.725 | 3785632.57 |
| 160 | brecciated sandstone and limestone | 432446.285 | 3785045.08 |
| 164 | brecciated sandstone | 432765.141 | 3785022.31 |
| 165 | brecciated sandstone | 432780.692 | 3785056.24 |
| 166 | brecciated sandstone | 432879.875 | 3784820.18 |
| 167 | fluorite rich zone | 432769.382 | 3784995.45 |
| 168 | fluorite rich zone | 432775.037 | 3784989.8 |
| 169 | fluorite rich zone | 432779.279 | 3784985.56 |
| 170 | fluorite rich zone | 432779.279 | 3784981.32 |
| 171 | brecciated zone in sandstone | 432745.349 | 3784961.52 |
| 172 | brecciated zone in sandstone | 432796.761 | 3784860.97 |
| 173 | brecciated sandstone | 432846.104 | 3784797.31 |
| 174 | fractured sandstone with minor breccia | 432838.146 | 3784827.55 |
| 175 | brecciated sandstone | 432865.205 | 3784814.81 |
| 176 | brecciated sandstone | 432876.852 | 3784832.27 |
| 177 | brecciated sandstone | 432898.63 | 3784818 |
| 179 | brecciated sandstone | 432710.809 | 3784792.53 |
| 183 | brecciated sandstone | 432616.899 | 3784854.61 |
| 184 | brecciated sandstone | 432610.532 | 3784827.55 |

| Sample | Description | UTM E | UTM N |
|---|---|---|---|
| 208 | fragments of brecciated sandstone | 432628.041 | 3784614.26 |
| 209 | brecciated sandstone | 432564.373 | 3784649.28 |
| 210 | fractured and brecciated sandstone | 432487.971 | 3784649.28 |
| 211 | brecciated sandstone-dolomite contact | 432464.096 | 3784607.89 |
| 212 | brecciated sandstone-dolomite contact | 432671.017 | 3784568.1 |
| 214 | brecciated sandstone | 432998.907 | 3784652.46 |
| 215 | brecciated sandstone | 433025.966 | 3784655.64 |
| 216 | fractured sandstone | 433024.375 | 3784630.18 |
| 226 | fractured and brecciated sandstone | 431865.052 | 3784057 |
| 227 | fractured and brecciated sandstone | 431872.97 | 3784041.16 |
| 228 | brecciated sandstone | 431834.509 | 3784018.54 |
| 229 | brecciated sandstone | 431834.509 | 3784001.57 |
| 230 | brecciated sandstone | 431819.804 | 3783990.26 |
| 231 | brecciated sandstone | 431816.41 | 3784053.61 |
| 232 | fragments of brecciated sandstone from dump | 431823.255 | 3784056.81 |
| 233 | brecciated sandstone | 431953.285 | 3784009.49 |
| 234 | brecciated sandstone | 431967.991 | 3784012.88 |
| 235 | brecciated sandstone | 431978.172 | 3784016.28 |
| 236 | brecciated sandstone | 431971.385 | 3783997.05 |
| 237 | fragments of brecciated sandstone | 431807.005 | 3783985.6 |
| 238 | fragments of conglomerate from dump | 432040.388 | 3783969.9 |
| 252 | fenitized and fractured trachyte dike | 432258.71 | 3783708.59 |
| 253 | fenitized and fractured trachyte dike | 432258.71 | 3783695.02 |
| 254 | fragments of brecciated sandstone from dump | 432284.727 | 3783690.49 |
| 255 | brecciated sandstone | 432313.007 | 3783731.22 |
| 256 | brecciated sandstone | 432315.27 | 3783718.77 |
| 257 | fragments of sandstone and brecciated sandstone from dump | 432316.401 | 3783698.41 |
| 293 | Rio Tinto breccia | 432323 | 3783697 |
| 294 | Rio Tinto breccia | 432323 | 3783697 |
| 295 | Red Cloud fluorite breccia | 431966 | 3784008 |
| 296 | Red Cloud fluorite breccia | 431966 | 3784008 |
| 297 | Red Cloud copper | 431825 | 3784047 |
| 1 | fenitized intrusive breccia | 430198.598 | 3786890.79 |
| 2 | carbonatized and fenitized intrusive breccia | 430180.19 | 3786886.19 |
| 3 | fenitized intrusive breccia | 430196.297 | 3786879.28 |
| 4 | fenitized intrusive breccia | 430212.405 | 3786883.88 |
| 5 | fenitized intrusive breccia | 430225.06 | 3786890.79 |
| 7 | fenitized intrusive breccia | 430134.17 | 3786857.42 |
| 8 | carbonatized and fenitized intrusive breccia | 430143.374 | 3786845.92 |
| 31 | fenitized intrusive breccia | 429942.299 | 3786082.92 |
| 35 | fragments of fenitized gneiss and intrusive breccia in tree roots | 430072.691 | 3786025.88 |
| 36 | fenitized and carbonatized intrusive breccia in tree roots | 430048.242 | 3786016.71 |
| 37 | fragments of fenitized and carbonatized intrusive breccia in tree roots | 430011.57 | 3786015.69 |
| 38 | fragments of fenitized and carbonatized intrusive breccia from dump | 430035 | 3785979.02 |
| 39 | fragments of fenitized and carbonatized intrusive breccia from dump | 430065.56 | 3785989.2 |
| 40 | fragments of silicified intrusive breccia from dump | 430082.878 | 3785999.39 |
| 41 | fenitized gneiss | 430093.065 | 3786009.58 |

| Sample | Description | UTM E | UTM N |
|---|---|---|---|
| 43 | carbonatized intrusive breccia | 429713.094 | 3786041.16 |
| 44 | fenitized intrusive breccia | 429406.468 | 3785972.91 |
| 45 | intrusive breccia | 429390.169 | 3785840.48 |
| 55 | fragments of fenitized intrusive breccia from dump | 429739.58 | 3785467.64 |
| 56 | fragments of fenitized intrusive breccia | 429826.168 | 3785379.01 |
| 57 | fragments of intrusive breccia | 429864.878 | 3785389.2 |
| 60 | fragments of intrusive breccia | 429780.327 | 3785029.6 |
| 62 | fragments of intrusive breccia | 429457.403 | 3784877.81 |
| 63 | fragments of intrusive breccia | 429388.132 | 3784846.23 |
| 64 | brecciated zone in sandstone | 429495.094 | 3784784.09 |
| 65 | fragments of intrusive breccia | 429357.571 | 3784467.28 |
| 66 | fragments of intrusive breccia | 429175.226 | 3784513.12 |
| 67 | fragments of intrusive breccia | 428540.583 | 3784725.01 |
| 68 | fragments of fenitized intrusive breccia | 428474.368 | 3784563.04 |
| 69 | outcrop of altered intrusive breccia | 428392.873 | 3784598.69 |
| 70 | fragments of altered intrusive breccia | 428297.116 | 3784532.48 |
| 71 | intrusive breccia | 428649.582 | 3784338.93 |
| 72 | fenitized intrusive breccia | 428655.694 | 3784313.46 |
| 73 | fenitized intrusive breccia | 428656.713 | 3784279.84 |
| 74 | fragments of fenitized intrusive breccia | 428657.732 | 3784254.38 |
| 75 | float | 428629.208 | 3784257.43 |
| 76 | fenitized intrusive breccia | 428597.629 | 3784225.85 |
| 77 | fenitized intrusive breccia | 428601.704 | 3784213.63 |
| 78 | fenitized and carbonatized trachyte | 428611.891 | 3784211.59 |
| 79 | fenitized intrusive breccia | 428622.078 | 3784221.78 |
| 80 | fenitized intrusive breccia | 428601.704 | 3784189.18 |
| 81 | fenitized intrusive breccia | 428589.48 | 3784202.42 |
| 82 | fenitized intrusive breccia | 428581.33 | 3784189.18 |
| 83 | fractured and fenitized trachyte near edge of intrusive breccia | 428497.798 | 3784228.91 |
| 84 | fragments of fenitized intrusive breccia | 428519.19 | 3784253.36 |
| 86 | fragments of fenitized intrusive breccia | 428797.292 | 3784267.62 |
| 87 | fenitized intrusive breccia | 428822.759 | 3784240.11 |
| 88 | outcrop of fractured trachyte | 428814.61 | 3784176.96 |
| 97 | fenitized and carbonatized intrusive breccia | 430808.567 | 3785416.32 |
| 98 | fenitized and carbonatized intrusive breccia | 430821.3 | 3785416.32 |
| 99 | fragments of intrusive breccia in float | 430983.017 | 3785324.64 |
| 100 | intrusive breccia | 430998.297 | 3785299.17 |
| 101 | brecciated sandstone | 431030.131 | 3785327.18 |
| 102 | brecciated sandstone | 431022.491 | 3785302.99 |
| 103 | brecciated sandstone | 431014.851 | 3785288.98 |
| GM-10-1 | M&E #13 intrusive breccia | 428588 | 3784201 |
| GM-10-2 | Conqueror #4 fluorite breccia | 432224 | 3784714 |
| 4094 | | 430175 | 3786882 |
| 58 | iron skarn in contact with trachyte | 429086.537 | 3785545.49 |
| 59 | fragments of iron skarn from dump | 428672.571 | 3785106.37 |
| 61 | fragments of iron skarn from dump | 429535.842 | 3784926.71 |
| 96 | fragments of magnetite-hematite with minor quartz from dump | 430417.776 | 3784814.74 |

| Sample | Description | UTM E | UTM N |
| --- | --- | --- | --- |
| 260 | magnetite-hematite | 433473.524 | 3778045.38 |
| GM-09-LC-2 | fragment of iron skarn | 431753 | 3784505 |
| 9671 | | 429093 | 3785541 |

| Sample | La | Ce | Nd | Sm | Eu | Dy | Ho | Yb | Lu |
| --- | --- | --- | --- | --- | --- | --- | --- | --- | --- |
| 21 | 155 | 200 | 67 | 12.1 | 3 | | | 3.1 | 0.41 |
| 22 | 65.4 | 76 | 16 | 2.8 | 0.6 | | | 2.2 | 0.27 |
| 23 | 217 | 280 | 69 | 10 | 2.5 | | | 2.5 | 0.33 |
| 26 | 159 | 250 | 48 | 8.68 | 1.7 | 6.5 | 1.8 | 5.9 | 0.9 |
| 27 | 110 | 193 | 50 | 7.11 | 1.1 | 3.7 | 1.7 | 6.5 | 1.08 |
| 28 | 96 | 178 | 56 | 7.64 | 1.4 | 5.8 | 2.2 | 7.5 | 1.13 |
| 29 | 76.4 | 120 | 47 | 7 | 1.6 | | | 2.4 | 0.27 |
| 30 | 75.2 | 120 | 35 | 4.7 | 1.1 | | | 2.1 | 0.28 |
| 32 | 35 | 49 | 17 | 3.6 | 1.3 | | | 1.3 | 0.17 |
| 33 | 86.5 | 120 | 37 | 5.9 | 1.2 | | | 3.9 | 0.65 |
| 34 | 29 | 47 | 14 | 3.2 | 1 | | | 1.9 | 0.22 |
| 42 | 34 | 58 | 19 | 4.5 | 0.9 | | | 1.7 | 0.26 |
| 47 | 297 | 285 | 54 | 9.79 | 2.5 | 7.6 | 1.7 | 5.6 | 0.74 |
| 48 | 91.4 | 98 | 24 | 4.2 | 0.8 | | | 2.7 | 0.37 |
| 54 | 91.1 | 170 | 45 | 7.4 | 1.7 | | | 4.6 | 0.62 |
| 85 | 83.2 | 130 | 42 | 8.4 | 1.9 | | | 4.3 | 0.63 |
| 104 | 88.8 | 118 | 36 | 6.52 | 1.4 | 3.1 | 1.5 | 3.2 | 0.47 |
| 259 | 41.1 | 74 | 27 | 6.9 | 1.6 | 5.5 | 1.4 | 3.9 | 0.52 |
| GM-09-LC-1 | <50 | <50 | <50 | | | <50 | <50 | | |
| GM-09-LC-4 | 82 | 160 | 71 | | | <50 | <50 | | |
| 153 | 450 | 755 | 179 | 25.5 | 4.4 | 5.1 | 1.6 | 4.2 | 0.54 |
| 258 | 120 | 224 | 76 | 12.8 | 3.4 | 4.1 | <1 | 3.7 | 0.56 |
| 10 | 2620 | 2350 | 315 | 35.2 | 7.8 | 11.6 | 3.6 | 5.6 | 0.61 |
| 11 | 283 | 300 | 44 | 7.11 | 1.4 | 2 | <1 | 2.6 | 0.31 |
| 13 | 2840 | 2990 | 438 | 66.8 | 14.2 | 23.9 | 4.1 | 7.7 | 0.85 |
| 14 | 2800 | 2970 | 422 | 63.5 | 12.4 | 21.8 | 5.5 | 13.4 | 1.75 |
| 15 | 2450 | 2410 | 324 | 45.3 | 9.5 | 17.7 | 4.1 | 7.2 | 0.81 |
| 16 | 902 | 871 | 116 | 18.4 | 3.9 | 8 | 2.6 | 10.9 | 1.68 |
| 17 | 780 | 796 | 118 | 18.9 | 4.1 | 5.6 | 1.6 | 4.2 | 0.52 |
| 18 | 2650 | 2370 | 284 | 37.3 | 7.9 | 8 | 2.3 | 7.2 | 0.93 |
| 19 | 3660 | 3580 | 627 | 77.7 | 16 | 20.9 | 5 | 14.3 | 1.7 |
| 24 | 237 | 390 | 120 | 22.2 | 5.1 | | | 8 | 1 |
| 25 | 1000 | 1540 | 470 | 105 | 27 | | | 28 | 3.2 |
| 46 | 1500 | 1570 | 250 | 43.3 | 10.2 | 11.5 | 2.1 | 7.4 | 0.93 |
| 49 | 522 | 520 | 86 | 15.2 | 3 | 10 | <1 | 7.3 | 1 |
| 50 | 780 | 793 | 120 | 20 | 4.9 | 8.5 | 2.9 | 7.3 | 0.93 |
| 51 | 956 | 1300 | 297 | 37.4 | 10 | 20.7 | 5 | 13.2 | 1.7 |
| 52 | 512 | 534 | 110 | 16.7 | 3.8 | | | 4.6 | 0.59 |
| 53 | 1970 | 2080 | 295 | 42.1 | 8.1 | 12.7 | 3.1 | 6.3 | 0.7 |
| 90 | 2290 | 2500 | 390 | 68.7 | 13.9 | 29.6 | 8.9 | 27.3 | 3.5 |
| 91 | 177 | 277 | 62 | 13.1 | 2.8 | 5.4 | 1.4 | 4.1 | 0.6 |
| 92 | 458 | 514 | 97 | 17.5 | 3.7 | 6 | 2.2 | 6.8 | 0.99 |

| Sample | La | Ce | Nd | Sm | Eu | Dy | Ho | Yb | Lu |
|---|---|---|---|---|---|---|---|---|---|
| 93 | 671 | 796 | 125 | 21 | 4.4 | 6.2 | 2.6 | 7.7 | 1.19 |
| 94 | 523 | 546 | 92 | 16 | 3.7 | 5.5 | 2.4 | 5.2 | 0.75 |
| 95 | 297 | 422 | 91 | 16.1 | 2.9 | 5.4 | 2.2 | 4.3 | 0.58 |
| 105 | 2340 | 3940 | 1060 | 190 | 45.3 | 42 | 8.3 | 12.9 | 1.73 |
| 106 | 242 | 380 | 108 | 16.8 | 3.4 | 8.8 | 2.7 | 8.2 | 1.22 |
| 107 | 63.3 | 97 | 35 | 7.73 | 1.8 | 6.6 | 1.7 | 5.2 | 0.68 |
| 108 | 2370 | 3410 | 780 | 107 | 20 | | | 17 | 2.1 |
| 109 | 2890 | 3200 | 650 | 61.7 | 10 | | | 7.1 | 0.83 |
| 110 | 35 | 58 | 25 | 8.4 | 2.7 | | | 5 | 0.64 |
| 111 | 997 | 1480 | 360 | 46.9 | 7.8 | | | 3.9 | 0.51 |
| 112 | 2540 | 3550 | 840 | 97.8 | 16 | | | 6.1 | 0.82 |
| 113 | 2330 | 2780 | 560 | 57.4 | 10 | | | 3.6 | 0.54 |
| 114 | 1310 | 1570 | 320 | 37.9 | 7.1 | | | 5.3 | 0.63 |
| 115 | 8880 | 8340 | 1450 | 107 | 21 | | | 7.5 | 1 |
| 116 | 9000 | 9310 | 1500 | 119 | 17 | | | 5.2 | 0.93 |
| 117 | 1910 | 1930 | 330 | 32.9 | 5.5 | | | 4.6 | 0.49 |
| 118 | 9000 | 11400 | 1930 | 155 | 25 | 25 | 6 | 11 | 1.3 |
| 119 | 2660 | 2480 | 400 | 33.4 | 5 | | | 5.2 | 0.6 |
| 120 | 5810 | 5320 | 840 | 63.8 | 12 | | | 7 | 1 |
| 121 | 9000 | 9130 | 1360 | 120 | 23 | | | 21 | 1.8 |
| 122 | 5970 | 5740 | 950 | 82.2 | 15 | | | 8.4 | 0.92 |
| 123 | 3790 | 3590 | 620 | 52.4 | 10 | | | 4.9 | 0.83 |
| 124 | 9000 | 8780 | 1460 | 112 | 22 | | | 13 | 1.4 |
| 125 | 2140 | 2030 | 370 | 33.9 | 6.3 | | | 8.3 | 0.94 |
| 126 | 739 | 742 | 140 | 17.4 | 3.3 | | | 5.5 | 0.67 |
| 127 | 80 | 110 | 40 | 8.9 | 2.1 | | | 5.9 | 0.75 |
| 128 | 5670 | 5260 | 860 | 69.9 | 12 | | | 8.2 | 0.74 |
| 129 | 142 | 160 | 48 | 8.3 | 1.9 | | | 3.7 | 0.51 |
| 130 | 6750 | 6320 | 1090 | 86.5 | 13 | | | 10.4 | 1 |
| 131 | 2130 | 2010 | 350 | 32.7 | 7.3 | | | 6.7 | 0.85 |
| 132 | 5680 | 5760 | 1060 | 92.8 | 17 | | | 10 | 1.1 |
| 133 | 9000 | 14400 | 2160 | 132 | 18.6 | 17 | 3.9 | 9.4 | 1.29 |
| 134 | 5410 | 4760 | 780 | 65.7 | 11 | | | 7.1 | 1 |
| 135 | 4950 | 8000 | 1570 | 282 | 54.2 | 59.4 | 12.4 | 24.7 | 2.81 |
| 136 | 1190 | 1980 | 410 | 79.8 | 16.6 | 34.9 | 6 | 16.1 | 2.17 |
| 138 | 1550 | 2450 | 486 | 92.4 | 19.9 | 40.6 | 8.9 | 17.6 | 2.18 |
| 140 | 526 | 900 | 260 | 45 | 10.9 | 28.7 | 6.6 | 12.5 | 1.53 |
| 141 | 270 | 470 | 150 | 28.5 | 7 | 22 | 4.1 | 10.7 | 1.32 |
| 142 | 1900 | 3280 | 704 | 141 | 29 | 24.8 | 9.6 | 11.8 | 1.37 |
| 143 | 4370 | 7470 | 1580 | 304 | 60 | 34.1 | 13.5 | 23.5 | 3.04 |
| 144 | 226 | 383 | 85 | 20 | 4.9 | 16.7 | 3 | 8.4 | 1.04 |
| 152 | 203 | 385 | 140 | 27.2 | 6.5 | 14.9 | 3.6 | 9.8 | 1.25 |
| 154 | 9000 | 20000 | 4150 | 200 | 48 | | | 31 | 1.6 |
| 155 | 283 | 350 | 89 | 15.6 | 3.5 | | | 6 | 0.73 |
| 156 | 784 | 1100 | 280 | 50.2 | 11 | | | 16 | 1.9 |
| 157 | 6180 | 5840 | 1000 | 90.2 | 15 | | | 12 | 0.89 |
| 158 | 9000 | 10500 | 1780 | 168 | 34 | | | 19 | 1.6 |

| Sample | La | Ce | Nd | Sm | Eu | Dy | Ho | Yb | Lu |
|---|---|---|---|---|---|---|---|---|---|
| 159 | 9000 | 10500 | 2050 | 200 | 39 | | | 19 | 1.6 |
| 161 | 5080 | 9860 | 2410 | 489 | 102 | 49.4 | 9.8 | 15.9 | 1.93 |
| 162 | 1290 | 2600 | 670 | 161 | 40 | 45 | 9.3 | 18.6 | 2.11 |
| 163 | 943 | 1750 | 486 | 74.6 | 15.7 | 10 | 1.7 | 2.2 | 0.28 |
| 178 | 5880 | 9570 | 1940 | 303 | 59.3 | 19.5 | 2.8 | 4.5 | 0.52 |
| 180 | 15700 | 22700 | 4100 | 539 | 100 | 24.9 | 2.9 | 5.5 | 0.89 |
| 181 | 3460 | 5090 | 1000 | 150 | 30.8 | 21.7 | 4.8 | 9.6 | 1.1 |
| 182 | 330 | 511 | 107 | 22.9 | 5.4 | 9.3 | 2.9 | 5.2 | 0.62 |
| 185 | 344 | 653 | 200 | 45.6 | 11.8 | 20.1 | 6.5 | 12.3 | 1.47 |
| 186 | 5020 | 6640 | 1160 | 149 | 29.8 | 23.3 | 5.9 | 10.3 | 1.23 |
| 187 | 3700 | 6200 | 1300 | 221 | 46.3 | 51.5 | 7.4 | 15.2 | 1.83 |
| 188 | 9720 | 14200 | 2700 | 389 | 71.8 | 58.4 | 7 | 8.7 | 1.47 |
| 189 | 9000 | 12000 | 2180 | 167 | 26 | | | 5.9 | 0.78 |
| 190 | 9000 | 11400 | 2030 | 162 | 28 | | | 6.9 | 0.65 |
| 191 | 2500 | 2100 | 360 | 27.3 | 5.6 | | | 4.8 | 0.64 |
| 192 | 591 | 744 | 140 | 17.9 | 3.3 | | | 5.9 | 0.7 |
| 193 | 5720 | 5310 | 860 | 79.9 | 16 | | | 9.5 | 1.4 |
| 194 | 4630 | 5200 | 1030 | 104 | 21 | | | 94 | 1.1 |
| 195 | 2700 | 3210 | 680 | 81 | 16 | | | 8.9 | 0.82 |
| 196 | 383 | 400 | 96 | 13.2 | 2.8 | | | 4.9 | 0.65 |
| 197 | 6030 | 5720 | 1050 | 94.5 | 19 | | | 9.1 | 1 |
| 198 | 223 | 230 | 62 | 10.4 | 2.5 | | | 4.7 | 0.62 |
| 199 | 4350 | 4290 | 810 | 82.4 | 16 | | | 12 | 1.1 |
| 200 | 3420 | 3240 | 560 | 50.9 | 10 | | | 5.8 | 0.72 |
| 201 | 9000 | 9040 | 1410 | 102 | 17 | | | 11 | 1.7 |
| 202 | 8970 | 8130 | 1320 | 107 | 20 | | | 7.4 | 1 |
| 203 | 520 | 561 | 110 | 12.3 | 2.2 | | | 2.5 | 0.32 |
| 204 | 2630 | 2720 | 480 | 44.9 | 7.5 | | | 5.7 | 0.7 |
| 205 | 887 | 1130 | 238 | 33.3 | 7.2 | 19 | 5.1 | 17.4 | 2.47 |
| 206 | 19100 | 19300 | 3520 | 390 | 66.8 | 70 | 16 | 35.4 | 4.55 |
| 207 | 250 | 335 | 85 | 17 | 4.5 | 14 | 3 | 8 | 1.05 |
| 213 | 92.7 | 186 | 77 | 18.9 | 5.4 | 12 | 3.1 | 7.5 | 0.95 |
| 217 | 95.8 | 160 | 61 | 11.1 | 2.5 | 4.9 | 1.2 | 3.5 | 0.55 |
| 218 | 2830 | 4900 | 1250 | 178 | 37.7 | 29 | 4.4 | 9.2 | 1.06 |
| 219 | 1570 | 2780 | 760 | 106 | 28.7 | 19.2 | 3.9 | 7.4 | 0.65 |
| 220 | 280 | 533 | 160 | 29.2 | 7.3 | 10.7 | 2.5 | 5.5 | 0.7 |
| 221 | 7230 | 9970 | 1780 | 261 | 53 | 38 | <3 | 12 | 0.6 |
| 222 | 278 | 780 | 140 | 23.9 | 5.9 | 11 | 3 | 12 | 1.83 |
| 223 | 102 | 172 | 56 | 9.96 | 2.8 | 6.9 | 2.5 | 7.7 | 1.15 |
| 224 | 617 | 1520 | 580 | 148 | 37.7 | 42.6 | 5.5 | 14.8 | 1.86 |
| 225 | 950 | 1180 | 209 | 38.5 | 8.5 | 19.1 | 3.3 | 8.5 | 1.03 |
| 239 | 264 | 350 | 70 | 15.4 | 3.8 | 11.1 | 3.7 | 9.4 | 1.2 |
| 240 | 374 | 502 | 107 | 22.7 | 4.3 | 12.2 | 2.9 | 8 | 1.1 |
| 241 | 2.7 | <5 | <10 | 0.27 | <0.1 | <1 | <1 | <0.5 | <0.1 |
| 242 | 16 | 21 | 10 | 2.19 | 0.6 | 1 | <1 | 0.7 | 0.12 |
| 243 | 174 | 205 | 49 | 7.87 | 1.8 | 3.4 | 1 | 3.5 | 0.46 |
| 244 | 26 | 43 | 18 | 4.37 | 1.2 | 4.1 | <1 | 3 | 0.42 |

| Sample | La | Ce | Nd | Sm | Eu | Dy | Ho | Yb | Lu |
|---|---|---|---|---|---|---|---|---|---|
| 245 | 47 | 78 | 36 | 63 | 1.6 | 4.1 | <1 | 2.6 | 0.38 |
| 246 | 255 | 360 | 87 | 17.7 | 4.4 | 13 | 2.9 | 9.6 | 1.3 |
| 247 | 4320 | 5980 | 658 | 77.7 | 13.6 | 18.2 | 6 | 7.3 | 1.09 |
| 248 | 831 | 1320 | 164 | 26.9 | 5.4 | 15.2 | 4 | 10.3 | 1.4 |
| 249 | 8630 | 9080 | 1340 | 149 | 27.4 | 28.3 | 4.8 | 12 | 1.42 |
| 250 | 6480 | 6430 | 880 | 94.9 | 17 | 11.1 | 2.6 | 9.1 | 1.03 |
| 251 | 10800 | 12300 | 1900 | 220 | 39.1 | 24.3 | 4.2 | 9 | 0.96 |
| GM-09-LC-3 | 5900 | 6700 | 1100 | | | <50 | <50 | | |
| 4088 | 7290 | 9040 | 1380 | 71 | 23 | 25 | | 6.1 | |
| 4089 | 10550 | 14060 | 1980 | 129 | 36 | 39 | | 10 | |
| 4090 | 7610 | 9320 | 1550 | 143 | 40 | 44 | | 11 | |
| 4091 | 275 | 230 | 174 | 14 | | | | | |
| 4092 | 123 | 7570 | 2010 | 425 | 96 | 101 | 5.8 | 13 | |
| 4093 | 3300 | 1790 | 264 | 26 | 5.8 | 23 | | 6 | |
| 6 | 1920 | 2020 | 265 | 35.7 | 7.3 | 12.5 | 2.8 | 6.2 | 0.7 |
| 9 | 2100 | 1960 | 290 | 32.4 | 6.8 | | | 8.9 | 1 |
| 12 | 2570 | 2440 | 323 | 54 | 12.1 | 26.4 | 4.9 | 9.5 | 1.07 |
| 20 | 4210 | 3940 | 565 | 86.3 | 18.8 | 31 | 6.8 | 13.4 | 1.47 |
| 89 | 7690 | 8790 | 1390 | 231 | 48.4 | 53.6 | 14.7 | 32.2 | 3.76 |
| 137 | 3330 | 5440 | 1100 | 200 | 39.8 | 47.6 | 8.2 | 18.1 | 2.27 |
| 139 | 1860 | 3140 | 780 | 130 | 27.8 | 46 | 9.4 | 18.6 | 2.22 |
| 145 | 1870 | 3590 | 770 | 184 | 41.1 | 82.4 | 16.9 | 34.3 | 4.02 |
| 146 | 333 | 697 | 160 | 30 | 9.4 | 16.7 | 4 | 10 | 1.25 |
| 147 | 169 | 270 | 62 | 13.8 | 4.4 | 6.4 | <3 | 5 | 0.7 |
| 148 | 847 | 1110 | 197 | 45.3 | 10.4 | 15.3 | 3.3 | 7.5 | 0.83 |
| 149 | 799 | 1720 | 510 | 98.9 | 22.2 | 32 | 5.6 | 13.9 | 1.74 |
| 150 | 469 | 934 | 260 | 51 | 12.9 | 17 | 3 | 8.9 | 1.18 |
| 151 | 72 | 153 | 52 | 18.1 | 6.1 | 35.8 | 6.7 | 24.2 | 3.12 |
| 160 | 5670 | 7940 | 1800 | 200 | 45 | | | 11 | 0.94 |
| 164 | 1380 | 2230 | 567 | 76.8 | 16.8 | 17.2 | 4.4 | 6.2 | 0.78 |
| 165 | 7380 | 10000 | 1900 | 254 | 48.1 | 21.9 | 4 | 9.4 | 1.05 |
| 166 | 5100 | 6570 | 1200 | 152 | 27.8 | 28 | 6.3 | 8.3 | 0.87 |
| 167 | 6130 | 8020 | 1520 | 200 | 40.1 | 32 | 3.9 | 8.2 | 0.99 |
| 168 | 10300 | 13400 | 2570 | 315 | 58 | 38 | 7.7 | 10 | 0.94 |
| 169 | 10800 | 13600 | 2490 | 291 | 52.5 | 31.8 | 5.9 | 11.2 | 1.17 |
| 170 | 10500 | 12800 | 2260 | 260 | 49.5 | 22.6 | 5.2 | 9.1 | 1.07 |
| 171 | 312 | 672 | 208 | 43 | 10 | 15.6 | 3.1 | 7.1 | 0.89 |
| 172 | 130 | 273 | 115 | 25.8 | 8.2 | 14 | 3.1 | 5.7 | 0.73 |
| 173 | 156 | 306 | 100 | 21.5 | 5.6 | 11 | 2.4 | 4.4 | 0.51 |
| 174 | 166 | 304 | 100 | 23.8 | 6 | 13.4 | 4.1 | 8.7 | 1.08 |
| 175 | 600 | 1170 | 320 | 53.9 | 13.4 | 17 | 3.5 | 6.7 | 0.71 |
| 176 | 3400 | 4450 | 818 | 119 | 24 | 27 | 6.3 | 8 | 1.18 |
| 177 | 549 | 952 | 320 | 57.6 | 13.9 | 18 | 4.1 | 8.9 | 1.03 |
| 179 | 3720 | 5870 | 1400 | 173 | 33 | 28.8 | 6.1 | 12.6 | 1.49 |
| 183 | 6040 | 9450 | 1960 | 317 | 63.8 | 32.8 | 6.3 | 6.5 | 0.77 |
| 184 | 847 | 1460 | 420 | 79.6 | 21.7 | 28 | 7.3 | 9.2 | 1.03 |
| 208 | 3440 | 5260 | 1060 | 173 | 35.9 | 40 | 5.9 | 9.9 | 1.16 |

| Sample | La | Ce | Nd | Sm | Eu | Dy | Ho | Yb | Lu |
|---|---|---|---|---|---|---|---|---|---|
| 209 | 4070 | 7560 | 2100 | 357 | 75.3 | 53.2 | 9.7 | 11.7 | 1.49 |
| 210 | 1310 | 2110 | 430 | 80 | 17.3 | 20.7 | 4 | 6.7 | 0.84 |
| 211 | 1060 | 1940 | 510 | 91.6 | 21.1 | 29.3 | 4.7 | 9.1 | 1.09 |
| 212 | 3130 | 5630 | 1340 | 282 | 65 | 53.3 | 10.2 | 16 | 1.75 |
| 214 | 54.7 | 77 | 24 | 6.76 | 2.1 | 6.6 | <3 | 2.4 | 0.16 |
| 215 | 14 | 36 | 20 | 6.8 | 2.5 | 8.3 | 2 | 3.6 | 0.44 |
| 216 | 20 | 33 | 18 | 5.32 | 2 | 4.9 | <1 | 3.1 | 0.41 |
| 226 | 81.7 | 126 | 50 | 7.69 | 1.9 | 6.8 | 1.4 | 4.2 | 0.55 |
| 227 | 701 | 1030 | 205 | 42.6 | 9.1 | 18.8 | 2.4 | 9.9 | 1.13 |
| 228 | 354 | 416 | 119 | 27.7 | 7.3 | 14 | 4 | 5.2 | 0.87 |
| 229 | 113 | 199 | 53 | 15.8 | 3.9 | 10.8 | 2.4 | 6 | 0.75 |
| 230 | 625 | 783 | 190 | 36.9 | 9 | 13 | <9 | 5.5 | 0.8 |
| 231 | 44.7 | 78 | 40 | 7.23 | 1.5 | 5.9 | 1.2 | 4.2 | 0.53 |
| 232 | 822 | 1120 | 204 | 35.9 | 7 | 9.6 | 3 | 7.8 | 0.92 |
| 233 | 3110 | 3690 | 615 | 92.6 | 17.8 | 16.9 | 4.3 | 7.6 | 0.81 |
| 234 | 9610 | 10200 | 1490 | 201 | 40 | 36 | <4 | 17 | 1.1 |
| 235 | 734 | 822 | 185 | 25.3 | 5.1 | 9.2 | 2.3 | 6.3 | 0.8 |
| 236 | 11700 | 12800 | 2040 | 254 | 43.2 | 35 | 10 | 25.2 | 2.6 |
| 237 | 4760 | 5590 | 890 | 124 | 24 | 28 | <2 | 11 | 0.9 |
| 238 | 11600 | 12900 | 1920 | 216 | 41.1 | 21.2 | 2.9 | 8.3 | 0.95 |
| 252 | 120 | 209 | 63 | 12.8 | 3.1 | 14 | 2.8 | 9.4 | 1.42 |
| 253 | 38.8 | 74 | 25 | 5.05 | 1.1 | 4.1 | 1.2 | 4.8 | 0.8 |
| 254 | 92.4 | 146 | 60 | 12.2 | 3.6 | 10.7 | 2.8 | 4.2 | 0.45 |
| 255 | 249 | 370 | 85 | 20.7 | 5 | 11 | 1 | 6.3 | 0.9 |
| 256 | 84 | 175 | 67 | 15.3 | 4.2 | 12 | 1.9 | 8.4 | 1.02 |
| 257 | 467 | 692 | 140 | 26 | 6 | 10 | <1 | 5.4 | 0.8 |
| 293 |  | 1160 |  | 33.5 | 4 |  |  | 14 | 0.8 |
| 294 |  | 3600 | 840 | 130 | 20 | 22 | 11 | 12 | 1.2 |
| 295 |  | 2620 |  | 70.88 |  |  |  | 18 | 2.2 |
| 296 |  | 5500 | 1000 | 140 | 20 | 27 | 6.3 | 14 | 1.5 |
| 297 |  | 180 |  | 8.3 | 5 |  |  | 35 |  |
| 1 | 2320 | 2550 | 362 | 50.5 | 11.7 | 17.8 | 3.7 | 6.9 | 0.82 |
| 2 | 1230 | 1570 | 340 | 41.7 | 9 |  |  | 8.8 | 1.1 |
| 3 | 1190 | 1290 | 215 | 27.3 | 4.2 | 9.1 | 2.3 | 6.4 | 0.85 |
| 4 | 1830 | 1990 | 291 | 42.2 | 9.5 | 12.2 | 2.9 | 5.2 | 0.68 |
| 5 | 1430 | 1480 | 225 | 27.8 | 6.1 | 8.7 | 2.2 | 6.5 | 0.85 |
| 7 | 1160 | 1410 | 330 | 43 | 8.1 |  |  | 8.1 | 1 |
| 8 | 754 | 912 | 180 | 26.3 | 5.2 |  |  | 5.6 | 0.59 |
| 31 | 149 | 232 | 82 | 13.5 | 3.1 | 4.2 | <1 | 3.7 | 0.5 |
| 35 | 60.7 | 120 | 43 | 7.5 | 1.9 |  |  | 3.1 | 0.47 |
| 36 | 283 | 310 | 64 | 13.4 | 2.7 |  |  | 4.2 | 0.5 |
| 37 | 106 | 180 | 63 | 12.8 | 3.2 |  |  | 2.7 | 0.34 |
| 38 | 310 | 340 | 86 | 14.6 | 3.3 |  |  | 3.5 | 0.39 |
| 39 | 139 | 210 | 81 | 14.9 | 3.7 |  |  | 3 | 0.39 |
| 40 | 281 | 340 | 110 | 19 | 4 |  |  | 4.2 | 0.49 |
| 41 | 49 | 68 | 21 | 3.5 | 1 |  |  | 1.8 | 0.24 |
| 43 | 127 | 210 | 71 | 14.1 | 3.4 |  |  | 3.1 | 0.43 |

| Sample | La | Ce | Nd | Sm | Eu | Dy | Ho | Yb | Lu |
|---|---|---|---|---|---|---|---|---|---|
| 44 | 200 | 311 | 94 | 15.5 | 3.5 | 4.8 | 1.6 | 3.9 | 0.55 |
| 45 | 205 | 327 | 79 | 16 | 3.8 | 4.1 | 1.2 | 3.7 | 0.55 |
| 55 | 79.5 | 130 | 50 | 10.5 | 2.4 | | | 3.7 | 0.5 |
| 56 | 113 | 189 | 57 | 13.9 | 3.3 | <4.0 | <1 | 3.8 | 0.45 |
| 57 | 101 | 171 | 48 | 11.8 | 2.8 | 3.3 | <1 | 3.1 | 0.44 |
| 60 | 100 | 182 | 46 | 10.2 | 2.5 | 5.9 | 1.5 | 2.9 | 0.43 |
| 62 | 193 | 278 | 66 | 13.6 | 2.9 | 6.5 | <1 | 3.8 | 0.59 |
| 63 | 159 | 245 | 64 | 13.4 | 3.3 | 7 | 2 | 3.9 | 0.5 |
| 64 | 813 | 966 | 161 | 27.8 | 6.5 | 18.3 | 3.6 | 7.8 | 0.95 |
| 65 | 107 | 162 | 41 | 9.01 | 2.1 | 7.4 | 1.6 | 3.3 | 0.46 |
| 66 | 123 | 180 | 53 | 10 | 2 | | | 3.8 | 0.51 |
| 67 | 131 | 198 | 43 | 8.76 | 1.9 | 6.1 | <1 | 4 | 0.58 |
| 68 | 112 | 180 | 37 | 8.66 | 1.7 | 2.8 | <1 | 3.6 | 0.52 |
| 69 | 118 | 183 | 57 | 8.65 | 1.8 | 4.4 | <1 | 3.7 | 0.54 |
| 70 | 153 | 231 | 48 | 8.92 | 1.8 | 6.1 | 1.6 | 4.4 | 0.64 |
| 71 | 9000 | 13400 | 2900 | 200 | 67.8 | 92 | 17 | 20.9 | 1.8 |
| 72 | 1290 | 1960 | 412 | 54.3 | 10.2 | 18 | 5.5 | 16 | 2.36 |
| 73 | 698 | 899 | 190 | 32 | 7.1 | | | 16 | 2.2 |
| 74 | 358 | 470 | 130 | 22.7 | 4.9 | | | 13 | 1.7 |
| 75 | 18900 | 22100 | 4360 | 514 | 109 | 160 | 34 | 60.6 | 6.97 |
| 76 | 4500 | 4930 | 732 | 85.4 | 14.6 | 12.2 | 2.3 | 11.1 | 1.43 |
| 77 | 4240 | 5010 | 785 | 103 | 17.6 | 16.7 | 4.6 | 21.4 | 2.6 |
| 78 | 466 | 572 | 130 | 18.9 | 4.1 | | | 5.2 | 0.66 |
| 79 | 8560 | 9560 | 1440 | 169 | 28.3 | 33.8 | 7.4 | 26.2 | 3.71 |
| 80 | 11900 | 15600 | 2630 | 337 | 58.8 | 59.2 | 17.9 | 55 | 5.97 |
| 81 | 880 | 1130 | 197 | 28.7 | 5.4 | 4.4 | 1.3 | 6.7 | 1.01 |
| 82 | 5860 | 7260 | 1170 | 156 | 27.7 | 24.8 | 7.2 | 19.3 | 2.64 |
| 83 | 183 | 230 | 64 | 12.1 | 2.9 | | | 8 | 1 |
| 84 | 158 | 220 | 67 | 14.4 | 3.4 | | | 12 | 1.5 |
| 86 | 306 | 380 | 83 | 19.5 | 4.7 | | | 40 | 5 |
| 87 | 8860 | 11000 | 2480 | 330 | 67.7 | 89 | 19.3 | 43.2 | 5.26 |
| 88 | 190 | 299 | 87 | 14 | 3.4 | 5.3 | 1.8 | 5.8 | 0.83 |
| 97 | 157 | 226 | 64 | 11.3 | 2.5 | <2 | <2 | 3.8 | 0.51 |
| 98 | 113 | 175 | 41 | 9.34 | 2.1 | 4.1 | <2 | 4 | 0.61 |
| 99 | 190 | 264 | 62 | 12 | 2.9 | 4.1 | <1 | 3.3 | 0.49 |
| 100 | 344 | 391 | 68 | 12.1 | 2.4 | 6.7 | 2.7 | 5.3 | 0.65 |
| 101 | 96 | 112 | 24 | 5.14 | 1 | 2.9 | 1.2 | 2.1 | 0.3 |
| 102 | 6280 | 7280 | 1180 | 122 | 21.7 | 15.7 | 4.1 | 7.6 | 1.07 |
| 103 | 720 | 755 | 117 | 18.7 | 3.7 | 8.5 | 3.6 | 8 | 1.06 |
| GM-10-1 | 410 | 600 | 120 | | | <50 | <50 | | |
| GM-10-2 | 19000 | 21000 | 2700 | | | <100 | <100 | | |
| 4094 | 1680 | 3690 | 563 | 58 | 3440 | 2.4 | | 5.2 | |
| 58 | 436 | 410 | 53 | 5.8 | 1 | 2 | <1 | 4.1 | 1.2 |
| 59 | 62.9 | 89 | 13 | 2.05 | 0.6 | 1.6 | <1 | 0.9 | 0.13 |
| 61 | 177 | 251 | 54 | 8.84 | 1.7 | 3.5 | 1.5 | 6.5 | 1.51 |
| 96 | 41.4 | 47 | 10 | 1.9 | <0.5 | <1 | <1 | 0.6 | 0.1 |
| 260 | 64.4 | 86 | 23 | 2.9 | <1 | <1 | <1 | 0.8 | <0.1 |

| Sample | La | Ce | Nd | Sm | Eu | Dy | Ho | Yb | Lu |
|---|---|---|---|---|---|---|---|---|---|
| GM-09-LC-2 | <50 | 260 | <50 | | | <50 | <50 | | |
| 9671 | | | | | | | | | |

| Sample | Y | Sc | Th | U | Au ppb | Ag | Cu | Pb | Zn |
|---|---|---|---|---|---|---|---|---|---|
| 21 | 33 | 14.9 | 30 | 6.8 | <5 | <0.2 | 50 | 32 | 83 |
| 22 | 27 | 0.55 | 23 | 8.7 | 71 | <0.2 | 10 | 52 | 43 |
| 23 | 30 | 1 | 71.3 | 6.4 | 12 | <0.2 | 17 | 17 | 51 |
| 26 | 59 | 0.97 | 120 | 23.6 | <5 | <0.2 | 14 | 178 | 7 |
| 27 | 57 | 0.53 | 120 | 19 | 45 | <0.2 | 6 | 26 | 8 |
| 28 | 76 | 0.52 | 130 | 23 | 19 | <0.2 | 5 | 52 | 10 |
| 29 | 27 | 0.62 | 274 | 8.8 | <5 | <0.2 | 9 | 10 | 15 |
| 30 | 14 | 0.8 | 34 | 4.5 | <5 | <0.2 | 6 | 17 | 21 |
| 32 | 15 | 4.6 | 5.1 | 1.2 | 25 | <0.2 | 18 | 10 | 20 |
| 33 | 33 | 1.5 | 36 | 4.1 | 12 | <0.2 | 30 | 102 | 62 |
| 34 | 11 | 0.38 | 56.6 | 13 | <5 | <0.2 | 8 | 23 | 20 |
| 42 | 20 | 5.4 | 5.3 | <1 | 7 | <0.2 | 12 | 5 | 15 |
| 47 | 78 | 6.81 | 7.1 | 2.4 | <5 | 0.4 | 11 | 51 | 41 |
| 48 | 37 | 5.7 | 6.3 | 1.7 | <5 | <0.2 | 2 | 21 | 29 |
| 54 | 42 | 0.63 | 63.4 | 10 | 9 | <0.2 | 4 | 8 | 30 |
| 85 | 54 | 0.94 | 50.5 | 3.8 | <5 | <0.2 | 2 | 3 | 11 |
| 104 | 47 | 6.86 | 8.7 | 2.8 | 15 | <0.2 | 5 | 25 | 76 |
| 259 | 52 | 10.5 | 9.4 | 2.6 | 24 | <0.2 | 7 | 4 | 8 |
| GM-09-LC-1 | 12 | | <20 | <20 | | | 21 | <10 | <10 |
| GM-09-LC-4 | 180 | | <20 | <20 | | | 48 | 26 | 1152 |
| 153 | 68 | 2.92 | 10 | 10.8 | <5 | <0.2 | 16 | 26 | 30 |
| 258 | 47 | 8.37 | 33 | 6.1 | 94 | <0.2 | 10 | 6 | 30 |
| 10 | 74 | 1.82 | 5.5 | 4.5 | 30 | <0.2 | 81 | 584 | 89 |
| 11 | 28 | 3.21 | 4.8 | 2.4 | 35 | 0.6 | 62 | 350 | 100 |
| 13 | 66 | 3.75 | 6.4 | 10.5 | 135 | <0.2 | 415 | 1869 | 911 |
| 14 | 134 | 7.34 | 9.2 | 10.2 | 28 | <0.2 | 158 | 205 | 529 |
| 15 | 106 | 3.96 | 5.9 | 13.3 | 19 | <0.2 | 263 | 181 | 297 |
| 16 | 92 | 2.11 | 5.9 | 4 | 32 | 0.2 | 19 | 81 | 103 |
| 17 | 61 | 3.1 | 20.5 | 7.7 | 63 | 0.9 | 108 | 799 | 547 |
| 18 | 79 | 4.75 | 3.2 | 5.9 | 33 | <0.2 | 32 | 321 | 239 |
| 19 | 126 | 6.66 | 14.4 | 10 | 80 | <0.2 | 63 | 519 | 201 |
| 24 | 101 | 1 | 49 | 14 | 41 | <0.2 | 18 | 503 | 123 |
| 25 | 418 | 2.8 | 20 | 20 | 19 | <0.2 | 29 | 711 | 321 |
| 46 | 106 | 6.15 | 27.8 | 14 | 21 | <0.2 | 18 | 63 | 53 |
| 49 | 64 | 4.9 | 18 | 7 | 5 | <0.5 | 22 | 64 | 156 |
| 50 | 87 | 6.7 | 10.3 | 9.3 | <5 | <0.2 | 27 | 63 | 87 |
| 51 | 162 | 6.4 | 16 | 18 | <5 | <0.2 | 9 | 84 | 35 |
| 52 | 57 | 3.7 | 19 | 6.9 | <5 | <0.2 | 9 | 33 | 88 |
| 53 | 117 | 5.25 | 12.4 | 14.7 | 14 | <0.2 | 20 | 70 | 20 |
| 90 | <370 | 2.21 | 69.7 | 13 | 18 | <0.2 | 206 | 3441 | 174 |
| 91 | 56 | 8.14 | 37.2 | 5.7 | <5 | <0.2 | 19 | 79 | 21 |
| 92 | 97 | 0.82 | 47.3 | 6.2 | 13 | <0.2 | 10 | 29 | 23 |
| 93 | 80 | 2 | 37.3 | 7.6 | 55 | <0.2 | 21 | 67 | 77 |

| Sample | Y | Sc | Th | U | Au ppb | Ag | Cu | Pb | Zn |
|---|---|---|---|---|---|---|---|---|---|
| 94 | 68 | 2.4 | 45.4 | 7.4 | 15 | <0.2 | 17 | 43 | 115 |
| 95 | 52 | 1.44 | 43.1 | 3.7 | 10 | <0.2 | 29 | 28 | 35 |
| 105 | 402 | 1.5 | 110 | 14 | 49 | <0.2 | 135 | 86 | 51 |
| 106 | 122 | 0.93 | 63.6 | 8.1 | 32 | <0.2 | 39 | 12 | 5 |
| 107 | 79 | 9.06 | 9 | 4.4 | 116 | 2.5 | 40 | 34 | 83 |
| 108 | 315 | 4.8 | 40 | 5.7 | 145 | <0.2 | 14 | 31 | 203 |
| 109 | 95 | 4.8 | 23 | 4.9 | 43 | <0.2 | 3 | 39 | 140 |
| 110 | 57 | 3.2 | 6.2 | 2.1 | <5 | 0.5 | 8 | 18 | 52 |
| 111 | 79 | 1.4 | 20 | 5.5 | <5 | <0.2 | 109 | 42 | 26 |
| 112 | 129 | 3.8 | 25 | 12 | 6 | <0.2 | 26 | 59 | 54 |
| 113 | 64 | 4.3 | 21 | 4.9 | 7 | <0.2 | 16 | 32 | 109 |
| 114 | 75 | 4.5 | 13 | 4.3 | <5 | <0.2 | 12 | 21 | 99 |
| 115 | 83 | 2.4 | 26 | 5.6 | 12 | <0.2 | 65 | 80 | 51 |
| 116 | 89 | 3.7 | 28 | 18 | 29 | <0.2 | 87 | 113 | 117 |
| 117 | 66 | 3.2 | 11 | 6.9 | 51 | <0.2 | 32 | 76 | 93 |
| 118 | 112 | 3.4 | 38 | 19 | 45 | <0.2 | 196 | 236 | 175 |
| 119 | 45 | 4.7 | 18 | 5.5 | 28 | <0.2 | 126 | 53 | 166 |
| 120 | 80 | 6.5 | 28 | 4.3 | 49 | <0.2 | 9 | 47 | 125 |
| 121 | 108 | 4.9 | 39 | 7.1 | 94 | <0.2 | 166 | 168 | 182 |
| 122 | 93 | 3.1 | 21 | 7.4 | 22 | <0.2 | 31 | 95 | 90 |
| 123 | 54 | 4.5 | 18 | 6.3 | 404 | 0.2 | 758 | 84 | 858 |
| 124 | 75 | 4.9 | 30 | 12 | 66 | <0.2 | 39 | 228 | 268 |
| 125 | 105 | 4 | 15 | 5.7 | 78 | <0.2 | 17 | 35 | 96 |
| 126 | 85 | 6.7 | 12 | 4.2 | 98 | 0.5 | 16 | 27 | 182 |
| 127 | 88 | 5.9 | 8.6 | 3.2 | 17 | 0.5 | 18 | 27 | 74 |
| 128 | 74 | 3.4 | 24 | 7.2 | 755 | <0.2 | 299 | 66 | 130 |
| 129 | 30 | 9 | 10 | 3.1 | 30 | 0.2 | 11 | 9 | 241 |
| 130 | 96 | 4 | 30 | 13 | 75 | <0.2 | 22 | 62 | 75 |
| 131 | 90 | 6.1 | 14 | 5.8 | 28 | <0.2 | 5 | 50 | 183 |
| 132 | 112 | 2.7 | 23 | 12 | <5 | <0.2 | 108 | 154 | 110 |
| 133 | 88 | 2.6 | 41 | 65 | 10 | <0.2 | 19 | 58 | 2 |
| 134 | 84 | 4.5 | 24 | 5.1 | 21 | <0.2 | 138 | 74 | 90 |
| 135 | 390 | 7.93 | 26 | 7.1 | 72 | <0.2 | 270 | 127 | 360 |
| 136 | 333 | 8.2 | 13 | 4.9 | 85 | <0.2 | 405 | 71 | 369 |
| 138 | 331 | 8.35 | 11.7 | 3.1 | 157 | 1.1 | 435 | 95 | 579 |
| 140 | 229 | 10.8 | 10.8 | 4.2 | 367 | 1.2 | 824 | 112 | 247 |
| 141 | 171 | 11 | 10 | 3 | 329 | 1 | 423 | 129 | 192 |
| 142 | 356 | 21.4 | 12.5 | 18.2 | 96 | <0.2 | 64 | 405 | 410 |
| 143 | 416 | 22.1 | 27 | 3.6 | 118 | <0.2 | 186 | 1711 | 423 |
| 144 | <160 | 4 | 6.7 | 4.1 | 130 | 1.4 | 727 | 2151 | 180 |
| 152 | 110 | 4.16 | 47.4 | 12.3 | 79 | 2.5 | 282 | 55 | 30 |
| 154 | 84 | 6.3 | 68 | 6.7 | 29 | <0.2 | 99 | 406 | 152 |
| 155 | 75 | 9 | 6.9 | 4.2 | 45 | 0.3 | 73 | 236 | 87 |
| 156 | 218 | 5.5 | 10 | 6.9 | 21 | <0.2 | 228 | 52 | 225 |
| 157 | 90 | 5.2 | 21 | 4.6 | <5 | <0.2 | 211 | 85 | 164 |
| 158 | 113 | 3.8 | 27 | 2.9 | 42 | <0.2 | 237 | 88 | 96 |
| 159 | 97 | 4.9 | 49 | 7.1 | 14 | <0.2 | 393 | 82 | 194 |

| Sample | Y | Sc | Th | U | Au ppb | Ag | Cu | Pb | Zn |
|---|---|---|---|---|---|---|---|---|---|
| 161 | 384 | 5.49 | 123 | 8.9 | 74 | <0.2 | 216 | 409 | 328 |
| 162 | 399 | 2.66 | 19 | 1.6 | 29 | <0.2 | 575 | 294 | 234 |
| 163 | 212 | 0.71 | 15 | 2.6 | 74 | <0.2 | 448 | 1680 | 400 |
| 178 | <100 | 2.75 | 77.3 | 37.6 | 150 | <0.2 | 660 | 13800 | 726 |
| 180 | 144 | 7.51 | 150 | 19 | 66 | <0.2 | 423 | 220 | 80 |
| 181 | 168 | 2.55 | 48.8 | 16 | 25 | <0.2 | 314 | 247 | 48 |
| 182 | 57 | 8.51 | 7.3 | 5 | 23 | 0.5 | 313 | 125 | 160 |
| 185 | 197 | 12 | 17.4 | 9.2 | 167 | 1.5 | 548 | 72 | 393 |
| 186 | 175 | 3.72 | 55 | 10.9 | 107 | <0.2 | 570 | 510 | 237 |
| 187 | 183 | 1.8 | 40 | 10 | 15 | <0.2 | 563 | 1546 | 42 |
| 188 | <200 | 3.3 | 93.5 | <20 | 57 | <0.2 | 884 | 6457 | 324 |
| 189 | 97 | 2.4 | 53.1 | 4.4 | <5 | <0.2 | 42 | 86 | 103 |
| 190 | 99 | 2.2 | 46 | 7.2 | <5 | <0.2 | 30 | 93 | 85 |
| 191 | 74 | 2.8 | 12 | 3.4 | 13 | <0.2 | 21 | 29 | 100 |
| 192 | 75 | 3.7 | 11 | 7 | 9 | <0.2 | 52 | 52 | 235 |
| 193 | 130 | 2.3 | 16 | 3.6 | <5 | <0.2 | 7 | 78 | 38 |
| 194 | 131 | 3.3 | 29 | 6.4 | <5 | <0.2 | 14 | 80 | 156 |
| 195 | 116 | 1.4 | 45 | 22 | <5 | <0.2 | 10 | 48 | 34 |
| 196 | 69 | 4.5 | 8.5 | 3.7 | 14 | <0.2 | 42 | 43 | 86 |
| 197 | 128 | 4 | 25 | 14 | 23 | <0.2 | 17 | 84 | 61 |
| 198 | 77 | 5.3 | 8 | 2 | 53 | 0.3 | 18 | 31 | 97 |
| 199 | 134 | 2.2 | 12 | 21 | 6 | <0.2 | 4 | 64 | 41 |
| 200 | 85 | 3.4 | 15 | 6 | 20 | <0.2 | 7 | 34 | 43 |
| 201 | 106 | 2.4 | 43 | 9.1 | <5 | <0.2 | 19 | 99 | 25 |
| 202 | 92 | 2.5 | 28 | 10 | 8 | <0.2 | 7 | 57 | 9 |
| 203 | 34 | 2.5 | 8 | 3.8 | <5 | <0.2 | 13 | 23 | 34 |
| 204 | 62 | 2.6 | 19 | 6.7 | 15 | <0.2 | 13 | 41 | 39 |
| 205 | 221 | 2.64 | 59 | 16.6 | 25 | <0.2 | 45 | 41 | 211 |
| 206 | 501 | 10 | 30 | 38 | 48 | <0.2 | 230 | 331 | 690 |
| 207 | 162 | 4.3 | 6.2 | 3.7 | 28 | 0.6 | 22 | 30 | 63 |
| 213 | 115 | 8.38 | 14 | 4 | 23 | 0.7 | 186 | 93 | 126 |
| 217 | 42 | 4.41 | 30 | 7 | 15 | <0.2 | 110 | 18 | 61 |
| 218 | 203 | 3.13 | 52.4 | 7.7 | 34 | 1.9 | 606 | 158 | 578 |
| 219 | <150 | 4.09 | 28.6 | 16 | 40 | 1.9 | 606 | 16800 | 241 |
| 220 | <110 | 3 | 12.5 | 9 | 73 | 4.1 | 957 | 3561 | 166 |
| 221 | 149 | 5.81 | 52.4 | 9 | 27 | 5.3 | 175 | 70 | 228 |
| 222 | 155 | 1.33 | 77.5 | 18 | 18 | <0.2 | 84 | 38 | 36 |
| 223 | 96 | 1.08 | 90.7 | 22 | 28 | <0.2 | 12 | 86 | 42 |
| 224 | 263 | 9.34 | 27.7 | 8.6 | 47 | 0.7 | 533 | 116 | 694 |
| 225 | 179 | 3.05 | 17.6 | 4.4 | 7 | <0.2 | 54 | 41 | 61 |
| 239 | 90 | 4.39 | 11.7 | 6.4 | 28 | 0.2 | 167 | 1057 | 148 |
| 240 | 75 | 4.59 | 50.2 | 9.7 | 22 | <0.2 | 156 | 178 | 133 |
| 241 | 3 | 0.13 | <0.5 | <1 | <5 | 0.3 | 6 | 3 | 45 |
| 242 | 15 | 2.63 | 2.6 | <1 | 9 | 0.4 | 8 | 5 | 8 |
| 243 | 50 | 6.81 | 3.8 | 2.4 | 36 | 1.9 | 543 | 241 | 181 |
| 244 | 49 | 4.26 | 7.8 | 2 | 10 | 0.7 | 173 | 12 | 44 |
| 245 | 45 | 2.34 | 9.2 | 1.7 | 7 | 0.9 | 171 | 26 | 24 |

| Sample | Y | Sc | Th | U | Au ppb | Ag | Cu | Pb | Zn |
|---|---|---|---|---|---|---|---|---|---|
| 246 | 154 | 6.9 | 16 | 3 | 61 | 0.9 | 222 | 69 | 208 |
| 247 | 80 | 9.59 | 67.1 | 12.3 | 41 | <0.2 | 311 | 440 | 182 |
| 248 | 95 | 10.6 | 28.8 | 9.1 | 30 | <0.2 | 148 | 99 | 231 |
| 249 | 142 | 4.47 | 38.3 | 41.8 | 80 | <0.2 | 678 | 148 | 624 |
| 250 | 81 | 4.63 | 29.4 | 24.8 | 29 | <0.2 | 594 | 171 | 1463 |
| 251 | 76 | 4.61 | 52.9 | 50.7 | 63 | <0.2 | 529 | 200 | 766 |
| GM-09-LC-3 | 215 | | 25 | <20 | | | 43 | 70 | 68 |
| 4088 | 186 | | | | | | 60 | 280 | |
| 4089 | 286 | | | | | | 130 | 350 | |
| 4090 | 310 | | | | | | 290 | 2240 | |
| 4091 | 46 | | | | | | 40 | 80 | |
| 4092 | 752 | | | | | | 102 | 430 | |
| 4093 | 181 | | | | | | 70 | 110 | |
| 6 | 58 | 8.65 | 32.4 | 27.2 | 170 | 3.7 | 7220 | 337 | 411 |
| 9 | 74 | 4.5 | 45 | 8 | 54 | <0.2 | 11 | 47 | 323 |
| 12 | <160 | 2.09 | 24.1 | 10.9 | 496 | 27.3 | 4250 | 29700 | 182 |
| 20 | <200 | 3.76 | 19.3 | 42.7 | 610 | 11.2 | 5823 | 33400 | 933 |
| 89 | <350 | 4.06 | 122 | 26 | 71 | 2.9 | 5254 | 61800 | 554 |
| 137 | 302 | 18 | 22.4 | 7.2 | 131 | 0.7 | 1482 | 166 | 668 |
| 139 | 349 | 9.46 | 14 | 4.2 | 378 | <0.2 | 1240 | 157 | 355 |
| 145 | <600 | 9.65 | 16.2 | 14 | 615 | 22.2 | 10409 | 24500 | 1578 |
| 146 | <230 | 6.81 | 6 | 25 | 307 | 1.52opt | 24400 | 228700 | 4342 |
| 147 | <180 | 1.48 | 2.2 | 16 | 264 | 10.1opt | 89200 | 370900 | 3424 |
| 148 | 60 | 1.6 | 7.9 | 13.9 | 770 | 14.3 | 10627 | 1578 | 433 |
| 149 | <220 | 2.1 | 7.8 | 16 | 1707 | 2.05opt | 45300 | 29300 | 2750 |
| 150 | <180 | 2 | 8.7 | 34 | 531 | 5.75opt | 88000 | 98500 | 3541 |
| 151 | <270 | 3.05 | 9 | 9 | 1137 | 39.7 | 6648 | 4094 | 670 |
| 160 | 129 | 4.1 | 63.3 | 19 | 289 | 3.1 | 3551 | 575 | 204 |
| 164 | 120 | 4.56 | 19 | 8.1 | 163 | <0.2 | 127 | 348 | 74 |
| 165 | <70 | 4.65 | 90.6 | 17 | 293 | 3.2 | 3813 | 8284 | 453 |
| 166 | <90 | 7.18 | 52.7 | 14 | 594 | 13.8 | 8774 | 4288 | 986 |
| 167 | 95 | 5.42 | 47.8 | 33.6 | 246 | 4.6 | 4240 | 3260 | 2670 |
| 168 | <70 | 3.84 | 69 | 65 | 600 | <0.2 | 2577 | 5429 | 3337 |
| 169 | <100 | 3.91 | 78.2 | 52 | 526 | 6.9 | 5174 | 8144 | 9726 |
| 170 | <60 | 3.26 | 89 | 36.5 | 307 | 2.5 | 2800 | 9219 | 1935 |
| 171 | 140 | 4.7 | 13 | 7.9 | 208 | 0.5 | 219 | 115 | 161 |
| 172 | <110 | 3.54 | 4.7 | 69 | 596 | 36.2 | 18267 | 17100 | 3853 |
| 173 | 82 | 3.61 | 6.8 | 10 | 25 | 2.6 | 365 | 301 | 154 |
| 174 | 119 | 9.2 | 12.2 | 6.6 | 11 | 1.3 | 540 | 296 | 1115 |
| 175 | 105 | 7.48 | 16.4 | 26.8 | 99 | 25.8 | 19600 | 1094 | 2001 |
| 176 | <140 | 2.64 | 60.6 | 78.9 | 67 | 13.6 | 18118 | 21400 | 189 |
| 177 | 117 | 9.26 | 24.7 | 15 | 20 | 6 | 1297 | 446 | 317 |
| 179 | 190 | 5.2 | 50 | 15 | 76 | 0.9 | 1749 | 266 | 300 |
| 183 | <130 | 5.4 | 85.8 | 19.6 | 250 | <0.2 | 1042 | 14200 | 792 |
| 184 | <120 | 4.43 | 10 | 17.9 | 920 | 9.4 | 7297 | 14300 | 1259 |
| 208 | 148 | 1.68 | 37.8 | 9.4 | 107 | <0.2 | 196 | 411 | 40 |
| 209 | 209 | 13 | 93 | 10.9 | 102 | <0.2 | 875 | 506 | 827 |

| Sample | Y | Sc | Th | U | Au ppb | Ag | Cu | Pb | Zn |
|---|---|---|---|---|---|---|---|---|---|
| 210 | 117 | 3.3 | 22.1 | 9.8 | 31 | 6 | 376 | 322 | 113 |
| 211 | 154 | 5.51 | 24.1 | 50 | 25 | <0.2 | 222 | 190 | 105 |
| 212 | 250 | 3.17 | 39.7 | 23 | <5 | <0.2 | 1073 | 731 | 128 |
| 214 | 20 | 3.88 | 8.5 | 75 | 61 | 2.38opt | 37000 | 1062 | 5717 |
| 215 | 71 | 8.16 | 2.9 | 5.4 | 19 | 36.8 | 10471 | 28 | 841 |
| 216 | 74 | 6.36 | 3.1 | 3 | 12 | 9.2 | 4387 | 23 | 549 |
| 226 | 54 | 4.75 | 6.9 | 3.8 | 7 | 0.9 | 270 | 796 | 588 |
| 227 | <150 | 5.64 | 13.1 | 22.5 | 27 | 13.1 | 5962 | 9815 | 2778 |
| 228 | <150 | 4.37 | 8.5 | 70 | 67 | 3opt | 13067 | 210600 | 2128 |
| 229 | <120 | 3.8 | 7.9 | 13.1 | 14 | 4.5 | 1876 | 5012 | 4716 |
| 230 | 54 | 5.87 | 12 | 195 | <58 | 2.44opt | 15173 | 93400 | 2954 |
| 231 | 59 | 13.4 | 10.3 | 4.5 | 30 | 2.6 | 728 | 747 | 397 |
| 232 | <110 | 8.32 | 14.7 | 17 | 31 | 9.4 | 3798 | 27600 | 6914 |
| 233 | 120 | 5.72 | 15.1 | 23.6 | 24 | <0.2 | 150 | 115 | 174 |
| 234 | 173 | 21 | 31 | 19 | <19 | 0.6 | 73 | 131 | 462 |
| 235 | 92 | 7 | 10 | 6.2 | 7 | 1.3 | 201 | 378 | 303 |
| 236 | 271 | 33 | 50 | 32.7 | 5 | <0.2 | 29 | 125 | 481 |
| 237 | 153 | 2.8 | 16 | 24 | <12 | <0.5 | 135 | 753 | 65 |
| 238 | 79 | 7.03 | 68.5 | 28.5 | 15 | <0.2 | 1832 | 752 | 158 |
| 252 | 110 | 1.45 | 97.6 | 16.6 | 17 | <0.2 | 75 | 1078 | 111 |
| 253 | 41 | 0.45 | 77 | 19 | 8 | <0.2 | 158 | 764 | 116 |
| 254 | <90 | 5.92 | 4.2 | 36.4 | 93 | 21 | 23200 | 12900 | 1782 |
| 255 | 43 | 2.7 | 10 | 19 | 170 | 13 | 4727 | 30000 | 249 |
| 256 | <140 | 2.79 | 9.2 | 13.8 | 149 | 9 | 1305 | 9077 | 416 |
| 257 | 49 | 4.1 | 17 | 7 | 94 | 3.1 | 903 | 1987 | 194 |
| 293 | | | | | 39 | | 1679 | 331 | 3449 |
| 294 | | | | | 170 | 8 | 5786 | 10000 | 142 |
| 295 | | | | | 12 | | 21 | 60 | 219 |
| 296 | | | | | | 11 | 374 | 1186 | 169 |
| 297 | | | | | | 2.08 | 15105 | 10000 | 10200 |
| 1 | 59 | 4.13 | 28.1 | 26.5 | 174 | 0.2 | 1266 | 559 | 309 |
| 2 | 109 | 4.2 | 22 | 6.5 | 139 | 0.5 | 301 | 141 | 398 |
| 3 | 44 | 4.22 | 38.2 | 9.2 | 222 | 1 | 223 | 318 | 1330 |
| 4 | 54 | 3.45 | 25.8 | 18.9 | 175 | 3.5 | 3121 | 367 | 232 |
| 5 | 68 | 4.39 | 29.1 | 11.7 | 117 | 2.5 | 559 | 278 | 698 |
| 7 | 113 | 2.5 | 67.5 | 14 | 37 | <0.2 | 14 | 68 | 279 |
| 8 | 62 | 2.8 | 38 | 7.9 | 31 | <0.2 | 17 | 22 | 57 |
| 31 | 51 | 17 | 24 | 5 | 5 | <0.2 | 26 | 19 | 62 |
| 35 | 27 | 3.9 | 33 | 5.2 | <5 | <0.2 | 25 | 71 | 62 |
| 36 | 57 | 4.5 | 23 | 3.1 | 165 | <0.2 | 193 | 16 | 108 |
| 37 | 26 | 20.1 | 23 | 5 | 18 | <0.2 | 54 | 18 | 120 |
| 38 | 39 | 17.7 | 25 | 4.7 | 73 | <0.2 | 47 | 28 | 144 |
| 39 | 31 | 19 | 31 | 4.9 | 11 | <0.2 | 53 | 20 | 133 |
| 40 | 55 | 18.2 | 23 | 5.5 | 15 | <0.2 | 30 | 20 | 113 |
| 41 | 9 | 0.37 | 60.7 | 6.6 | <5 | <0.2 | 10 | 17 | 42 |
| 43 | 36 | 10.2 | 27 | 6.2 | <5 | <0.2 | 56 | 12 | 71 |
| 44 | 55 | 10.4 | 27.8 | 3.9 | 20 | <0.2 | 34 | 18 | 69 |

| Sample | Y | Sc | Th | U | Au ppb | Ag | Cu | Pb | Zn |
|---|---|---|---|---|---|---|---|---|---|
| 45 | 53 | 10.7 | 32.5 | 5.7 | 12 | <0.2 | 10 | 19 | 45 |
| 55 | 46 | 8.4 | 18 | 3.9 | <5 | <0.2 | 14 | 8 | 25 |
| 56 | 44 | 6.11 | 20.5 | 5.8 | 12 | 0.4 | 48 | 233 | 66 |
| 57 | 42 | 8.3 | 22.7 | 3.4 | 7 | 0.2 | 64 | 52 | 65 |
| 60 | 32 | 7.41 | 20.9 | 3.2 | <5 | 0.2 | 22 | 55 | 39 |
| 62 | 40 | 8.59 | 28 | 5.5 | 15 | <0.2 | 28 | 88 | 45 |
| 63 | 48 | 6.57 | 31.3 | 6.2 | <5 | <0.2 | 12 | 26 | 57 |
| 64 | 144 | 1.3 | 56.4 | 4.5 | 30 | <0.2 | 86 | 109 | 19 |
| 65 | 38 | 8.82 | 19.6 | 4.2 | <5 | 0.5 | 11 | 23 | 32 |
| 66 | 37 | 5.7 | 43 | 9.5 | <5 | <0.2 | 7 | 5 | 33 |
| 67 | 38 | 4.82 | 59.7 | 11.2 | <5 | <0.2 | 41 | 19 | 32 |
| 68 | 35 | 5.14 | 54 | 12 | <5 | <0.2 | 23 | 81 | 78 |
| 69 | 41 | 4.5 | 56 | 11.5 | <5 | <0.2 | 5 | 18 | 39 |
| 70 | 39 | 4.45 | 67.9 | 12.8 | <5 | <0.2 | 16 | 55 | 31 |
| 71 | 458 | 2.2 | 20 | 7.6 | 141 | <0.2 | 6 | 72 | 16 |
| 72 | 187 | 1.9 | 49 | 9.8 | 27 | <0.2 | 9 | 36 | 37 |
| 73 | 125 | 1.6 | 38 | 10 | 58 | <0.2 | 25 | 1244 | 52 |
| 74 | 168 | 1.6 | 38 | 7.8 | 35 | <0.2 | 8 | 180 | 24 |
| 75 | 725 | 2.52 | 30 | 13 | 116 | <0.2 | 108 | 1353 | 17 |
| 76 | 110 | 4.29 | 47.6 | 6 | 19 | <0.2 | 30 | 402 | 47 |
| 77 | 177 | 3.64 | 36.3 | 6.8 | 24 | <0.2 | 15 | 685 | 58 |
| 78 | 56 | 2.2 | 42 | 5.3 | <5 | <0.2 | 9 | 78 | 150 |
| 79 | 221 | 6.3 | 52 | 9.2 | 29 | <0.2 | 34 | 1701 | 82 |
| 80 | 696 | 3 | 130 | 84 | 17 | <0.2 | 95 | 64 | 43 |
| 81 | 66 | 2.55 | 47.7 | 4.1 | 18 | <0.2 | 178 | 2124 | 79 |
| 82 | 235 | 4.43 | 42.5 | 7.2 | 24 | <0.2 | 14 | 968 | 113 |
| 83 | 93 | 0.68 | 56.4 | 7.8 | 11 | <0.2 | 12 | 389 | 43 |
| 84 | 160 | 2 | 43 | 7.5 | <5 | <0.2 | 4 | 148 | 24 |
| 86 | 548 | 1.5 | 40 | 13 | 27 | <0.2 | 6 | 44 | 6 |
| 87 | 664 | 1.93 | 100 | 17 | 32 | <0.2 | 11 | 75 | 53 |
| 88 | 82 | 1.5 | 41.6 | 6.2 | 48 | <0.2 | 9 | 7 | 58 |
| 97 | 52 | 6.62 | 29 | 5.7 | 23 | <0.2 | 19 | 18 | 74 |
| 98 | 52 | 6.64 | 28.5 | 5.7 | 17 | <0.2 | 11 | 13 | 80 |
| 99 | 101 | 9.09 | 28.4 | 5.2 | <5 | <0.2 | 11 | 25 | 56 |
| 100 | 85 | 6.9 | 9.6 | 4.1 | 16 | <0.2 | 10 | 22 | 56 |
| 101 | 30 | 7.27 | 6.5 | 2 | 11 | 0.2 | 5 | 6 | 11 |
| 102 | 127 | 3.08 | 25.5 | 24.6 | 7 | <0.2 | 15 | 255 | 52 |
| 103 | 112 | 7.14 | 8.4 | 4.8 | <5 | <0.2 | 75 | 11 | 67 |
| GM-10-1 | 83 |  | <20 | <20 |  |  | <10 | 114 | 76 |
| GM-10-2 | 100 |  | <50 | <50 |  |  | <50 | 228 | <50 |
| 4094 | 189 |  |  |  |  |  | 8580 | 22200 |  |
| 58 | 16 | 2.5 | 8 | 20 | 8 | 0.7 | 12 | 13 | 30 |
| 59 | 8 | 0.5 | 13.8 | 18.9 | <5 | <0.2 | 88 | 31 | 41 |
| 61 | 28 | 4.97 | 3.6 | <1 | <5 | <0.2 | 70 | 340 | 53 |
| 96 | 5 | 0.56 | 2.1 | 8.4 | 6 | <0.2 | 104 | 56 | 77 |
| 260 | 7 | 0.79 | 1.8 | 4 | <2 | <0.5 | 13 | 14 | 55 |
| GM-09-LC-2 | 32 |  | 83 | <20 |  |  | 198 | 704 | <10 |

| Sample | Y | Sc | Th | U | Au ppb | Ag | Cu | Pb | Zn |
|---|---|---|---|---|---|---|---|---|---|
| 9671 | | | | 700 | | | | | |

| Sample | Mo | Nb | Ni | Co | As | Hg | Ba | Sr | F |
|---|---|---|---|---|---|---|---|---|---|
| 21 | 2 | | 14 | 18 | <5 | <0.01 | 3700 | 1431 | |
| 22 | 2 | 118 | 1 | 1 | <5 | <0.01 | 690 | 63 | 907 |
| 23 | <1 | 118 | 1 | 4 | <5 | <0.01 | 1800 | 749 | 1435 |
| 26 | 6 | | 2 | <1 | 13 | 0.034 | 1200 | 168 | |
| 27 | 2 | | 1 | <1 | <5 | 0.018 | 110 | 47 | |
| 28 | 1 | | 3 | <1 | <5 | <0.01 | 50 | 27 | 141 |
| 29 | 1 | | 3 | 2 | <5 | <0.01 | 1800 | 508 | 317 |
| 30 | 1 | 89 | 4 | 2 | <5 | <0.01 | 2000 | 77 | |
| 32 | 2 | 3 | 4 | 5 | <5 | <0.01 | 1500 | 350 | 94 |
| 33 | 4 | 55 | 11 | 5 | <5 | <0.01 | 1100 | 298 | 79 |
| 34 | 1 | 150 | 5 | 2 | <5 | <0.01 | 2400 | 896 | 100 |
| 42 | <1 | 9 | 5 | 2 | <5 | 0.014 | 330 | 453 | 1231 |
| 47 | 3 | | 6 | 3 | 24 | 0.024 | 2200 | 436 | |
| 48 | 4 | | 12 | 3 | <5 | <0.01 | 700 | 640 | |
| 54 | 3 | 181 | 2 | 2 | <5 | <0.01 | 430 | 107 | 140 |
| 85 | 2 | 135 | 3 | 2 | <5 | <0.01 | 770 | 247 | 602 |
| 104 | 2 | | 17 | 5 | <5 | <0.01 | 580 | 117 | |
| 259 | 2 | | 24 | 4 | 9 | 0.038 | 160 | 116 | |
| GM-09-LC-1 | <10 | <10 | <10 | <10 | <20 | | | 134 | |
| GM-09-LC-4 | 40 | 13 | 42 | 16 | 69 | | | 82 | |
| 153 | 123 | | 10 | 4 | <5 | <0.01 | 4700 | 213 | |
| 258 | 2 | | 7 | 8 | 24 | <0.01 | 1900 | 96 | |
| 10 | 194 | | 6 | 2 | 34 | 0.042 | >20000 | >2000 | |
| 11 | 22 | | 10 | 4 | 21 | 0.064 | 1700 | 378 | |
| 13 | 364 | | 5 | 3 | 42 | 0.13 | 18700 | 1175 | |
| 14 | 44 | | 10 | 4 | 40 | 0.087 | >20000 | >2000 | |
| 15 | 11 | | 6 | 8 | 19 | 0.052 | 17100 | >2000 | |
| 16 | 37 | | 5 | 2 | 8 | 0.063 | 8200 | 463 | |
| 17 | 93 | | 14 | 14 | 116 | 0.121 | 7300 | 1335 | |
| 18 | 22 | | 5 | 3 | 20 | 0.038 | 14500 | 683 | |
| 19 | 24 | | 9 | 5 | 16 | 0.085 | >20000 | 973 | |
| 24 | 41 | | 3 | 2 | 16 | 0.051 | 4000 | 224 | |
| 25 | 81 | | 10 | 6 | 23 | 0.087 | 16200 | 380 | |
| 46 | 13 | | 4 | 2 | 9 | 0.026 | >20000 | 1369 | |
| 49 | 14 | | 14 | <5 | 3.8 | 100 | 2900 | 530 | |
| 50 | 7 | | 6 | 4 | 14 | 0.033 | 14400 | 848 | |
| 51 | 6 | | 4 | 2 | <5 | <0.01 | 11000 | 861 | |
| 52 | 5 | | 4 | 5 | 10 | <0.01 | 6200 | 1797 | |
| 53 | 7 | | 4 | 3 | 11 | 0.035 | 16900 | 1316 | |
| 90 | 25 | | 7 | 3 | 83 | 0.198 | 6500 | 524 | |
| 91 | <1 | | 15 | 4 | 6 | 0.033 | 970 | 534 | |
| 92 | 4 | | 2 | <1 | <5 | 0.062 | 3300 | 190 | |
| 93 | 4 | | 2 | 4 | 8 | 0.031 | 2900 | 309 | |
| 94 | 26 | | 4 | 3 | <5 | 0.014 | 2800 | 178 | |

| Sample | Mo | Nb | Ni | Co | As | Hg | Ba | Sr | F |
|---|---|---|---|---|---|---|---|---|---|
| 95 | 1 | | 3 | 2 | <5 | 0.036 | 1700 | 802 | |
| 105 | 113 | | 4 | 2 | 13 | 0.138 | 16000 | 1036 | |
| 106 | 5 | | 1 | <1 | 12 | 0.067 | 2100 | 366 | |
| 107 | 7 | | 14 | 7 | <5 | 0.117 | 3100 | 199 | |
| 108 | 7 | | 17 | 8 | <5 | 0.045 | >20000 | 528 | |
| 109 | 6 | | 15 | 8 | 7 | <0.01 | 19100 | 384 | |
| 110 | 3 | | 8 | 5 | 14 | <0.01 | 1800 | 333 | 240000 |
| 111 | 11 | | 7 | 5 | 50 | 0.017 | 10200 | 430 | 62500 |
| 112 | 14 | | 9 | 4 | 5 | 0.012 | 20000 | 1056 | 135000 |
| 113 | 14 | | 12 | 6 | 12 | <0.01 | 14900 | 385 | 116000 |
| 114 | 8 | | 11 | 5 | <5 | <0.01 | 8700 | 342 | 145000 |
| 115 | 16 | | 5 | 3 | 15 | 0.029 | >20000 | 1836 | 245000 |
| 116 | 18 | | 12 | 6 | 7 | 0.024 | >20000 | 1900 | 202500 |
| 117 | 8 | | 14 | 7 | 5 | 0.02 | 7100 | 639 | 107500 |
| 118 | 32 | | 15 | 6 | 27 | 0.19 | >20000 | >2000 | 263500 |
| 119 | 23 | | 20 | 10 | 12 | 0.024 | 9200 | >2000 | 79000 |
| 120 | 9 | | 20 | 11 | <5 | <0.01 | 16100 | >2000 | 184800 |
| 121 | 19 | | 13 | 5 | 14 | 0.098 | >20000 | >2000 | 306500 |
| 122 | 7 | | 9 | 5 | <5 | 0.018 | >20000 | 1557 | 295000 |
| 123 | 15 | | 18 | 11 | 328 | 0.373 | 13300 | >2000 | 168500 |
| 124 | 26 | | 19 | 8 | 17 | 0.039 | >20000 | 1653 | 219000 |
| 125 | 8 | | 12 | 5 | 10 | <0.01 | 11000 | 795 | 168500 |
| 126 | 10 | | 19 | 10 | 44 | <0.01 | 3000 | 365 | 85500 |
| 127 | 6 | | 18 | 5 | 15 | 0.012 | 740 | 193 | 47800 |
| 128 | 18 | | 12 | 7 | 189 | 0.73 | >20000 | >2000 | 158000 |
| 129 | 1 | | 29 | 8 | 23 | <0.01 | 840 | >2000 | 44500 |
| 130 | 14 | | 8 | 5 | 17 | <0.01 | >20000 | 1758 | 219000 |
| 131 | 9 | | 14 | 6 | 6 | <0.01 | 7800 | 1080 | 164000 |
| 132 | 29 | | 7 | 4 | 14 | 0.09 | 18800 | 1947 | 317500 |
| 133 | 4 | | 5 | 3 | <5 | 0.011 | >20000 | 1153 | 184800 |
| 134 | 15 | | 7 | 3 | 31 | 0.099 | >20000 | 1222 | 254000 |
| 135 | 7 | | 27 | 10 | 77 | 0.15 | >20000 | 911 | 160000 |
| 136 | 5 | | 27 | 10 | 83 | 0.179 | 11400 | 436 | 85600 |
| 138 | 5 | | 26 | 10 | 183 | 0.972 | 11800 | 631 | 147200 |
| 140 | 4 | | 21 | 8 | 265 | 0.601 | 16000 | 687 | 179200 |
| 141 | 3 | | 23 | 9 | 210 | 1.118 | 8900 | 460 | 121600 |
| 142 | 14 | | 30 | 9 | 129 | 0.89 | 17400 | 481 | 35600 |
| 143 | 22 | | 44 | 15 | 50 | 0.196 | >20000 | 553 | 13500 |
| 144 | 6 | | 17 | 8 | 638 | 0.535 | 4100 | 377 | 26000 |
| 152 | 69 | | 3 | 2 | 39 | 0.166 | 5000 | 1827 | |
| 154 | 5 | | 8 | 3 | <5 | 0.081 | >20000 | 1483 | |
| 155 | 6 | | 15 | 6 | 33 | 0.066 | 3300 | 358 | |
| 156 | 17 | | 18 | 6 | 47 | 0.092 | 13500 | 510 | |
| 157 | 7 | | 10 | 5 | 8 | 0.059 | >20000 | 1052 | |
| 158 | 5 | | 7 | 3 | 17 | 0.133 | >20000 | 1036 | |
| 159 | 27 | | 11 | 4 | 46 | 0.258 | >20000 | 1085 | |
| 161 | 178 | | 28 | 7 | 7 | 0.229 | >20000 | 1111 | |

| Sample | Mo | Nb | Ni | Co | As | Hg | Ba | Sr | F |
|---|---|---|---|---|---|---|---|---|---|
| 162 | 58 | | 4 | 1 | 155 | 0.192 | >20000 | 980 | |
| 163 | 58 | | 3 | 1 | 420 | 0.149 | >20000 | 941 | |
| 178 | 246 | | 6 | 4 | 264 | 1.47 | >20000 | >2000 | |
| 180 | 7 | | 5 | 3 | 43 | 0.418 | >20000 | 915 | |
| 181 | 43 | | 6 | 3 | 80 | 0.266 | >20000 | >2000 | |
| 182 | 6 | | 8 | 5 | 65 | 0.265 | 3300 | 426 | |
| 185 | 16 | | 26 | 8 | 162 | 0.271 | 4000 | 1541 | |
| 186 | 15 | | 5 | 2 | 180 | 1.156 | >20000 | 1141 | |
| 187 | 3 | | 2 | 2 | 101 | 0.552 | >20000 | >2000 | |
| 188 | 50 | | 7 | 4 | 385 | 1.188 | >20000 | >2000 | |
| 189 | 12 | | 6 | 2 | <5 | 0.02 | >20000 | >2000 | 116000 |
| 190 | 9 | | 7 | 3 | <5 | 0.014 | >20000 | >2000 | 156500 |
| 191 | 14 | | 11 | 4 | 15 | 0.042 | 9200 | 634 | 103500 |
| 192 | 20 | | 23 | 15 | 28 | 0.032 | 6700 | 777 | 46000 |
| 193 | 6 | | 3 | 2 | <5 | <0.01 | >20000 | 1579 | 385000 |
| 194 | 22 | | 8 | 3 | <5 | 0.049 | >20000 | 1648 | 355000 |
| 195 | 20 | | 5 | 3 | <5 | 0.01 | 15100 | 737 | 235000 |
| 196 | 6 | | 15 | 5 | 16 | 0.029 | 3100 | 263 | 62500 |
| 197 | 9 | | 8 | 4 | <5 | 0.065 | >20000 | 1437 | 245000 |
| 198 | 6 | | 17 | 6 | 24 | 0.071 | 1500 | 269 | 92300 |
| 199 | 6 | | 3 | 2 | <5 | <0.01 | >20000 | 1744 | 370000 |
| 200 | 7 | | 6 | 4 | 25 | 0.03 | 11200 | 1130 | 159500 |
| 201 | 29 | | 4 | 3 | <5 | 0.031 | >20000 | 1232 | 227000 |
| 202 | 68 | | 3 | 2 | <5 | <0.01 | >20000 | >2000 | 306500 |
| 203 | 13 | | 11 | 5 | 8 | <0.01 | 3000 | 215 | 38000 |
| 204 | 8 | | 9 | 5 | 7 | <0.01 | 12700 | 347 | 88500 |
| 205 | 24 | | 7 | 3 | <5 | 0.015 | 4500 | 236 | |
| 206 | 9 | | 28 | 9 | 22 | 0.186 | >20000 | 588 | |
| 207 | 16 | | 10 | 3 | <5 | 0.033 | 3500 | 168 | |
| 213 | 3 | | 10 | 10 | 54 | 0.646 | 1500 | 592 | |
| 217 | 2 | | 9 | 3 | 34 | 0.453 | 800 | 976 | |
| 218 | 74 | | 7 | 3 | 248 | 1.317 | 17300 | 689 | |
| 219 | 511 | | 5 | 3 | 688 | 19 | 14800 | 1427 | |
| 220 | 30 | | 7 | 9 | 434 | 1.077 | 2400 | 357 | |
| 221 | 22 | | 17 | 12 | 80.5 | 2000 | 59100 | >2000 | |
| 222 | 6 | | 4 | 2 | 12 | 0.439 | 2000 | 153 | |
| 223 | 2 | | 2 | <1 | <5 | 0.21 | 690 | 94 | |
| 224 | 30 | | 42 | 8 | 94 | 0.398 | 16700 | 1073 | |
| 225 | 5 | | 6 | 2 | <5 | 0.032 | 5700 | 410 | |
| 239 | 5 | | 12 | 4 | 49 | 0.059 | 2600 | 267 | |
| 240 | 9 | | 10 | 6 | 62 | 0.153 | 3200 | 341 | |
| 241 | <1 | | 1 | 1 | <5 | 0.017 | <20 | 608 | |
| 242 | <1 | | 6 | 2 | <5 | 0.079 | 640 | 131 | |
| 243 | 5 | | 19 | 19 | 225 | 0.481 | 440 | 282 | |
| 244 | 2 | | 9 | 4 | 69 | 0.232 | 120 | 13 | |
| 245 | 2 | | 5 | 2 | 54 | 0.196 | 180 | 521 | |
| 246 | 5 | | 17 | 3 | 59 | 0.105 | 2300 | 177 | |

| Sample | Mo | Nb | Ni | Co | As | Hg | Ba | Sr | F |
|---|---|---|---|---|---|---|---|---|---|
| 247 | 33 | | 31 | 23 | 142 | 0.233 | 16700 | 345 | |
| 248 | 35 | | 32 | 14 | 101 | 0.211 | 3400 | 331 | |
| 249 | 27 | | 10 | 6 | 114 | 0.275 | 18200 | 708 | |
| 250 | 28 | | 48 | 9 | 106 | 0.213 | >20000 | 1008 | |
| 251 | 13 | | 16 | 13 | 54 | 0.149 | >20000 | >2000 | |
| GM-09-LC-3 | 52 | 32 | <10 | <10 | 20 | | | 502 | |
| 4088 | | | | | | | | | |
| 4089 | | | | | | | | | |
| 4090 | | | | | | | | | |
| 4091 | | | | | | | | | |
| 4092 | | | | | | | | | |
| 4093 | | | | | | | | | |
| 6 | 9 | | 5 | 6 | 124 | 0.097 | 8400 | >2000 | |
| 9 | 5 | | 6 | 8 | 44 | 0.016 | 8200 | 876 | |
| 12 | 618 | | <1 | 2 | 985 | 1.403 | 9000 | >2000 | |
| 20 | 1316 | | 2 | 4 | 1039 | 2.659 | 15800 | >2000 | |
| 89 | 134 | | 8 | 5 | >2000 | 5.081 | 20000 | 502 | |
| 137 | 7 | | 34 | 9 | 276 | 0.868 | >20000 | 1009 | 208000 |
| 139 | 2 | | 19 | 7 | 393 | 1.653 | >20000 | 875 | 252800 |
| 145 | 49 | | 28 | 12 | 1852 | 12.174 | >20000 | 658 | |
| 146 | 1194 | | 5 | 5 | >2000 | 28 | 5300 | 235 | |
| 147 | 136 | | <1 | 2 | >2000 | 89 | 5100 | 1564 | |
| 148 | 13 | | 7 | 3 | >2000 | 13.624 | >20000 | 1126 | |
| 149 | 46 | | 6 | 8 | >2000 | 53 | 18100 | 505 | |
| 150 | 65 | | 2 | 11 | >2000 | 121 | 11300 | 1487 | |
| 151 | 12 | | 2 | 2 | >2000 | 39 | 2500 | 1801 | |
| 160 | 56 | | 6 | 4 | 788 | 5.523 | >20000 | >2000 | |
| 164 | 6 | | 9 | 4 | 69 | 0.125 | 9400 | 471 | 131200 |
| 165 | 246 | | 7 | 6 | 1999 | 5.299 | >20000 | 1903 | 225600 |
| 166 | 50 | | 7 | 8 | 1877 | 9.371 | 15500 | 1285 | 179200 |
| 167 | 18 | | 12 | 4 | 713 | 4.113 | >20000 | >2000 | 296000 |
| 168 | 10 | | 14 | 7 | 640 | 2.465 | >20000 | >2000 | 264000 |
| 169 | 35 | | 6 | 5 | 1377 | 4.845 | >20000 | >2000 | 264000 |
| 170 | 111 | | 7 | 3 | 742 | 3.86 | >20000 | >2000 | 318400 |
| 171 | 20 | | 18 | 6 | 79 | 0.153 | 2400 | 179 | |
| 172 | 51 | | 17 | 4 | >2000 | 22 | 3300 | 308 | |
| 173 | 25 | | 8 | 3 | 292 | 1.302 | 7000 | 295 | |
| 174 | 35 | | 44 | 10 | 232 | 2.052 | 2400 | 225 | |
| 175 | 16 | | 13 | 6 | >2000 | 46 | 5300 | 289 | |
| 176 | 262 | | 2 | 2 | >2000 | 14.555 | 12700 | 794 | |
| 177 | 68 | | 12 | 6 | 660 | 0.692 | 7500 | 1003 | |
| 179 | 76 | | 23 | 8 | 284 | 1.215 | 18700 | 1331 | |
| 183 | 78 | | 4 | 3 | 266 | 1.139 | >20000 | >2000 | |
| 184 | 32 | | 6 | 5 | >2000 | 3.958 | >20000 | 1140 | |
| 208 | 14 | | 3 | 2 | 25 | 0.159 | >20000 | >2000 | |
| 209 | 96 | | 32 | 7 | 206 | 0.54 | >20000 | 1657 | |
| 210 | 19 | | 12 | 4 | 75 | 0.261 | 9400 | 1461 | |

| Sample | Mo | Nb | Ni | Co | As | Hg | Ba | Sr | F |
|---|---|---|---|---|---|---|---|---|---|
| 211 | 13 | | 9 | 5 | 40 | 0.243 | 10400 | 1394 | |
| 212 | 5 | | 8 | 6 | 200 | 1.412 | >20000 | >2000 | |
| 214 | 8 | | 15 | 6 | >2000 | 154 | 1600 | 708 | |
| 215 | 2 | | 10 | 10 | 1261 | 27 | 250 | 115 | |
| 216 | 4 | | 11 | 11 | 746 | 9.04 | 140 | 155 | |
| 226 | 16 | | 14 | 5 | 66 | 0.173 | 1300 | 127 | |
| 227 | 73 | | 13 | 9 | 1473 | 2.024 | 5700 | 324 | |
| 228 | 1198 | | 3 | 3 | >2000 | 54 | 5600 | 154 | |
| 229 | 41 | | 14 | 6 | 461 | 1.052 | 800 | 152 | |
| 230 | 298 | | 8 | <10 | >9000 | >5000 | 4400 | 317 | |
| 231 | 10 | | 26 | 29 | 184 | 0.432 | 690 | 172 | |
| 232 | 486 | | 27 | 13 | >2000 | 3.281 | 5800 | 318 | |
| 233 | 13 | | 18 | 5 | 48 | 0.137 | 19400 | 453 | |
| 234 | 26 | | 17 | 26 | 35 | 175 | 79000 | 942 | |
| 235 | 5 | | 20 | 8 | 58 | 0.225 | 5000 | 230 | |
| 236 | 29 | | 20 | 7 | 12 | 0.075 | 16100 | 709 | |
| 237 | 15 | | 8 | <5 | 143 | 395 | 26900 | 750 | |
| 238 | 11 | | 10 | 4 | 492 | 1.697 | >20000 | >2000 | |
| 252 | 153 | | 3 | <1 | 37 | 0.081 | 830 | 76 | |
| 253 | 8 | | 2 | <1 | 71 | 0.202 | 400 | 59 | |
| 254 | 76 | | 44 | 22 | 1571 | 3.61 | 4500 | 577 | |
| 255 | 34 | | 6 | <5 | 1270 | 2800 | 4100 | 2091 | |
| 256 | 56 | | 6 | 2 | 1688 | 0.991 | 1700 | 287 | |
| 257 | 90 | | 13 | <5 | 386 | 570 | 5130 | 378 | |
| 293 | | | | | | | | | |
| 294 | | | | | | | | | |
| 295 | | | | | | | | | |
| 296 | | | | | | | | | |
| 297 | | | | | | | | | |
| 1 | 6 | | 3 | 3 | 50 | 0.298 | >20000 | 1126 | |
| 2 | 7 | | 9 | 4 | 121 | 0.028 | 4900 | 467 | |
| 3 | 8 | | 6 | 6 | 123 | 0.125 | 13000 | 966 | |
| 4 | 11 | | 3 | 3 | 70 | 0.1 | 15600 | 1174 | |
| 5 | 6 | | 7 | 4 | 97 | 0.096 | 10700 | 987 | |
| 7 | 8 | | 5 | 5 | 94 | <0.01 | 6100 | 943 | |
| 8 | 5 | | 7 | 7 | 42 | <0.01 | 4700 | 1482 | |
| 31 | 3 | | 22 | 15 | <5 | 0.02 | 1900 | 534 | |
| 35 | 2 | | 14 | 7 | <5 | <0.01 | 1600 | 459 | 201 |
| 36 | 7 | | 19 | 10 | <5 | <0.01 | 1600 | 329 | 395 |
| 37 | 3 | 57 | 22 | 23 | 5 | <0.01 | 3000 | 542 | 676 |
| 38 | 3 | 52 | 21 | 16 | <5 | <0.01 | 2800 | 1104 | 867 |
| 39 | 5 | 74 | 24 | 19 | <5 | <0.01 | 3700 | 1368 | 772 |
| 40 | 6 | 61 | 25 | 20 | <5 | <0.01 | 6000 | 515 | 889 |
| 41 | <1 | 102 | 3 | 2 | <5 | <0.01 | 3200 | 801 | 131 |
| 43 | 4 | | 17 | 16 | 10 | 0.018 | 2000 | 1089 | |
| 44 | 3 | | 18 | 14 | <5 | 0.044 | 1500 | 1375 | |
| 45 | <1 | | 27 | 12 | 7 | <0.01 | 1400 | 399 | |

| Sample | Mo | Nb | Ni | Co | As | Hg | Ba | Sr | F |
|---|---|---|---|---|---|---|---|---|---|
| 55 | <1 | | 19 | 16 | <5 | <0.01 | 1100 | 445 | |
| 56 | 9 | | 22 | 6 | 34 | 0.066 | 1600 | 68 | |
| 57 | 3 | | 19 | 9 | 18 | 0.069 | 1500 | 469 | |
| 60 | 2 | | 17 | 10 | 16 | 0.024 | 1100 | 646 | |
| 62 | 12 | | 16 | 12 | <5 | 0.054 | 2500 | 393 | |
| 63 | 11 | | 15 | 11 | 12 | 0.032 | 2600 | 559 | |
| 64 | 10 | | 4 | 2 | 39 | 0.04 | 8100 | 735 | |
| 65 | 3 | | 14 | 11 | <5 | 0.037 | 1100 | 434 | |
| 66 | 3 | | 15 | 11 | 5 | 0.028 | 1000 | 295 | |
| 67 | 1 | | 13 | 11 | 16 | 0.014 | 820 | 236 | |
| 68 | 5 | | 13 | 8 | 14 | 0.049 | 770 | 309 | |
| 69 | 2 | | 9 | 6 | 8 | 0.067 | 700 | 205 | |
| 70 | 2 | | 16 | 12 | <5 | 0.029 | 710 | 332 | |
| 71 | 20 | <1 | 5 | 2 | <5 | <0.01 | >20000 | 1325 | >20000 |
| 72 | 20 | | 5 | 3 | <5 | 0.021 | 3300 | 352 | |
| 73 | 41 | 72 | 3 | 2 | 7 | 0.013 | 4000 | 202 | 786 |
| 74 | 6 | 93 | 5 | 3 | <5 | <0.01 | 3300 | 246 | 345 |
| 75 | 72 | | 3 | 2 | 46 | 0.027 | >20000 | >2000 | |
| 76 | 63 | | 6 | 3 | 26 | 0.052 | 11100 | 428 | 54800 |
| 77 | 33 | | 5 | 5 | <5 | 0.041 | 9500 | 439 | 56000 |
| 78 | 10 | 148 | 2 | 8 | 7 | <0.01 | 4000 | 639 | 10186 |
| 79 | 54 | | 7 | 3 | <5 | 0.05 | 9700 | 496 | 116800 |
| 80 | 34 | | 3 | 4 | <5 | 0.044 | 12900 | 839 | 235200 |
| 81 | 232 | | 4 | 3 | 49 | 0.055 | 3100 | 566 | 21500 |
| 82 | 20 | | 4 | 2 | <5 | 0.052 | 10500 | 405 | 164800 |
| 83 | 9 | 132 | 3 | 2 | 9 | <0.01 | 1500 | 188 | 187 |
| 84 | 6 | 102 | 5 | 4 | <5 | <0.01 | 2000 | 140 | 226 |
| 86 | 46 | 69 | 4 | 2 | 18 | 0.014 | 2700 | 90 | 363 |
| 87 | 150 | | 4 | 3 | <5 | <0.01 | >20000 | 437 | |
| 88 | 3 | | 3 | 3 | <5 | 0.012 | 3600 | 168 | |
| 97 | 4 | | 14 | 7 | 24 | 0.021 | 2200 | 445 | |
| 98 | 6 | | 15 | 8 | 10 | 0.016 | 1800 | 417 | |
| 99 | 3 | | 18 | 10 | 13 | 0.016 | 1900 | 481 | |
| 100 | 22 | | 17 | 7 | 11 | <0.01 | 2500 | 409 | |
| 101 | 2 | | 16 | 4 | 14 | 0.018 | 1800 | 85 | |
| 102 | 17 | | 5 | 5 | <5 | <0.01 | 18700 | 591 | |
| 103 | 23 | | 15 | 5 | <5 | 0.133 | 3000 | 347 | |
| GM-10-1 | 343 | 94 | <10 | <10 | 20 | | | 279 | |
| GM-10-2 | <50 | <100 | <50 | <50 | <50 | | | 2322 | |
| 4094 | | | | | | | | | |
| 58 | 24 | | 11 | 120 | 7 | 40 | 280 | 29 | |
| 59 | 6 | | 11 | 34 | <5 | 0.027 | 950 | 31 | |
| 61 | <1 | | 6 | 7 | <5 | 0.073 | 1000 | 165 | |
| 96 | 14 | | 10 | 17 | <5 | 0.054 | 230 | 47 | |
| 260 | 7 | | <1 | 78 | 29 | 30 | 200 | 53 | |
| GM-09-LC-2 | 359 | 114 | <10 | 21 | 563 | | | 513 | |
| 9671 | | | | | | | | | |

## APPENDIX 3. GEOCHEMICAL PLOTS

Turquoise triangles are breccia pipes and fenite samples, red circle is rhyolite, pink diamond is latite, blue diamond is trachyte/syenite, and open blue triangle is fenitized trachyte/syenite. Chemical analyses are from Schreiner (1993) and this report (Appendix 1).

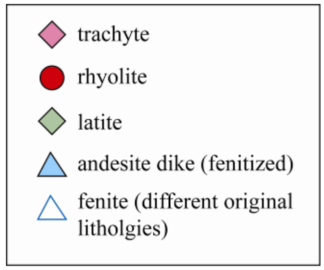


Key

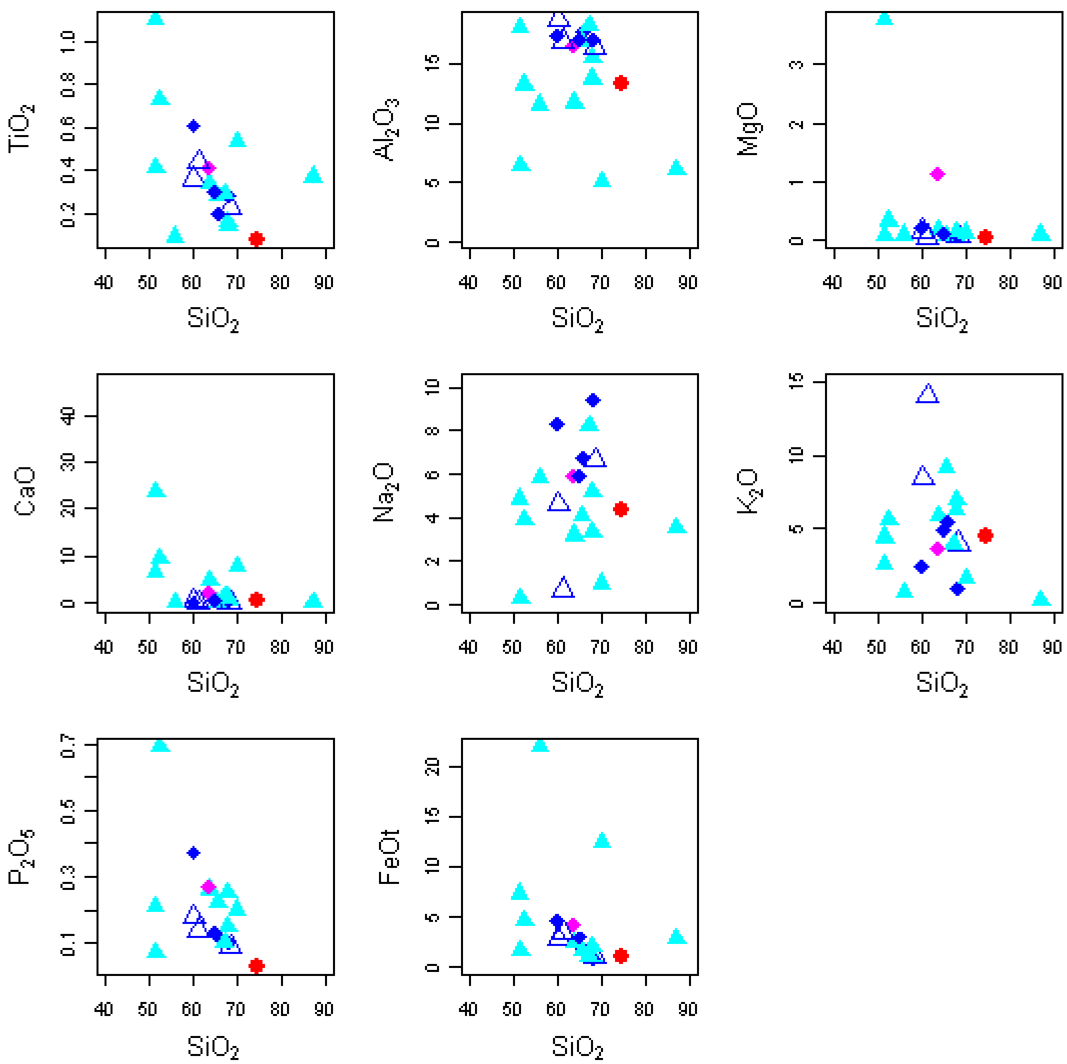


Scatter plots of major elements verses $SiO_2$ (in percent), showing similar differentiation of igneous rocks. This shows that the igneous rocks are geochemically and likely genetically related.

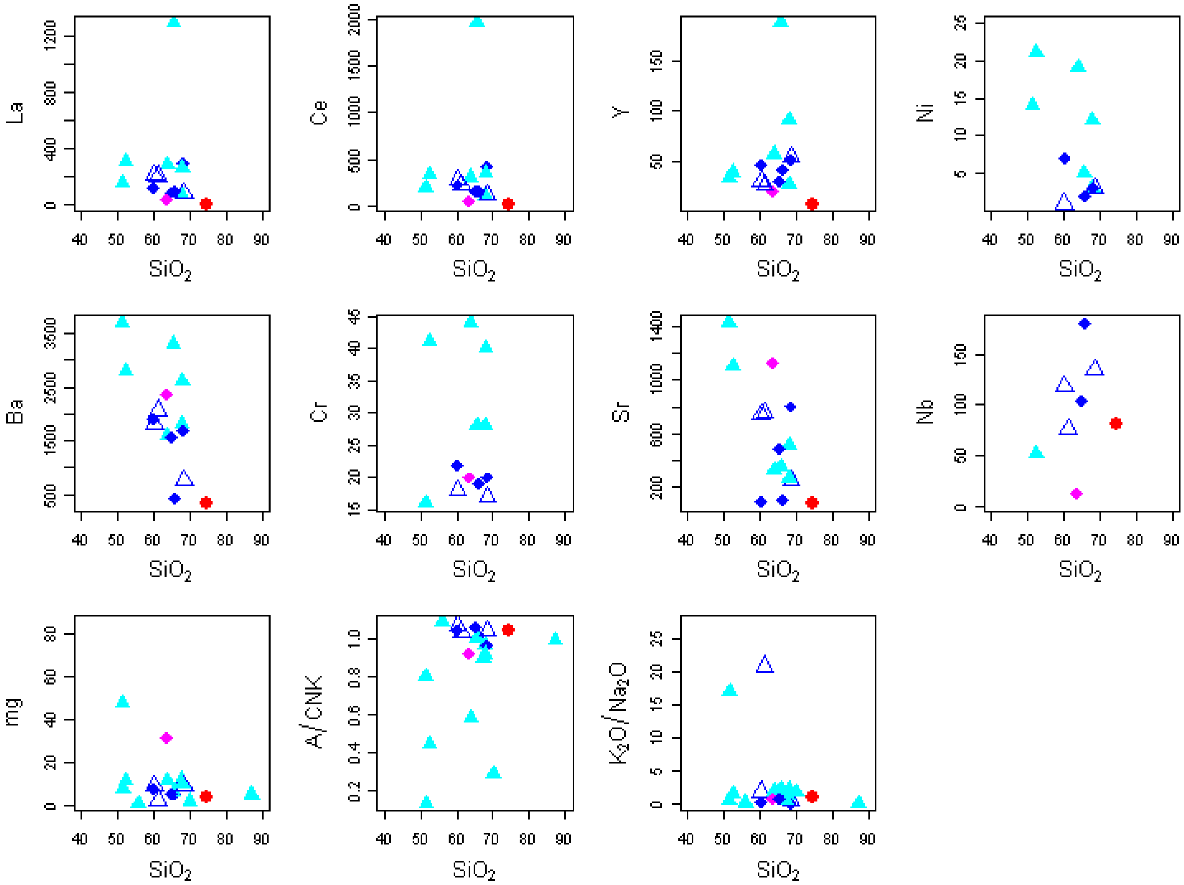


Scatter plots of trace elements (in parts per million, ppm) verses $SiO_2$ (in percent), showing similar differentiation of igneous rocks. This shows that the igneous rocks are geochemically and likely genetically related.

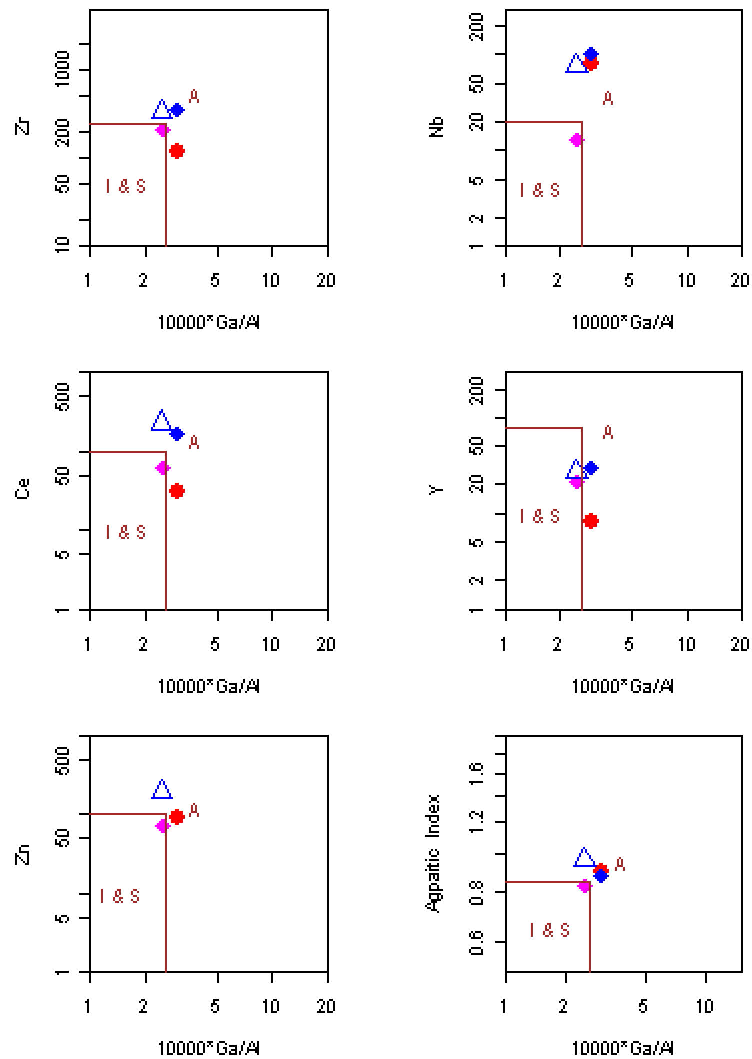


Geochemical plots from Whalen, et al. (1987) showing that the igneous rocks from the Gallinas Mountains are similar in chemistry to A-type granitoids.

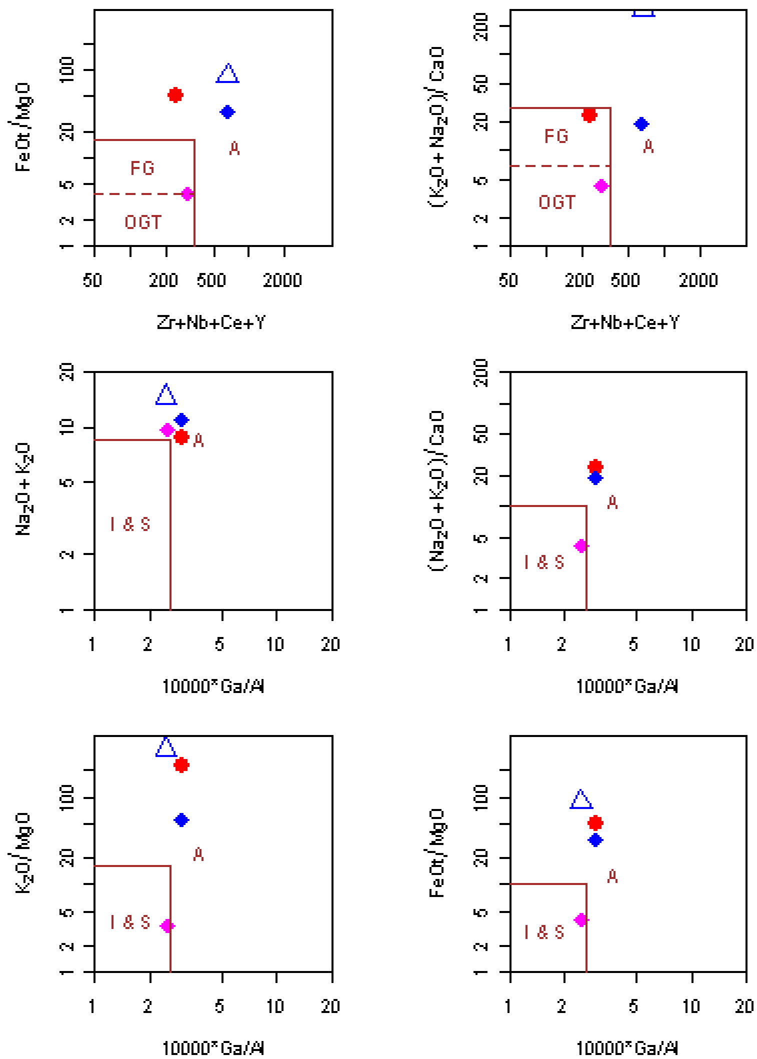


Geochemical plots from Whalen, et al. (1987) showing that the igneous rocks from the Gallinas Mountains are similar in chemistry to A-type granitoids.